University of São Paulo
"Luiz de Queiroz" College of Agriculture

Parameterization and evaluation of mechanistic crop models for estimating *Urochloa brizantha* cv. BRS Piatã productivity under full sun and in silvopastoral system

Cristiam Bosi

Thesis presented to obtain the degree of Doctor in Science. Area: Agricultural Systems Engineering

Piracicaba
2017

Cristiam Bosi
Agronomist

Parameterization and evaluation of mechanistic crop models for estimating *Urochloa brizantha* cv. BRS Piatã productivity under full sun and in silvopastoral system

Advisor:
Prof. Dr. **PAULO CESAR SENTELHAS**

Co-advisor:
Dr. **JOSÉ RICARDO MACEDO PEZZOPANE**

Thesis presented to obtain the degree of Doctor in Science. Area: Agricultural Systems Engineering

Piracicaba
2017

Dados Internacionais de Catalogação na Publicação
DIVISÃO DE BIBLIOTECA – DIBD/ESALQ/USP

Bosi, Cristiam

Parameterization and evaluation of mechanistic crop models for estimating *Urochloa brizantha* cv. BRS Piatã productivity under full sun and in silvopastoral system / Cristiam Bosi. - - Piracicaba, 2017.

158 p.

Tese (Doutorado) - - USP / Escola Superior de Agricultura “Luiz de Queiroz”.

1. Agroflorestal 2. APSIM 3. CROPGRO 4. Interações árvore-cultura 5. Radiação solar 6. Água no solo I. Título

ACNOWLEDGEMENTS

I would like to thank God for my life, health, for all the opportunities, for this work finished, and for his love. To Our Lady Mary for her love and intercession.

To my parents Jovir P. Bosi and Valdecira P. Bosi, for their support, education, and love. To my wife Dulcineia Camargo Bosi for her love, support and understanding during this time of study. To my brother Cassiano, my sister Carine, my grandmother Francisca and my aunt Olinda for their love and prayers. To my mother-in-law Lucy for her prayers.

To my professor adviser Dr. Paulo Cesar Sentelhas for his mentoring, friendship, teachings, and all the assistance during the development of my Ph.D. studies. To my co-adviser Dr. José Ricardo M. Pezzopane for his support, friendship, and assistance during all this time of research and study. To my supervisor in Australia Dr. Neil I. Huth for his help with the models development and adaptation, his friendship, support, and for the drives and walkings through many places of Queensland.

To Mariana P. Andreucci for the support and friendship during my stay in Australia. To Clare and John Dimes for the support and help in Toowoomba and Brisbane. To Cui Chenfeng for the talkings and company. To Dean Holzworth and Jeremy Wish for the help and support. To Brett Cocks and his family for the beautiful and nice Australian Christmas.

To the professors Carlos G. S. Pedreira, Peterson R. Fiorio, Marcus V. Folegatti, Patricia A. A. Marques, Ciro A. Righi, Fabio R. Marin, Sérgio O. Moraes, Fernando C. Mendonça and Patrícia M. Santos for the teachings and good experiences.

To my friends at “Cúpula” Rafael Battisti, Leonardo A. Monteiro, Leandro G. Costa, Murilo S. Vianna, Fabiani D. Bender, Henrique B. Dias, Gustavo C. Beruski, Fernando D. Hinnah, Yury N. Duarte, Elvis F. Elli, Silvane I. Brand, Juliana C. Rodrigues, Cleverson H. Freitas, Maiara A. Despontin, Paola Bongiovani and Rogério S. Nóia Jr. for the friendship.

To my friends at Embrapa Pecuária Sudeste Larissa R. M. Bernarde, Vitoria dos S. Toni da Silva, Willian L. Bonani, Daiane M. Parra, Mateus H. Marconato, Cristian A. Camargo (in memorian), Luis F. Gallo, Guilherme R. Oliveira, Ana G. Dentello, Mauricio Gava, Cristiana G. Pezzopane, and Mariana V. Azenha for the support.

To ESALQ and Embrapa Pecuária Sudeste for the opportunity to develop my Ph.D. To FAPESP for the scholarships (grant nº 2014/11931-8 and grant nº 2016/01532-4). To CAPES for the scholarship during the first 6 months of my Ph.D. To CSIRO for the opportunity to realize an internship overseas.

To everyone that in some way contributed for my evolution. Thank you very much.

EPIGRAPH

“Imagination is more important than knowledge. For knowledge is limited to all we now know and understand, while imagination embraces the entire world, and all there ever will be to know and understand.”

“We are in the position of a little child, entering a huge library whose walls are covered to the ceiling with books in many different tongues. The child knows that someone must have written those books. It does not know who or how. It does not understand the languages in which they are written. The child notes a definite plan in the arrangement of the books, a mysterious order, which it does not comprehend, but only dimly suspects. That, it seems to me, is the attitude of the human mind, even the greatest and most cultured, toward God. We see a universe marvelously arranged, obeying certain laws, but we understand the laws only dimly. Our limited minds cannot grasp the mysterious force that sways the constellations.”

Albert Einstein

CONTENTS

RESUMO

Parametrização e avaliação de modelos mecanísticos para estimativa da produtividade de *Urochloa brizantha* cv. BRS Piatã a pleno sol e em sistema silvipastoril

Os sistemas silvipastoris são um tipo de sistema agroflorestal em que árvores ou arbustos são combinados com animais e pastagens. Os sistemas silvipastoris são importantes para a intensificação de pastagens e para a mitigação dos efeitos das mudanças climáticas. Entretanto, poucos estudos vêm sendo realizados visando à adaptação de modelos para a simulação desses sistemas. O objetivo desse estudo foi parametrizar e testar os modelos mecanísticos APSIM e CROPGRO para estimar a produtividade de *Urochloa brizantha* cv. BRS Piatã a pleno sol e em um sistema silvipastoril, avaliar o desempenho dos modelos para simular as interações árvore-pastagem e desenvolver ferramentas para aprimorar tais simulações. Para isso, foram conduzidos quatro experimentos de campo, a pleno sol, para avaliar diferentes manejos da pastagem: corte, em irrigado e sequeiro; e pastejo, em sequeiro e com alto ou baixo suprimento de nitrogênio. Outro experimento foi conduzido em um sistema silvipastoril com as árvores arranjadas em renques simples, com orientação Leste-Oeste, com espaçamento de 15 m entre renques e 2 m entre plantas nos renques. Esse experimento foi conduzido sob pastejo e em sequeiro, com avaliações das variáveis da pastagem, microclima e água no solo em quatro distâncias em relação ao renque Norte (0,00 m; 3,75 m; 7,50 m and 11,25 m). As estimativas de massa de forragem a pleno sol, realizadas com o modelo APSIM-*Tropical Pasture*, apresentaram boa concordância entre os dados observados e os estimados (R^2 entre 0,82 e 0,97, d entre 0,92 e 0,98 e NSE de 0,72 a 0,92), enquanto que, as estimativas geradas pelo modelo CROPGRO-*Perennial Forage* alcançaram boa precisão (R^2 entre 0,65 e 0,93) e boa exatidão (d entre 0,86 e 0,97 e NSE de 0,60 a 0,90), para os diferentes manejos e condições ambientais. Mesmo considerando o desempenho promissor de ambos os modelos para simular pastagens a pleno sol, para confirmar a acurácia e a eficiência destes, são necessários testes em outros locais, condições climáticas, tipos de solo e intensidades de corte ou pastejo. As simulações do crescimento da pastagem no sistema silvipastoril indicaram que o modelo APSIM-*Tropical Pasture*, foi eficiente quando somente a competição por radiação solar foi considerada (R^2 de 0,69 a 0,88, d entre 0,90 e 0,96 e NSE de 0,51 a 0,85), mas ineficiente quando somente a competição por água no solo foi considerada (R^2 entre 0,58 e 0,85, d entre 0,58 e 0,82 e NSE de -4,07 a -0,14). O modelo CROPGRO-*Perennial Forage* atingiu bom desempenho na simulação do crescimento da pastagem para as distâncias 0,00 m, 3,75 m e 7,50 m em relação às árvores (R^2 de 0,75 a 0,90, d entre 0,93 e 0,96, NSE de 0,74 a 0,85). Apesar dos bons resultados, ambos os modelos devem ser melhorados para simular todos os fatores que afetam o crescimento de pastagens em sistemas silvipastoris.

Palavras-chave: Agroflorestal; APSIM; CROPGRO; Interações árvore-cultura; Radiação solar; Água no solo

ABSTRACT

Parameterization and evaluation of mechanistic crop models for estimating *Urochloa brizantha* cv. BRS Piatã productivity under full sun and in silvopastoral system

Silvopastoral systems are a kind of agroforestry system in which trees or shrubs are combined with animals and pastures. Silvopastoral systems are important to intensify pasture production and mitigate climate change effects. However, very few studies have been performed to adapt crop models to simulate these systems. The aim of this study was to parameterize and test the mechanistic crop models APSIM and CROPGRO for estimating *Urochloa brizantha* cv. BRS Piatã productivity under full sun and in a silvopastoral system, to evaluate the models' performance to simulate tree-crop interactions, and to develop tools to improve these simulations. For this purpose, four field experiments were conducted under full sun to investigate cutting management under irrigated and rainfed conditions and grazing management under rainfed conditions with high and low N supply. Another experiment was carried out in a silvopastoral system with the trees arranged in simple rows, in East-West orientation, with 15 m between rows and 2 m between plants in the rows. This experiment was conducted under grazing management and rainfed conditions with the pasture variables, microclimate and soil water content being assessed at four distances from the North row (0.00 m, 3.75 m, 7.50 m and 11.25 m). The forage mass simulations for the pasture at full sun, performed using the APSIM-Tropical Pasture model, showed good agreement between observed and estimated data (R^2 between 0.82 and 0.97, d between 0.92 and 0.98, and NSE ranging from 0.72 to 0.92), while the simulations with the CROPGRO-Perennial Forage model achieved good precision (R^2 between 0.65 and 0.93) and good accuracy (d from 0.86 to 0.97, and NSE from 0.60 to 0.90), for the various managements and environmental conditions. Even considering the promising performance of both models for pastures under full sun, they already needs to be tested in other locations, climate conditions, soils, and grazing or cutting intensities, to prove its accuracy and reach enough confidence. The pasture growth simulations at the silvopastoral system indicated that the APSIM-Tropical Pasture was efficient when only competition by solar radiation was considered (R^2 from 0.69 to 0.88, d from 0.90 to 0.96, and NSE between 0.51 and 0.85), but inefficient when considering only competition by soil water (R^2 between 0.58 and 0.85, d between 0.58 and 0.82, and NSE from -4.07 to -0.14). The CROPGRO-Perennial Forage achieved good performance on pasture growth simulation at the distances 0.00 m, 3.75 m, and 7.50 m from the trees (R^2 from 0.75 to 0.90, d from 0.93 to 0.96, NSE between 0.74 and 0.85). Despite the good results, improvements should be performed in both models for simulating all factors that affect forage growth in silvopastoral systems.

Keywords: Agroforestry; APSIM; CROPGRO; Tree-crop interactions; Solar radiation; Soil water

1. INTRODUCTION

Agroforestry systems (AFS) are forms of land use where timber trees or fruit trees are combined with crops and/or livestock, simultaneously or in a sequence of time, aiming to improve ecological interactions and economic returns (Lundgren and Raintree 1982). According to Elevitch and Kim (2001), AFS are dynamic systems based on ecological management of the natural resources that, through integration between trees and agricultural or pastoral systems, diversify and keep good levels of productivity and promote social, economic and environmental improvements.

The main aim of an AFS is to optimize land use (Alao and Shuaibu 2013), combining forest and food productions (King 1979), improving the soil conservation (Pattanayak and Mercer 1998), and reducing the need for new lands for agriculture (Schroeder 1994), minimizing pressure for deforestation. For example, areas with secondary vegetation, which has no economic and social importance, can be recovered and rationally used through agroforestry practices (Vieira et al. 2009). Another important aspect of this kind of system is its design which requires less external resources input (Filius 1982).

Agroforestry systems are also classified as crop-livestock-forest integration systems. Systems based on crop-livestock-forest integration are more complex than single crops. In these systems, many interactions occur between plants with different height, shape and root architecture (trees, shrubs, crops), and between plants and animals, with their intensity varying spatially and temporally (Silva 2012). Gillespie et al. (2000) indicated that the intensity of such interactions is determined by the resource competition patterns, mainly by water, solar radiation, and nutrients.

In integrated systems, the interactions between their components may be positive, neutral or negative (competition). During system planning, the main aim must be that trees and the other components interact successfully, optimizing the system productivity (Nicodemo et al. 2004). For tropical and subtropical regions, there is not enough knowledge about planning and management of integrated systems, mainly for regions with warm and wet summer, and dry winter.

AFS are very important systems for the Brazilian government plan for mitigation and adaptation to climatic changes and reduction of greenhouse gases emission from agriculture, named ABC Plan, which is divided into seven programs, of which three are related to AFS: a) Recovery of degraded pastures; b) Implementation of AFS; c) Adaptation of Brazilian agriculture to climate changes (MAPA 2014).

Silvopastoral systems (SPS) are a kind of AFS in which pastures and trees are grown together interacting with animals. These systems aim to be more sustainable than conventional systems, increasing total productivity, diversifying agricultural production and improving resources use efficiency (Mijail et al. 2005). Besides that, as already mentioned, these systems are a good tool to recover degraded pastures (Nair et al. 2009), to adapt agricultural systems, and to mitigate the effects of climate change on plants and animals, with several social, economic and environmental benefits (Steinfeld et al. 2006).

Such kind of integrated system may promote: higher land use efficiency; increase of economic returns per hectare; erosion control; improvements on soil fertility by increasing nutrient cycling and biological activity; higher forage allowance and quality due to the good conditions for pasture growth; flexibility for the trees use (for building, timber, firewood, charcoal, honey production, among others); and higher biodiversity, mainly when native species are employed (Carvalho et al. 2007). Also, higher carbon sequestration and mitigation of the effects of extreme weather conditions can be listed as benefits of SPS.

SPS may have as main purpose animal production, giving a secondary economic importance for trees, which may be used for timber and several other products, or only for shading animals, and eventually for animal feeding. The other possible option is when the main economic components are the trees, with the animals being employed to graze weeds and to reduce the management costs, giving also an additional economic return (Engel 1999).

In SPS, the shading promoted by the tree canopy changes the solar radiation and soil water availability for the understory plants, altering microclimate and, consequently, crop growth and development (Menezes et al. 2002). Therefore, the efficiency of these systems depends on the use of species that are adapted to these environmental conditions. In the case of forage species, they must be tolerant to shading, have good potential yield, and be adapted to management and regional soil and climatic conditions (Garcia and Andrade 2001).

According to Benavides et al. (2009), microclimatic alterations occur in SPS independently of the type of tree used, deciduous or perennial; however, the intensity of these alterations varies according to the tree species. Benavides et al. (2009) also observed the effect of trees on solar radiation, water dynamics, wind speed, and air temperature. Such microclimatic changes were also observed in several other studies in the last ten years (Amadi et al. 2016; Böhm et al. 2014; Gomes et al. 2016; Karki and Goodman 2015; Oliveira et al. 2007; Pezzopane et al. 2015; Prasad et al. 2010; Siles et al. 2010; Tamang et al. 2010).

The microclimate alterations in SPS are very important to determine pasture evapotranspiration and soil water availability, affecting the water balance (Feldhake 2009; Lin

2010), and reducing pasture productivity when competition by water is important (Bosi et al. 2014). On the other hand, trees may also improve soil structure, porosity, water holding capacity, reduce surface runoff (Benegas et al. 2014), increase infiltrability (Benegas et al. 2014; Sahin et al. 2016) and improve the water use, mainly from deeper soil layers (Gyenge et al. 2002; Pollock et al. 2009).

For plants, high solar radiation incidence increases leaf temperature. Excessively high leaf temperatures can result in stress, reducing photosynthesis (Boyer 1971), affecting plant growth and productivity. Therefore, shading promoted by trees in SPS may keep leaf temperature within suitable levels. For example, Siles et al. (2010) observed that under full sun the leaf temperature of coffee plants was higher than air temperature, while in shaded coffee area, leaf temperature was always lower than air temperature.

For animals, thermal stress occurs when air temperature reaches values higher than the thermoneutral range (Armstrong 1994). Such condition causes increase of animals' body temperature, which is determinant to their thermal comfort (Baliscei et al. 2012), which affects productivity and reproductive efficiency (Garcia et al. 2010). As consequences of such stress, physiological and behavior adaptations occur, like preference for shaded places, increases of water intake, peripheral vasodilation, sweating, and respiratory rate (Blackshow and Blackshow 1994), and, as consequence, reduction of animal productivity. These problems may be minimized by adopting SPS, as confirmed by Baliscei et al. (2013) who found lower values of measured black globe temperature, which represents animals' body temperature, inside a SPS.

According to Valle et al. (2000), the pastures of Urochloa (syn. Brachiaria) genus have been of great importance for Brazilian livestock, since they allowed the occupation of acid and low fertility soils in the Brazilian savannah (Cerrado biome) with beef cattle farms. Currently, Brazilian cultivated pastures are still based on those species. Besides that, such genus stimulated the development of pasture seeds production, making Brazil the largest exporter of this kind of seed to tropical regions around the world.

The capacity to feed animals in the Brazilian savannah was almost triplicated with the introduction of brachiariagrasses. Native pastures were explored with approximately 0.25 animals ha^{-1}, while molasses grass (*Melinis minutiflora*) and jaragua grass (*Hyparrhenia rufa*) with 0.3 to 0.6 animals ha^{-1}. Brachiariagrasses support between 1.0 and 1.5 animals ha^{-1}, in average. Therefore, brachiariagrasses are still considered very important for Brazilian livestock (Valle et al. 2010).

Urochloa brizantha is the most cultivated forage species in Brazil, mainly the Marandu cultivar (*U. brizantha* cv. Marandu) (Miles et al. 2004). This species is recommended for wet tropical regions, with total rainfall about 1000 mm year^{-1}, being tolerant to drought periods with duration between three and six months (Cook et al. 2004). The optimal temperatures for *Urochloa sp.* growth and development are between 30 and 35ºC (Miles et al. 2004).

Piatã cultivar is less productive than the most sowed ones. However, it is still a good option for regions with intense water deficit. The main reason for that, according to Santos et al. (2013), is its higher control on stomatic conductance.

Soil moisture, solar radiation, air temperature and daylength are the most important factors for determining pastures growth and development (Pedreira 2009). Although solar radiation and temperature are of similar importance for biomass production, they have different functions under an ecophysiological point of view. Solar radiation is more associated to the conversion of radiative energy into chemical energy during photosynthesis (Zhu et al. 2008), while temperature is associated to the metabolic processes involved in such conversion, affecting mainly the biochemical phase of photosynthesis (Bonhomme 2000).

Due to the great importance of environmental factors to determine forage productivity, mathematical models have been developed and used for estimating pasture growth, taking into account genetic, soil and climatic factors. These models are employed since the 80s of the last century for pasture production dynamics (Andrade et al. 2015). Different approaches and studies using models allowed to estimate pasture yield and production parameters based only on climatic factors (Fitzpatrick and Nix 1973; Ometto 1981; Villa Nova et al. 1983).

Among the several types of crop models, the mechanistic ones are those based on the understanding and systematization of the main plant physiological processes and the interactions with other processes in the agroecosystem (Andrade et al. 2015). This kind of approach has being applied for tropical pastures simulation by the following models: ALMANAC (Agricultural Land Management Alternative with Numerical Assessment Criteria) (Kiniry et al. 2007), Century (Parton et al. 1993), Orchidee Grassland Management (Coltri et al. 2014), CROPGRO Perennial Forage (Alderman 2008; Lara et al. 2012; Pedreira et al. 2011; Pequeno et al. 2014; Pequeno et al. 2017; Rymph et al. 2004), APSIM (Agricultural production systems simulator) (Araújo et al. 2013), and STICS (*Simulateur mulTIdisciplinaire pour les Cultures Standard*) (Santos 2016), all of them with satisfactory performance.

Specifically for pastures of *U. brizantha*, just CROPGRO Perennial Forage model of DSSAT (Decision Support System for Agrotechnology Transfer) was adapted for Xaraés palisadegrass (*U. brizantha* cv. Xaraés) (Pedreira et al. 2011) and Marandu palisadegrass (*U. brizantha* cv. Marandu) (Pequeno et al. 2014), and STICS model for Piatã palisadegrass (*U. brizantha* cv. BRS Piatã) (Santos 2016). Therefore, CROPGRO Perennial Forage and APSIM were never parameterized for simulating Piatã palisadegrass.

The APSIM is a farming systems modeling framework that contains interconnected models to simulate systems comprising soil, crop, tree, pasture and livestock biophysical processes. It is used extensively by researchers to assess on-farm management practices, climate risk, climate change and adaptation strategies, mixed pasture/livestock strategies, agroforestry resource competition, nutrient leaching under various conditions, gene trait expression, among many other applications (Holzworth et al. 2014).

CROPGRO is a mechanistic model that predicts crop yield and composition based on plant, climate, management and soil information. It also simulates water balance, organic matter, surface residue dynamics and pests and diseases damages (Rymph 2004). Such model is written in FORTRAN programming language and is considered a generic model, being used for modeling several crops, which is possible because it has flexibility for changing the input files related to species and cultivar characteristics (Lara 2011).

Modelling crop development and growth in agroforestry systems is much more complex than for single crops. This complexity comes from the large heterogeneity caused by the association of crops or grasses with trees, which changes mass and energy fluxes among themselves, causing interdependence. Thereby, a model to describe these systems behavior needs not only to simulate plant´s dynamic processes, but also the changes and interactions between their components (Huth et al. 2002).

Many models have been used to simulate agroforestry systems, taking into account the abstraction of the interaction of crops and trees. Zuidema et al. (2005) used the SUCROS-Cocoa model to estimate cacao productivity, considering light interception and photosynthesis, maintenance respiration, biomass accumulation and competition for resources, and showed that the model produced realistic outputs for bean yield, standing biomass, leaf area and size–age relations. Johnson et al. (2009), combining the models ALMANAC and SWAT (Douglas-Mankin et al. 2010), estimated trees and crops yields in an agroforestry system and concluded that the model can improve the accuracy of watershed scale simulations of plant competition and agroforestry systems, and provide a basis for developing improved tropical systems routines. The *Yield*-SAFE model (Van Der Werf et al.

2007) was also applied in agroforestry systems by Graves et al. (2010) to simulate tree and crop growth in France and England. These authors showed that this model is able to provide useful predictions of yields in silvoarable systems, relative to arable and forestry systems.

Qi et al. (2001) used the CROPGRO model (Boote et al. 1998) to estimate soybean yield under windbreak, while Zamora et al. (2009) applied such model to estimate cotton yield under different shading intensities, in an agroforestry system with pecan trees.

Huth et al. (2002) applied the APSIM model to estimate the yield of eucalyptus and chickpea, through a multi-point approach, assessing each point in the field and aiming to find a distribution which could represent the whole system. Taking into account this abstraction, it was possible to simulate many agroforestry systems with different arrangements, management and several combinations of species, representing an enormous advance for understanding this kind of production system.

In the context of several efforts to simulate growth and development of the important crops for agriculture and livestock, and in front of the need for planning and understanding useful systems for mitigating the effects of climate change, it is important to adapt tools such as APSIM and CROPGRO for estimating palisadegrass growth in silvopastoral systems, in order to simulate the interactions that occur between pasture, trees and animals, and the differences of these systems when compared to single pastures. For this, the hypothesis of this study is that the APSIM and CROPGRO models are effective tools for estimating *U. brizantha* cv. BRS Piatã productivity under full sun and in a silvopastoral system.

1.1. Objectives

1.1.1. General

The general objective of this study was to parameterize and test the mechanistic crop models APSIM and CROPGRO for estimating *Urochloa brizantha* cv. BRS Piatã productivity under full sun and in a silvopastoral system, to evaluate the models' performance to simulate tree-crop interactions, and to develop tools to improve these simulations.

1.1.2. Specific

a) to assess the microclimate and soil water availability in two pastoral systems, one at a full sun pasture system of *Urochloa brizantha* cv. BRS Piatã and another at a silvopastoral system with the same pasture and rows of Eucalyptus trees, to use these data for the models parameterization and test;

b) to develop a state-of-the-art tropical pasture model in the APSIM Plant Modelling Framework and to parameterize and test this model for simulating Piatã palisadegrass growth under full sun, with cutting and rotational grazing managements;

c) to develop a two-dimensional model for simulating solar radiation transmission by eucalyptus trees arranged in rows to be implemented in the analysis with APSIM;

d) to calibrate the CROPGRO-Perennial Forage model for estimating Piatã palisadegrass growth under full sun, with cutting and rotational grazing managements.

e) to test the APSIM-Tropical Pasture and the CROPGRO-Perennial Forage models for estimating Piatã palisadegrass growth in a silvopastoral system with eucalyptus, considering competition by solar radiation and soil water.

REFERENCES

Alao, J.S., Shuaibu, R.B., 2013. Agroforestry practices and concepts in sustainable land use systems in Nigeria. J. Hortic. For. 5, 156-159. https://doi.org/10.5897/JHF11.055

Alderman, P.D., 2008. Simulating the regrowth dynamics of Tifton 85 bermudagrass as affected by nitrogen fertilization. MSc Thesis – University of Florida, Gainesville. 115 p.

Amadi, C.C., Van Rees, K.C.J., Farrell, R.E., 2016. Soil–atmosphere exchange of carbon dioxide, methane and nitrous oxide in shelterbelts compared with adjacent cropped fields. Agric. Ecosyst. Environ. 223, 123-134. https://doi.org/10.1016/j.agee.2016.02.026

Andrade, A.S., Santos, P.M., Pezzopane, J.R.M., Araujo, L.C., Pedreira, B.C., Pedreira, C.G.S., Marin, F.R., Lara, M.A.S., 2015. Simulating tropical forage growth and biomass accumulation: an overview of model development and application. Grass Forage Sci. 71, 54-65. https://doi.org/10.1111/gfs.12177

Araujo, L.C., Santos, P.M., Rodriguez, R., Pezzopane, J.R.M., Oliveira, P.P.A., Cruz, P.G., 2013. Simulating Guineagrass production: empirical and mechanistic approaches. Agron. J. 105, 61–69. https://doi.org/10.2134/agronj2012.0245

Armstrong, D.V., 1994. Heat stress interaction with shade and cooling. J. Dairy Sci. 77, 2044-2050. https://doi.org/10.3168/jds.S0022-0302(94)77149-6

Baliscei, M.A., Barbosa, O.R., Souza, W., Costa, M.A.T., Krutzmann, A., Queiroz, E.O., 2013. Microclimate without shade and silvopastoral system during summer and winter. Acta Sci. Anim. Sci. 35, 49-56. https://doi.org/10.4025/actascianimsci.v35i1.15155

Baliscei, M.A., Souza, W., Barbosa, O.R., Cecato, U., Krutzmann, A., Queiroz, E.O., 2012. Behavior of beef cattle and the microclimate with and without shade. Acta Sci. Anim. Sci. 34, 409-415. https://doi.org/10.4025/actascianimsci.v34i4.15055

Benavides, R., Douglas, G.B., Osoro, K., 2009. Silvopastoralism in New Zealand: review of effects of evergreen and deciduous trees on pasture dynamics. Agrofor. Syst. 76, 327-350. https://doi.org/10.1007/s10457-008-9186-6

Benegas, L., Ilstedt, U., Roupsard, O., Jones, J., Malmer, A., 2014. Effects of trees on infiltrability and preferential flow in two contrasting agroecosystems in Central America. Agric. Ecosyst. Environ. 183, 185-196. https://doi.org/10.1016/j.agee.2013.10.027

Blackshaw, J., Blackshaw, A., 1994. Heat stress in cattle and the effect of shade on production and behaviour: a review. Aust. J. Exp. Agric. 34, 285-295. https://doi.org/10.1071/EA9940285

Böhm, C., Kanzler, M., Freese, D., 2014. Wind speed reductions as influenced by woody hedgerows grown for biomass in short rotation alley cropping systems in Germany. Agrofor. Syst. 88, 579-591. https://doi.org/10.1007/s10457-014-9700-y

Bonhomme, R., 2000. Bases and limits to using “degree.day” units. Eur. J. Agron. 13, 1-10. https://doi.org/10.1016/S1161-0301(00)00058-7

Boote, K.J., Jones, J.W., Hoogenboom, G., Pickering, N.B., 1998. The CROPGRO model for grain legumes, in: Tsuji, G.Y., Hoogenboom, G., Thornton, P.K. (Eds.), Understanding Options for Agricultural Production. Kluwer, Dordrecht, pp. 99-128.

Bosi, C., Pezzopane, J.R.M., Sentelhas, P.C., Santos, P.M., Nicodemo, M.L.F., 2014. Productivity and biometric characteristics of signal grass in a silvopastural system. Pesqui. Agropecu. Bras. 49, 449-456. https://doi.org/10.1590/S0100-204X2014000600006

Boyer, J.S., 1971. Nonstomatal inhibition of photosynthesis in sunflower at low leaf water potentials and high light intensities. Plant. Physiol. 48, 532-536.

Carvalho, M.M., Paciullo, D.S.C., Castro, C.R.T., Wendling, I.J., Resende, A.S., Pires, M. de F. de A., 2007. Experiências com SSP’s no bioma Mata Atlântica na Região Sudeste, in: Fernandes, E.N., Paciullo, D.S., Castro, C.R.T., Muller, M.D., Arcuri, P.B., Carneiro, J. da C. (Eds.), Sistemas agrossilvipastoris na América do Sul: desafios e potencialidades. Embrapa Gado de Leite, Juiz de Fora, pp. 105-136.

Coltri, P.P., Viovy, N., Chang, J., Araújo, L.C., Barioni, L.G., Santos, P.M., Pezzopane, J.R.M., 2014. Evaluating the new Orchidee-GM (Grassland Management) model to tropical area in Brazil, in: Livestock, climate change and food security conference, Conference Abstract Book, INRA, Paris, pp.96.

Cook, B.G., Pengelly, B.C., Brown, S.D., Donnelly, J.L., Eagles, D.A., Franco, M.A., Hanson, J., Mullen, B.F., Partridge, I.J., Peters, M., Schultze-Kraft, R., 2004. Tropical Forages: an interactive selection tool. CSIRO-CIAT-ILRI, Brisbane.

Douglas-Mankin, K.R., Srinivasan, R., Arnold, J.G., 2010. Soil and Water Assessment Tool (SWAT) model: current developments and applications. Trans. ASABE, 53, 1423-1431. https://doi.org/10.13031/2013.34915

Elevitch, C.R., Kim, M.W., 2001. The overstory book: cultivating connections with trees. Permanent Agriculture Resources, Holualoa.

Engel, V.L., 1999. Sistemas Agroflorestais: conceitos e aplicações, in: Engel, V.L. (Ed.), Introdução aos Sistemas Agroflorestais. FEPAF, Botucatu.

Feldhake, C.M., 2009. Forage evapotranspiration and photosynthetically active radiation interception in proximity to deciduous trees. Agric. Water Manag. 96, 1170-1174. https://doi.org/10.1016/j.agwat.2009.02.011

Filius, A.M., 1982. Economic aspects of agroforestry. Agrofor. Syst. 1, 29-39.

Fitzpatrick, E.A, Nix, H.A., 1973. The Climatic Factor in Australian Grassland Ecology, in: Moore, R.M. (Ed.), Australian Grasslands. Australian National University Press, Canberra, pp. 3-36.

Garcia, A.R., Matos, L.B., Lourenco Junior, J.B., Nahum, B.S., Costa, N.A., 2010. Increased reproductive efficiency of dairy buffaloes due to silvopastoral system adoption in the Eastern Amazon. Rev. Vet. 21, 914-915.

Garcia, R., Andrade, C.M.S., 2001. Sistemas silvipastoris na região sudeste, in: Carvalho, M.M., Alvim. M.J., Carneiro, J. da C. (Eds.), Sistemas agroflorestais pecuários: opções de sustentabilidade para áreas tropicais e subtropicais. Embrapa Gado de Leite, Juiz de Fora, pp. 173-187.

Gillespie, A. R., Jose, S., Mengel, D. B., Hoover, W. L., Pope, P. E., Seifert, J.R., Biehle, D.J., Stall, T., Benjamin, T. J., 2000. Defining competition vectors in a temperate alley cropping system in the mid-western USA: 1. Production physiology. Agrofor. Syst. 48, 25-40. https://doi.org/10.1023/A:1006285205553

Gomes, L.C., Cardoso, I.M., Mendonca, E.S., Fernandes, R.B.A., Lopes, V.S., Oliveira, T.S., 2016. Trees modify the dynamics of soil CO_2 efflux in coffee agroforestry systems. Agric. For. Meteorol. 224, 30-39. https://doi.org/10.1016/j.agrformet.2016.05.001

Graves, A.R., Burgess, P.J., Palma, J., Keesman, K.J., Van Der Werf, W., Dupraz, C., Van Keulen, H., Herzog, F., Mayus, M., 2010. Implementation and calibration of the parameter-sparse Yield-SAFE model to predict production and land equivalent ratio in mixed tree and crop systems under two contrasting production situations in Europe. Ecol. Model. 221, 1744-1756. https://doi.org/10.1016/j.ecolmodel.2010.03.008

Gyenge, J.E., Fernández, M.E., Dalla Salda, G., Schlichter, T.M., 2002. Silvopastoral systems in Northwestern Patagonia II: water balance and water potential in a stand of *Pinus ponderosa* and native grassland. Agrofor. Syst. 55, 47-55. https://doi.org/10.1023/A:1020269432671

Holzworth, D.P., Huth, N.I., Devoil, P.G., Zurcher, E.J., Herrmann, N.I., Mclean, G., Chenu, K., Oosterom, E.J., Snow, V., Murphy, C., Moore, A.D., Brown, H., Whish, J.P.M., Verral, S., Fainges, J., Bell, L.W., Peake, A.S., Poulton, P.L., Hochman, Z., Thorburn, P.J., Gaydon, D.S., Dalgliesh, N.P., Rodriguez, D., Cox, H., Chapman, S., Doherty, A., Teixeira, E., Sharp, J., Cichota, R., Vogeler, I., Li, F.Y., Wang, E., Hammer, G.L., Robertson, M.J., Dimes, J.P., Whitbread, A.M., Hunt, J., Van Hees, H., Mcclelland, T., Carberry, PS., Hargreaves, J.N.G., Macleod, N., Mcdonald, C., Harsdorf, J., Wedgwood, S., Keating, B.A., 2014. APSIM - Evolution towards a new generation of agricultural systems simulation. Environ. Model. Softw. 62, 327-350.

Huth, N.I., Carberry, P.S., Poulton, P.L., Brennan, L.E., Keating, B.A., 2002. A framework for simulating agroforestry options for the low rainfall areas of Australia using APSIM. Eur. J. Agron. 18, 171-185. https://doi.org/10.1016/S1161-0301(02)00103-X

Johnson, M-V. V., Macdonald, J.D., Kiniry, J.R., Arnold, J., 2009. ALMANAC: a potential tool for simulating agroforestry yields and improving swat simulations of agroforestry watersheds. Int. Agric. Eng. J. 18, 51-58.

Karki, U., Goodman, M.S., 2015. Microclimatic differences between mature loblolly-pine silvopasture and open-pasture. Agrofor. Syst. 89, 319-325. https://doi.org/10.1007/s10457-014-9768-4

King, K.F.S., 1979. Agroforestry and the utilisation of fragile ecosystems. Agrofor. Syst. 2, 161-168.

Kiniry, J.R., Burson, B.L., Evers, G.W., Williams, J.R., Sanchez, H., Wade, C., Featherston, J.W., Greenwade, J., 2007. Coastal Bermudagrass, Bahiagrass, and native range simulation at diverse sites in Texas. Agron. J. 99, 450–461. https://doi.org/10.2134/agronj2006.0119

Lara, M.A.S., 2011. Respostas morfofisiológicas de genótipos de *Brachiaria spp.* sob duas intensidades de desfolhação e modelagem da produção de forragem em função das variações estacionais da temperatura e fotoperíodo: adaptação do modelo CROPGRO. PhD thesis– University of São Paulo, Piracicaba.

Lara, M.A.S., Pedreira, C.G.S., Boote, K.J., Pedreira, B.C., Moreno, L.S.B., Alderman, P.D., 2012. Predicting growth of *Panicum maximum*: an adaptation of the CROPGRO - perennial forage model. Agron. J. 104, 600–611. https://doi.org/ 10.2134/agronj2011.0272

Lin, B.B., 2010. The role of agroforestry in reducing water loss through soil evaporation and crop transpiration in coffee agroecosystems. Agric. For. Meteorol. 150, 510-518. https://doi.org/10.1016/j.agrformet.2009.11.010

Lundgren, B.O., Raintree, J.B., 1982. Sustained agroforestry. In: Nestel B (ed) Agricultural Research for Development: Potentials and Challenges in Asia. ISNAR, The Hague, pp. 37-49.

MAPA – Ministério da Agricultura Pecuária e Abastecimento, 2014. ABC Plan. http://www.agricultura.gov.br/desenvolvimento-sustentavel/plano-abc (acessed 06 March 2014).

Menezes, R.S.C., Salcedo, I.H., Elliott, E.T., 2002. Microclimate and nutrient dynamics in a silvopastoral system of semiarid northeastern Brazil. Agrofor. Syst. 56, 27-38. https://doi.org/10.1023/A:1021172530939

Mijail, A., Sotelo, M., Ramírez, F., Ramírez, I., López, A, Siria, I., 2005. Conservación de la biodiversidad en sistemas silvopastoriles de matiguás y río blanco, dpto. de matagalpa, Nicaragua, in: Congreso Internacional de Producción Animal Tropical, Anais del Congreso Internacional de Producción Animal Tropical. ACPA/ICA/CIMA/IIPF, Havana.

Miles, J.W., Valle, C.B., Rao, I.M., Euclides, V.P.B., 2004. Brachiariagrasses, in: Moser, L.E., Burson, B.L., Sollenberger, L.E. (Eds.), Warm-season (C4) grasses. ASA/CSSA/SSSA, Madison, pp.745-783.

Nair, P.K.R., Kumar, B.M., Nair, V.D., 2009. Agroforestry as a strategy for carbon sequestration. J. Plant Nutr. Soil Sci. 172, 10-23. https://doi.org/10.1002/jpln.200800030

Nicodemo, M.L.F., Porfírio-da-Silva, V., Thiago, L.R.L., Gontijo Neto, M.M., Laura, V.A., 2004. Sistemas Silvipastoris – Introdução de Árvores na Pecuária do Centro-Oeste Brasileiro. Embrapa Gado de Corte, Campo Grande.

Oliveira, T.K., Macedo, R.L.G., Venturin, N., Botelho, S.A., Higashikawa, E.M., Magalhaes, W.M., 2007. Solar radiation in understory of agrosilvopastoral system with eucalypt on different spacings. Cerne 13, 40-50.

Ometto, J.C., 1981. Bioclimatologia vegetal. Ceres, Piracicaba.

Parton, W.J., Scurlock, J.M.O., Ojima, D.S., Gilmanov, T.G., Scholes, R.J., Schimel, D.S., Kirchner, T., Menaut, J-C., Seastedt, T., Garcia Moya, E., Apinan Kamnalru, T., Kinyamario, J.I., 1993. Observations and modeling of biomass and soil organic matter dynamics for the grassland biome worldwide. Glob. Biogeochem. Cycles 7, 785–809.

Pattanayak, S., Mercer, D.E., 1998. Valuing soil conservation benefits of agroforestry: contour hedgerows in the Eastern Visayas, Philippines. Agric. Econ. 18, 31-46.

Pedreira, B.C., 2009. Capim Xaraés sob pastejo: respostas agronômicas e morfofisiológicas, e adaptação do modelo CROPGRO para a predição de crescimento. PhD thesis – University of São Paulo, Piracicaba.

Pedreira, B.C., Pedreira, C.G.S., Boote, K.J., Lara, M.A.S., Alderman, P.D., 2011. Adapting the CROPGRO perennial forage model to predict growth of *Brachiaria brizantha*. Field Crop. Res. 120, 370–379. https://doi.org/10.1016/j.fcr.2010.11.010

Pequeno, D.N.L., Pedreira, C.G.S., Boote, K.J., 2014. Simulating forage production of Marandu palisade grass (*Brachiaria brizantha*) with the CROPGRO-Perennial Forage model. Crop Pasture Sci. 65, 1335–1348. https://doi.org/10.1071/CP14058

Pequeno, D.N.L., Pedreira, C.G.S., Boote, K.J., Alderman, P.D., Faria, A.F.G., 2017. Species-genotypic parameters of the CROPGRO Perennial Forage Model: Implications for comparison of three tropical pasture grasses. Grass Forage Sci. (in press). https://doi.org/10.1111/gfs.12329

Pezzopane, J.R.M., Bosi, C., Nicodemo, M.L.F., Santos, P.M., Cruz, P.G., Parmejiani, R.S., 2015. Microclimate and soil moisture in a silvopastoral system in southeastern Brazil. Bragantia 74, 110-119. https://doi.org/10.1590/1678-4499.0334

Pollock, K.M., Mead, D.J., McKenzie, B.A., 2009. Soil moisture and water use by pastures and silvopastures in a sub-humid temperate climate in New Zealand. Agrofor. Syst. 75, 223-238. https://doi.org/10.1007/s10457-008-9172-z.

Prasad, J.V.N.S., Korwar, G.R., Rao, K.V. et al., 2010. Tree row spacing affected agronomic and economic performance of Eucalyptus-based agroforestry in Andhra Pradesh, Southern India. Agrofor. Syst. 78, 253-267. https://doi.org/10.1007/s10457-009-9275-1

Qi, X., Mize, C.W., Batchelor, W.D., Takle, E.S., Litvina, I.V., 2001. SBELTS: a model of soybean production under tree shelter. Agrofor. Syst. 52, 53-61. https://doi.org/10.1023/A:1010647118256

Rymph, S.J., 2004. Modeling growth and composition of perennial tropical forage grass. PhD thesis–University of Florida, Gainesville.

Rymph, S.J., Boote, K.J., Irmak, A., Mislevy, P., Evers, G.W., 2004. Adapting the CROPGRO model to predict growth and composition of tropical grasses: developing physiological parameters. Soil Crop Sci. Soc. Fla. Proc. 63, 37–51.

Sahin, H., Anderson, S.H., Udawatta, R.P., 2016. Water infiltration and soil water content in claypan soils influenced by agroforestry and grass buffers compared to row crop management. Agrofor. Syst. 90, 839-860. https://doi.org/10.1007/s10457-016-9899-x

Santos, D.C., 2016. Características do capim-piatã e desempenho de bovinos em sistemas silvipastoris no cerrado brasileiro. PhD thesis - Federal University of Goiás, Goiânia.

Santos, P.M., Cruz, P.G., Araújo, L.C., Pezzopane, J.R.M., Valle, C.B., Pezzopane, C.G., 2013. Response mechanisms of *Brachiaria brizantha* cultivars to water deficit stress. Rev. Bras. Zootec. 42, 767-773. https://doi.org/10.1590/S1516-35982013001100001

Schroeder, P., 1994. Carbon storage benefits of agroforestry systems. Agrofor. Syst. 27, 89-97.

Siles, P., Harmand, J-M., Vaast, P., 2010. Effects of Inga densiflora on the microclimate of coffee (*Coffea arabica* L.) and overall biomass under optimal growing conditions in Costa Rica. Agrofor. Syst. 78, 269-286. https://doi.org/10.1007/s10457-009-9241-y

Silva, V. P. da., 2012. Produtividade em sistema de integração lavoura-pecuária -floresta no subtrópico brasileiro. PhD thesis-Federal University of Paraná, Curitiba.

Steinfeld, H., Gerber, P., Wassenaar, T., Castel, V., Rosales, M., de Haan, C., 2006. Livestock’s long shadow: environmental issues and options. FAO, Rome.

Tamang, B., Andreu, M.G., Rockwood, D.L., 2010. Microclimate patterns on the leeside of single-row tree windbreaks during different weather conditions in Florida farms: implications for improved crop production. Agrofor. Syst. 79, 111-122. https://doi.org/10.1007/s10457-010-9280-4

Valle, C.B., Euclides, V.P.B., Macedo, M.C.M., 2000. Características das plantas forrageiras do gênero Brachiaria, in: Simpósio Sobre Manejo de Pastagem, Anais Simpósio Sobre Manejo de Pastagem. FEALQ, Piracicaba, pp. 21-64.

Valle, C.B., Macedo, M.C.M., Euclides, V.P.B., Jank, L., Resende, R.M.S., 2010. Gênero Brachiaria, in: Fonseca, D.M., Martuscello, J.A. (Eds.), Plantas forrageiras. UFV, Viçosa, pp. 537.

Van Der Werf, W., Keesman, K., Burgess, P.J., Graves, A.R., Pilbeam, D., Incoll, L.D., Metselaar, K., Mayus, M., Stappers, R., Van Keulen, H., Palma, J., Dupraz, C., 2007. Yield-SAFE: a parameter-sparse process-based dynamic model for predicting resource capture, growth and production in agroforestry systems. Ecol. Eng. 29, 419-433. https://doi.org/10.1016/j.ecoleng.2006.09.017

Vieira, D.L.M., Holl, K.D., Peneireiro, F.M., 2009. Agro-Successional Restoration as a Strategy to Facilitate Tropical Forest Recovery. Restor. Ecol. 17, 451-459. https://doi.org/10.1111/j.1526-100X.2009.00570.x

Villa Nova, N.A., Carretero, M.V., Scadua, R., 1983. Um modelo de avaliação do crescimento de cana-de-açúcar (Saccharum spp.) em termos da ação combinada do fotoperíodo e da temperatura média do ar, in: Congresso Brasileiro de Agrometeorologia, Anais do Congresso Brasileiro de Agrometeorologia, Sociedade Brasileira de Agrometeorologia, Campinas, pp.31-48.

Zamora, D.S., Jose, S., Jones, J.W., Cropper Junior, W.P., 2009. Modeling cotton production response to shading in a pecan alleycropping system using CROPGRO. Agrofor. Syst. 76, 423-435. https://doi.org/10.1007/s10457-008-9166-x

Zhu, X.-G., Long, S.P., Ort, D.R., 2008. What is the maximum efficiency with which photosynthesis can convert solar energy into biomass? Curr. Opin. Biotechnol. 19, 153-159. https://doi.org/10.1016/j.copbio.2008.02.004

Zuidema, P.A., Leffelaar, P.A., Gerritsma, W., Mommer, L., Anten, N.P.R., 2005. A physiological production model for cocoa (Theobroma cacao): model presentation, validation and application. Agric. Syst. 84, 195-225. https://doi.org/10.1016/j.agsy.2004.06.015

2. MICROCLIMATE ALTERATIONS IN A SILVOPASTORAL SYSTEM WITH EUCALYPTUS AND ITS POTENTIAL FOR MITIGATING CLIMATE CHANGE EFFECTS

ABSTRACT

The aim of this study was to assess the microclimate in an open pasture and in a silvopastoral system with rows of eucalyptus trees, oriented East-West, and the capacity of this system to mitigate climate change effects on agricultural systems. The experiment was composed by an open pasture of Piatã Palisadegrass and by an adjacent pasture with Eucalyptus rows. The trees were arranged in simple rows, in a near East-West orientation. The treatments considered the measurements at 0.00, 3.75, 7.50 and 11.25 m from the trees of the North row, and under full sun condition. Weather stations were installed in the open pasture and in the silvopastoral system for measuring micrometeorological conditions. The results demonstrated that the silvopastoral system caused higher shading in the inter-row, when solar declination was high; and higher shading close to trees, when solar declination was around -22º. Net radiation was strongly influenced by solar radiation incidence. Soil heat flux and soil temperature, were determined by solar radiation, wind speed and by the effect of tree canopy reducing radiation losses. Wind speed was always lower in the silvopastoral system, due to the windbreak effect of the Eucalyptus. Air temperature and relative humidity were not different among treatments. Analyzing the potential of this system to attenuate the climate change impacts, the protection from solar radiation may be important for locations where cloudiness will be decreased, resulting in reductions of net radiation, wind speed and, consequently, evapotranspiration, making the crop water balance less restrictive to plants growth.

Keywords: Agroforestry; Shading; Photosynthetically active radiation; Net radiation; Soil heat flux; Windbreak

2.1. Introduction

Agroforestry systems (AFS) are forms of land use where timber or fruit trees are combined with crops and/or livestock, simultaneously or in a sequence of time, aiming to improve ecological interactions and economic returns (Lundgren and Raintree 1982). Therefore silvopastoral systems are a kind of AFS in which trees or shrubs are combined with animals and pastures (Nair 1993).

One of the main aims of an AFS is to optimize the land use (Alao and Shuaibu 2013), combining forest and food productions (King 1979), improving the soil conservation (Pattanayak and Mercer 1998), reducing the need of new lands for agriculture (Schroeder 1994) and requiring less external inputs (Filius 1982). In this way, areas that have no economic and social importance can be recovered and rationally used through agroforestry practices (Vieira et al. 2009). However, AFS cause microclimatic changes (Monteith et al. 1991), which is mainly positive, but sometimes negative, if not properly planned.

Microclimate in AFS depends on the system design, arrangement, orientation, age, employed species and their architecture, among others, which interact with macro and meso scales. The main alterations in an AFS are caused by the shade promoted by the trees, which reduces solar radiation for the crops below the canopy (Pezzopane et al. 2015). The lower solar radiation affects microclimatic variables as air and soil temperatures, relative air humidity (RH), soil moisture (Pezzopane et al. 2015), evapotranspiration (Lin 2010), what results in changes on crop growth (Bosi et al. 2014). Additionally, the trees also reduce wind speed, depending on their arrangement, which affects other microclimate variables (Pezzopane et al. 2015).

According to Gomes et al. (2016), AFS can promote microclimate stability for the low layer species, reducing soil water losses and avoiding increase of air and soil temperatures, which was also observed by Amadi et al. (2016), in Saskatchewan, Canada, studying shelterbelts. Considering the capacity of AFS to promote microclimate changes, it can be an important strategy to adapt agricultural systems to climate changes (Montagnini et al. 2012), increasing the resilience of the agroecosystems and mitigating the risks associated to climate variability and change (Nguyen et al. 2013). In this context, the aim of this study was to assess the microclimate in an open pasture and in a silvopastoral system with rows of Eucalyptus trees, in the east-west orientation, and according to that to evaluate the capacity of this system to mitigate climate change effects on agricultural systems.

2.2. Material and methods

2.2.1. Experimental site

The experiment was carried out in São Carlos, state of São Paulo, Brazil (lat 22°01’ S, long 47°53’ W, alt 860 m), from August 2013 to June 2016. The climate of this location is Cwa (Köppen) with a cool and dry season, from April to September (average air temperature of 19.9ºC and total rainfall of 250 mm), and another warm and wet, from October to March (average air temperature of 23.0ºC and total rainfall of 1100mm) (Alvares et al. 2013). The trial was composed by an open pasture of *Urochloa* (syn. *Brachiaria*) *brizantha* (Hochst ex A. Rich.) Stapf cv. BRS Piatã, which was the full sun system, and by an adjacent pasture, of the same cultivar, with rows of *Eucalyptus urograndis* (*Eucalyptus grandis x Eucalyptus* *urophylla*) of the GG100 clonal, which was the silvopastoral system. The experimental area totaled 12 ha, being 6 ha in each system. The trees were planted in April 2011 and arranged in simple rows, in a near East-West orientation, with 15 m between rows and 2 m between plants in the rows, totaling 333 trees ha^{-1}.

The full sun pasture was considered a treatment (FS) and in the silvopastoral system other four treatments were established. The silvopastoral treatments were settle considering the distance from the North row, which was responsible for causing shading in the assessed area in the most of the year, due to solar declination. These treatments were: 0.00 m (SP1); 3.75 m (SP2); 7.50 m (SP3) and 11.25 m (SP4) from the North row (Figure 1).

2.2.2. Weather measurements

Three weather stations were installed, being one in the open pasture and two in the silvopastoral system, to measure photosynthetically active radiation (PAR), net radiation, soil heat flux, wind speed, air and soil temperature, and relative air humidity, continuously, in each treatment (Figure 1). PAR was measured in all positions, but the other variables were measured only at FS, SP1 and SP3. To measure these variables the following sensors were used: linear quantum sensor (Apogee, Logan, UT, USA), net radiometer (NR-Lite2, Kipp & Zonen, Delft, Netherlands), heat flux plate (HFP01, Hukseflux, Delft, Netherlands), ultrasonic anemometer (Windsonic, Gill, Lymington, Hampshire, UK), thermo-hygrometer (HC2-S3, Rotronic, Bassersdorf, Swiss) and soil temperature probe (thermistor 107, Campbell Scientific, Logan, UT, USA). These sensors were connected to a datalloger (CR3000, Campbell Scientific, Logan, UT, USA), configured to take measurements every 5 seconds and to record averages every 15 minutes and hour. Daily average, maximum and minimum (air temperature, relative air humidity and soil temperature), average and maximum (wind speed) and total values (PAR, net radiation and soil heat flux) were also recorded. The sensors were installed at 1.7 m height, except for linear quantum sensors, which were installed at 0.6 m above the ground, and the heat flux plates and soil temperature probes, which were deployed 0.05 m depth in the soil. PAR was measured in the whole experimental period (August 2013 to June 2016), whereas wind speed, air temperature, relative humidity and soil temperature were measured from June 2014 to June 2016, and net radiation and soil heat flux from December 2014 to June 2016 (Figure 2).

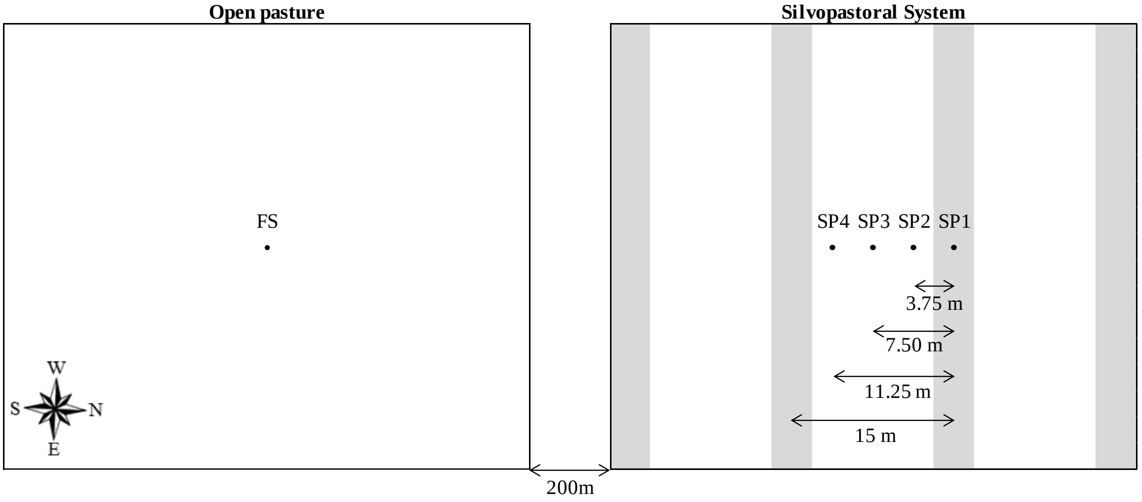

Figure 1. Schematic representation of the experimental area indicating where the data were collected in the open pasture (left) and in the silvopastoral system (right). FS: full sun, SP1: 0.00 m, SP2: 3.75 m, SP3: 7.50 m, SP4: 11.25 m from North row. Grey strips illustrate the tree rows.

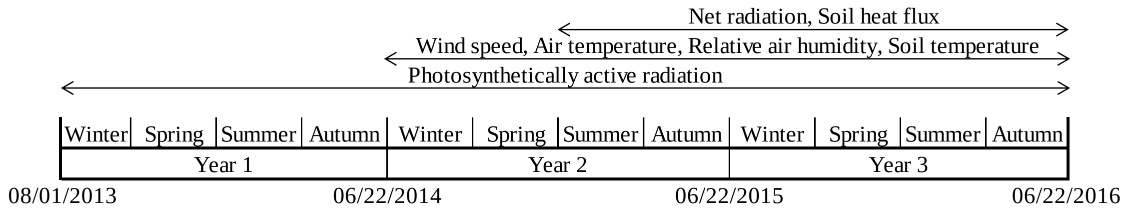

Figure 2. Weather measurements during the three years of experiments.

PAR transmission (PARt) was calculated through the ratio of PAR measured in each position of the silvopastoral system and at full sun condition. The potential of the silvopastoral system to mitigate climate change effects was considered as the reductions on PAR, net radiation, wind speed, air temperature and relative humidity, by comparing SP1 and SP3 with full sun condition, for each season of the year.

2.2.3. Statistical analysis

The experimental design was a completely randomized with repeated measures in time. The data were analyzed using the MIXED procedure of SAS (Littel et al. 2006). For the analysis of average and maximum wind speed; average, maximum and minimum air temperature, relative humidity and soil temperature; the repeated factors were years (2 and 3) and seasons of the year, being the comparison between seasons only within each experimental year, and each day of a season was considered as a replication (92 replications by season). For net radiation and soil heat flux, the analysis followed the same procedure used for the other variables, but the repeated factors were the seasons, comparing only the last six seasons (summer and autumn of the year 2 and all seasons of year 3). PAR and PARt were analyzed by a similar process, using data from the three years and considering each ten-day period as a replication (nine replications per season), which reduced the data variation by improving the normal distribution of the dataset. For comparison of means, the Tukey test was used with $p \geq 0.05$.

2.3. Results

2.3.1. Solar Radiation dynamics

During the winter and autumn, PAR at the full sun (FS) was higher than in the silvopastoral system (SP positions), except in the winter of year 1, when FS and SP4 were similar (Table 1). In these seasons of year, generally, the PAR at all SP positions was not different ($p<0.05$).

In the spring, PAR incidence was normally higher at FS than at the SP positions, except in the spring of year 1, when only SP1 received less PAR (difference of 7.24 MJ m^{-2} day^{-1}). In the summer, PAR at FS was higher to all the SP positions only in the third year, being different only to SP1 in the first two years. On average, PAR reduction at SP1 and SP3 was respectively 5.29 and 3.48 MJ m^{-2} day^{-1} (Table 2).

When PAR values of the seasons of the year were compared, within each distance, it was observed that at the SP1 the values were always similar and comprised between 1.60 and 3.86 MJ m^{-2} day^{-1}, being considered low. At the other SP positions, generally, PAR values were higher in the spring and summer.

PAR transmissions (PARt) in the winter and autumn were similar at all four SP positions, except in the first winter, when SP4 had higher PARt (86.6%) than SP2 (22.1%) (Figure 3 and Table 3). During the spring and summer, PARt was lower at SP1 than at the other positions, with few exceptions.

The PAR hourly dynamics was different between the three years. In the first year, PAR incidence was higher at FS, SP3 and SP4 than at SP1 and SP2, showing that the trees caused more shading in these two positions (Figure 4). In the subsequent years, PAR decreased at SP3 and SP4, which demonstrated shadow at these positions.

Table 1. Photosynthetically active radiation (PAR) incidence at the full sun (FS) and at the four positions within the silvopastoral system (SP1: 0.00 m, SP2: 3.75 m, SP3: 7.50 m and SP4: 11.25 m from the North row), in each season of the three experimental years.

Year	Position	PAR MJ m^{-2} day^{-1}				
		Winter	Spring	Summer	Autumn	Average
1	FS	8.08 Aab*	8.84 Aab	10.25 Aa	6.76 Ab	8.53
	SP1	3.86 BCa	1.60 Ba	1.97 Ba	2.90 Ba	2.43
	SP2	1.54 Cb	7.01 Aa	7.18 Aa	1.90 Bb	4.74
	SP3	5.16 BCab	7.39 Aa	8.38 Aa	2.16 Bb	5.86
	SP4	7.22 ABa	6.59 Aa	7.50 Aa	3.17 Bb	6.02
	Average	5.17	6.28	7.06	3.38	
2	FS	7.03 Aa	8.76 Aa	8.77 Aa	6.10 Aa	7.66
	SP1	3.55 Ba	3.03 Ca	2.46 Ba	1.99 Ba	2.78
	SP2	2.07 Bbc	5.07 BCab	5.32 ABa	1.67 Bc	3.58
	SP3	1.72 Bb	6.04 Ba	6.33 Aa	1.67 Bb	3.93
	SP4	3.06 Bbc	5.81 Ba	5.30 ABab	2.10 Bc	4.06
	Average	3.49	5.74	5.64	2.70	
3	FS	6.24 Aa	8.18 Aa	8.51 Aa	6.50 Aa	7.36
	SP1	2.16 Ba	2.86 Ba	2.27 Ba	1.93 Ba	2.31
	SP2	2.11 Ba	4.15 Ba	4.06 Ba	1.81 Ba	3.05
	SP3	1.86 Bb	5.12 Ba	4.70 Bab	1.75 Bb	3.40
	SP4	1.93 Bb	4.61 Ba	3.97 Bab	1.75 Bb	3.10
	Average	2.86	4.98	4.70	2.75	

*Means followed by the same upper case letter are not different in column, and those followed by the same lower case letter are not different in line ($P<0.05$).

Net radiation (Rn) was higher at FS than at the SP positions, except in the summer of year 2 when it was similar between FS and SP3 (11.32 and 10.13 MJ m^{-2} day^{-1}, respectively) (Table 4). In the comparison between SP1 and SP3, Rn was sometimes similar and sometimes higher in SP3. Rn average reduction was 5.17 and 3.08 MJ m^{-2} day^{-1}, respectively for SP1 and SP3, with the highest reductions occurring in the spring and summer for SP1 and in the winter and autumn for SP3 (Table 2).

Soil heat flux (SHF) was not always higher at FS, being sometimes similar to both the SP points and other times to only one of them (Table 4). Analyzing the average hourly Rn and SHF variations, in the night time period, the highest radiation and heat losses were observed at FS (Figure 5). In the day-time period, Rn and SHF presented the highest values at FS, intermediate at SP3 and lowest at SP1.

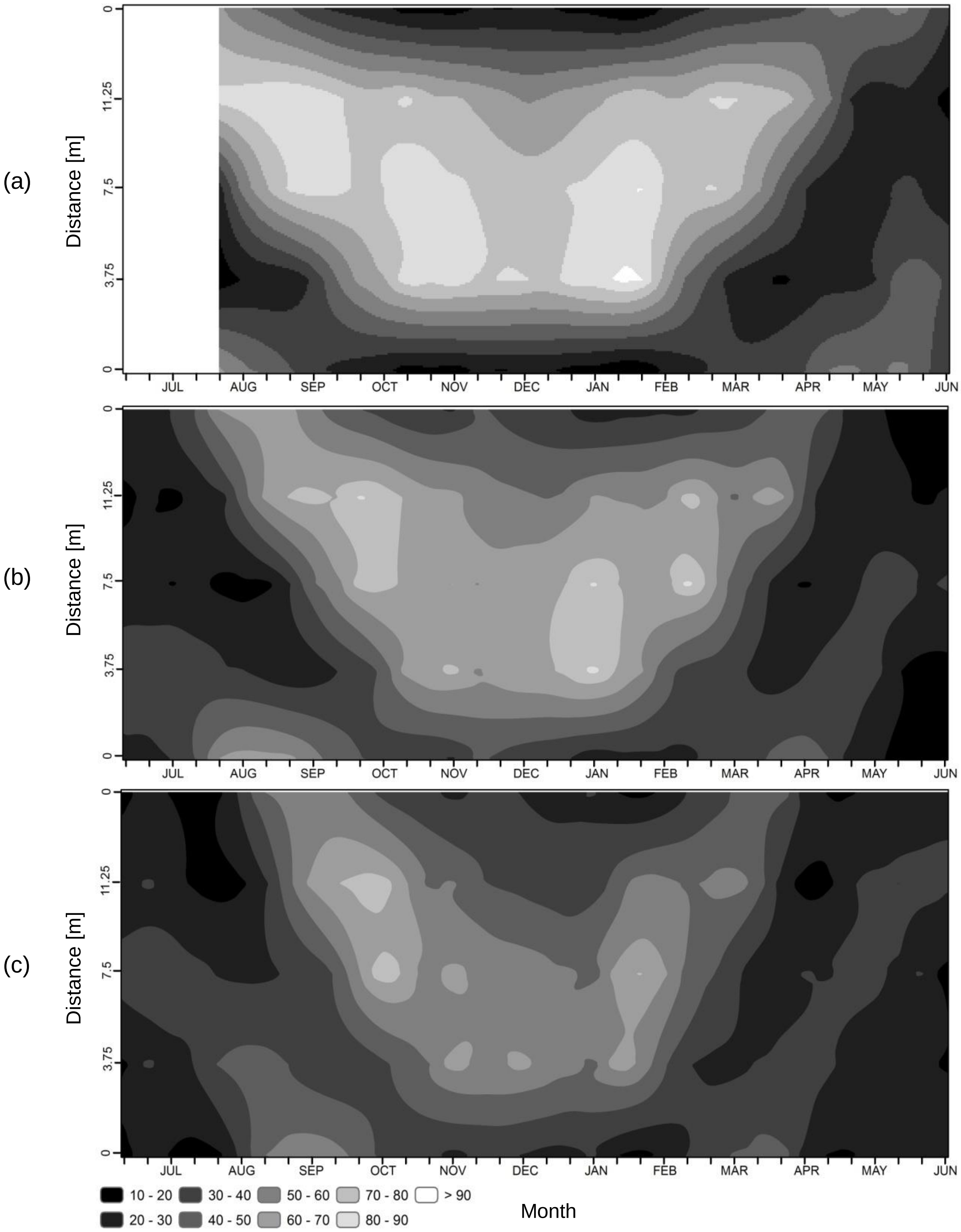

Figure 3. Spatial and temporal photosynthetically active radiation transmission (PARt) in the inter-row of a silvopastoral system, every ten-day period during three experimental years, from July to June. (a) year 1 (starting from August 2013), (b) year 2, and (c) year 3. Interpolation made by the Natural Neighbor method.

2.3.2. General microclimatic conditions

Average wind speed (WSavg) was higher at FS than at the SP positions, achieving a difference of 1.2 m s^{-1} between SP1 and FS (Table 5). The SP positions had always similar WSavg between them. Similar pattern was observed for maximum wind speed (WSmax), with reductions of up to 3.85 m s^{-1} at SP positions. The hourly wind speed dynamics demonstrated that the wind speed was higher at FS than at SP positions, all day long, with the highest difference in the morning (Figure 6a, 6b). On average, there was a substantial reduction of wind speed in all seasons, mainly for WSmax, which reached average reduction of 3.28 m s^{-1}, when comparing the silvopastoral system to the full sun condition (Table 2).

When weather differences between seasons were compared for each distance, at FS there was higher WSavg in the spring, generally, but at the SP positions, WSavg was more similar between seasons. WSmax was higher in the spring, decreasing gradually from the winter to autumn, at all positions (Table 5).

Average, maximum and minimum values of air temperature and relative humidity were not different ($p<0.05$) at the three assessed positions, for all seasons of the year, except for minimum relative humidity in the summer of year 3, when it was wetter at SP1 than at FS (64.8 and 54.9%, respectively) (Table 5). The hourly air temperature and relative humidity variations were similar between positions.

Table 2. Mean reductions of photosynthetically active radiation (PAR), net radiation (Rn), average wind speed (WSavg), maximum wind speed (WSmax), average air temperature (Tavg) and average relative air humidity (RHavg), every season of year, at 0.00 m (SP1) and 7.50 m (SP3) from the North row, in a silvopastoral system.

Variable	Position	Season of year				
		Winter	Spring	Summer	Autumn	Average
PAR (MJ m^{-2} day^{-1})	SP1	3.93	6.09	6.95	4.18	5.29
	SP3	4.21	2.41	2.71	4.59	3.48
Rn (MJ m^{-2} day^{-1})	SP1	2.87	6.67	7.90	3.25	5.17
	SP3	4.04	1.92	1.95	4.4	3.08
WSavg (m s^{-1})	SP1	0.91	1.01	0.80	0.64	0.84
	SP3	0.93	1.00	0.81	0.66	0.85
WSmax (m s^{-1})	SP1	3.30	3.59	3.50	2.84	3.30
	SP3	3.28	3.48	3.35	2.98	3.26
Tavg (°C)	SP1	0.03	-0.09	0.17	0.13	0.03
	SP3	0.10	-0.22	-0.04	0.29	0.02
RHavg (%)	SP1	-0.46	-0.12	-2.23	0.41	-0.50
	SP3	-0.84	0.00	-1.79	0.74	-0.36

Table 3. Photosynthetically active radiation (PAR) transmission at the four positions within the silvopastoral system (SP1: 0.00 m, SP2: 3.75 m, SP3: 7.50 m and SP4: 11.25 m from the North row), in each season of the three experimental years.

Year	Position	PAR transmission %				
		Winter	Spring	Summer	Autumn	Average
1	SP1	47.1 ABa*	20.5 Bb	20.3 Bb	43.8 Aa	31.3
	SP2	22.1 Bb	75.8 Aa	68.3 Aa	30.6 Ab	52.4
	SP3	62.2 ABab	80.3 Aa	80.4 Aa	32.3 Ab	64.2
	SP4	86.6 Aa	71.8 Aa	72.1 Aa	44.4 Ab	66.9
	Average	54.5	62.1	60.3	37.8	
2	SP1	48.1 Aa	35.9 Ba	29.4 Ba	30.2 Aa	36.0
	SP2	31.3 Aab	56.4 Aa	56.6 Aa	27.1 Ab	43.3
	SP3	25.0 Ab	66.5 Aa	67.7 Aa	28.8 Ab	47.0
	SP4	41.0 Aab	64.1 Aa	58.3 Aa	32.8 Ab	49.0
	Average	36.3	55.7	53.0	29.7	
3	SP1	32.7 Aa	35.3 Ba	27.7 Ba	28.8 Aa	31.2
	SP2	34.0 Aab	49.6 Aa	45.1 ABab	27.4 Ab	39.2
	SP3	31.5 Ab	60.1 Aa	52.2 Aab	27.5 Ab	43.3
	SP4	30.1 Aab	54.6 Aa	45.3 ABab	27.8 Ab	39.8
	Average	32.1	49.9	42.6	27.9	

*Means followed by the same upper case letter are not different in column, and those followed by the same lower case letter are not different in line ($P<0.05$).

Average (TSavg), maximum (TSmax) and minimum (TSmin) soil temperature were not always higher at FS, being sometimes similar to one or to both the SP points, and hardly ever lower than one of the SP points. Average hourly soil temperature variation, in general, showed greater differences in the diurnal period, with higher values always at FS (Figure 6c, 6d).

2.4. Discussion

2.4.1 Factors that determined microclimate

The eucalyptus trees arrangement in rows promoted a shadow range projection in the silvopastoral area, parallel to the tree rows. The east-west orientation of the tree rows resulted in little shadow movement throughout the day, which caused shadow projection on the same distance from the tree rows in great part of the day. On the other hand, this orientation promoted shadow variation throughout the year, due to the changes in solar declination, projecting shadow with different distances from the North row according to the period of the year (Figure 3, Table 1 and Table 2).

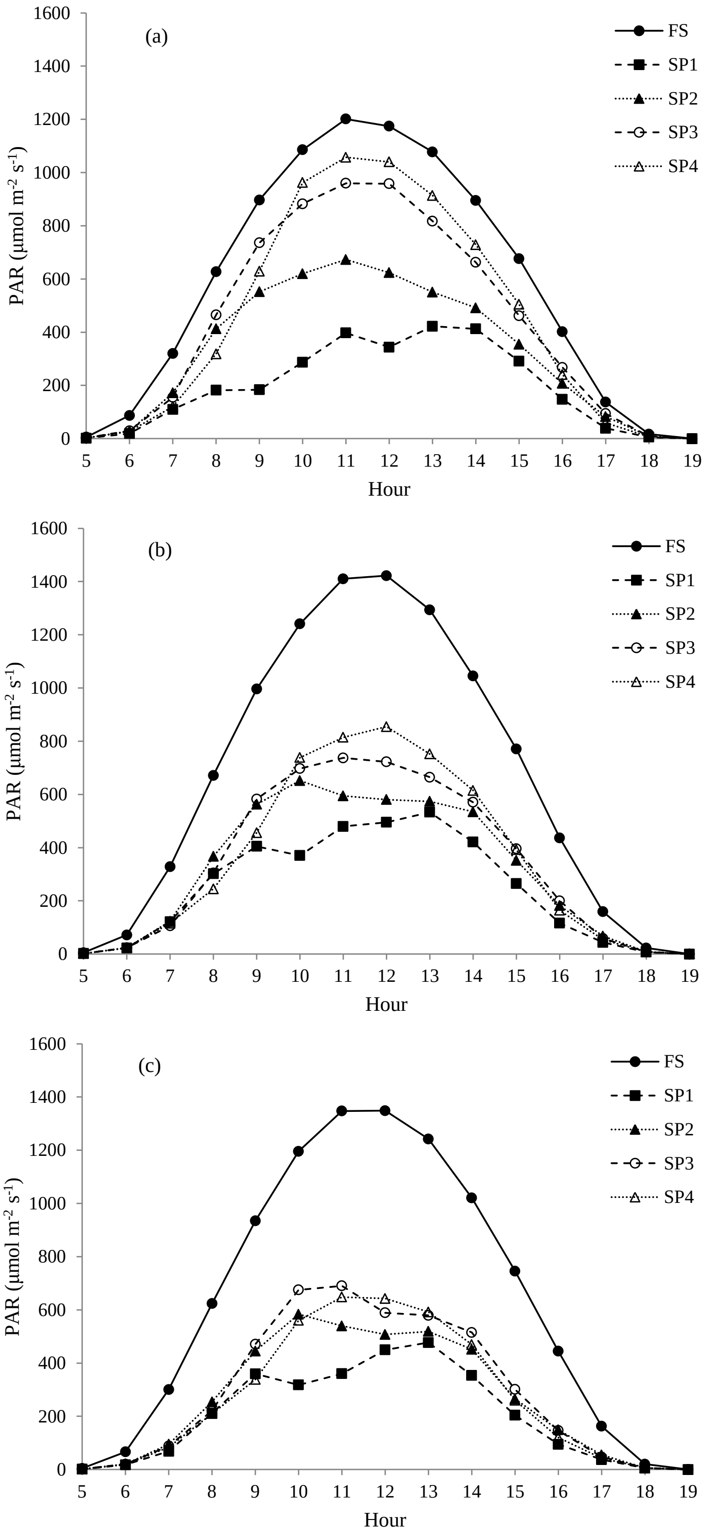

Figure 4. Average hourly photosinthetically active radiation at full sun (FS) and at the four positions within a silvopastoral system (SP1: 0.00 m, SP2: 3.75 m, SP3: 7.50 m and SP4: 11.25 m from the North row), in three experimental years. a: year 1, b: year 2, c: year 3.

Table 4. Net radiation and soil heat flux, at full sun (FS) and at two positions within a silvopastoral system (SP1: 0.00 m and SP3: 7.50 m from the North row), in six seasons of the year.

Position	Season of the year/Year						
	Summer/2	Autumn/2	Winter/3	Spring/3	Summer/3	Autumn/3	Average
	Net Radiation MJ m^{-2} day^{-1}						
FS	11.32 Aa*	6.25 Ab	5.43 Ab	10.43 Aa	10.60 Aa	6.03 Ab	8.34
SP1	2.85 Ba	3.00 Ba	2.56 Ba	3.76 Ca	3.27 Ca	2.79 Ba	3.04
SP3	10.13 Aa	1.74 Bc	1.39 Bc	8.51 Bab	7.90 Bb	1.74 Bc	5.27
Average	8.10	3.66	3.13	7.57	7.26	3.52	
	Soil Heat Flux MJ m^{-2} day^{-1}						
FS	-0.01 Aa	-0.11 Aab	0.13 Aa	0.02 ABa	-0.24 Abc	-0.42 Ac	-0.11
SP1	-0.13 ABa	-0.37 Bc	-0.15 Bab	-0.07 Ba	-0.12 Aa	-0.34 Abc	-0.19
SP3	-0.28 Bc	-0.27 ABc	-0.08 Bb	0.20 Aa	-0.07 Ab	-0.35 Ac	-0.14
Average	-0.14	-0.25	-0.03	0.05	-0.14	-0.37	

*Means followed by the same upper case letter are not different in column, and those followed by the same lower case letter are not different in line ($P<0.05$).

In the winter and autumn, PAR and PARt were not different among the SP positions, because the solar declination in these seasons was high (in the north direction), promoting high shade at all these positions. This pattern was not true when the trees' height was still low (around 12 m) and the solar declination was not enough to project significant shadow at SP4 (Table 1 and Table 3). The low tree height in the first year also allowed, in the spring and summer, significant shadow only at SP1, but according the trees were growing, the shadow increased significantly, mainly in the third year, with the trees' height around 25 m. This PAR dynamics, caused by tree growing, may be observed in the hourly dynamics of each experimental year (Figure 4).

Prasad et al. (2010) found PARt of 40% at 0.5 m from eucalyptus rows, spaced with 11 m, when the trees were four years old. Oliveira et al. (2007), also in a eucalyptus rows based system, spaced with 15 m and 4.5 years old, confirm that PAR was higher in the inter-rows than below trees canopies, achieving a difference of 762 μmol m^{-2} s^{-1}. Siles et al. (2010), in Costa Rica, assessed microclimate in a coffee based agroforestry system, shaded by *Inga densiflora*, and observed PARt of about 40% in the dry season and 25% during the wet season.

Net radiation (Rn) was highly influenced by solar radiation incidence, so tree height and solar declination were very important to define it. In the winter and autumn, Rn was higher at FS due to the high solar declination and lower solar radiation incidence in the silvopastoral system. In the spring and summer, the differences were based on the strong shading on SP1 and little on SP3.

Soil heat flux (SHF) was affected by solar radiation incidence, wind speed and by the effect of the trees canopies on radiation losses, reflecting and reemitting long wave radiation to the soil. Depending on the position and season of year, each one of these factors assumed more or less importance, being solar radiation incidence the most determinant factor.

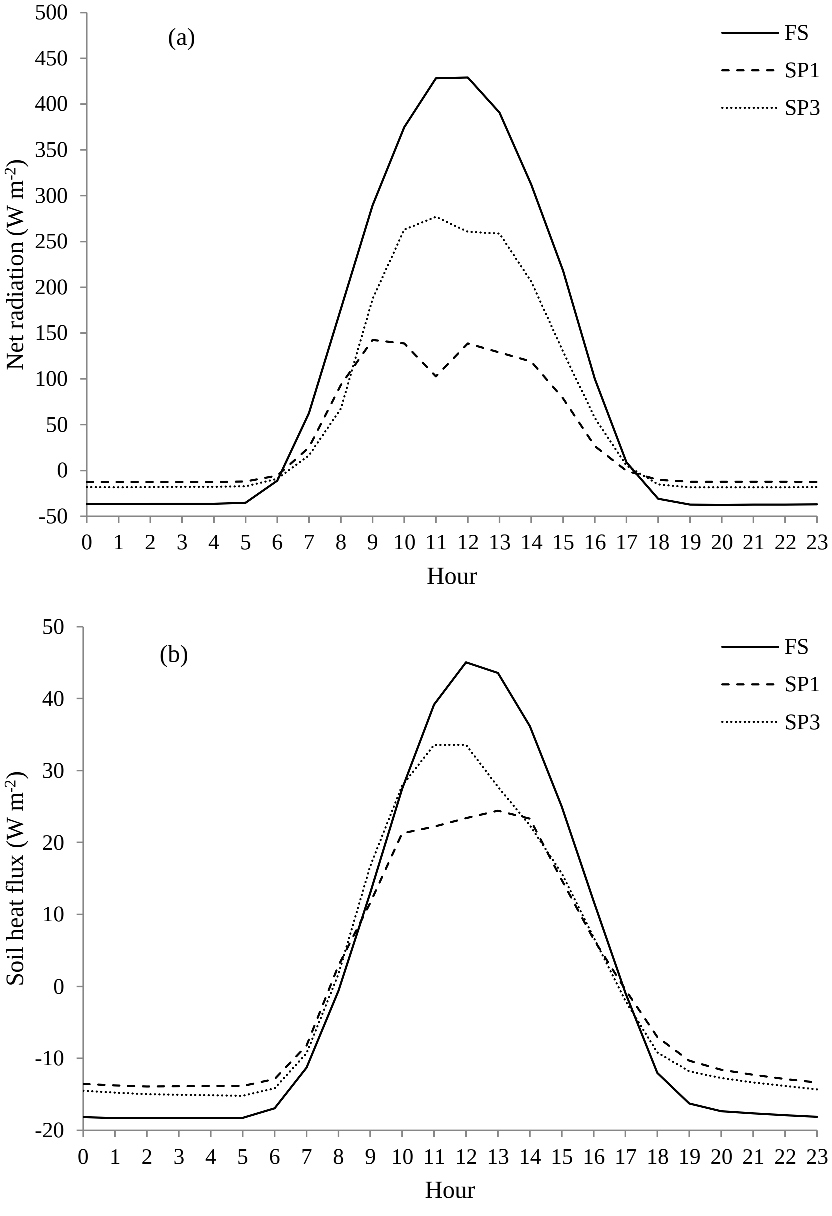

Figure 5. Average hourly net radiation (a) and soil heat flux (b) at full sun (FS) and at two different positions within a silvopastoral system (SP1: 0.00 m and SP3: 7.50 m from the North row).

Table 5. Mean average (WSavg) and maximum (WSmax) wind speed; average (Tavg), maximum (Tmax) and minimum (Tmin) air temperature; average (RHavg), maximum (RHmax) and minimum (RHmin) relative humidity; and average (TSavg), maximum (TSmax) and minimum (TSmin) soil temperature at full sun (FS) and at two positions within a silvopastoral system (SP1: 0.00 m and SP3: 7.50 m from the North row), in each season of the year of two experimental years.

Year	Season of year	Position	Variable										
			WSavg m s^{-1}	WSmax m s^{-1}	Tavg ºC	Tmax ºC	Tmin ºC	RHavg %	RHmax %	RHmin %	TSavg ºC	TSmax ºC	TSmin ºC
2	Winter	FS	2.24 Aab*	8.03 Ab	19.9 Ab	26.8 Ab	14.3 Ad	56.6 Ac	78.8 Ac	33.7 Ac	19.9 Ac	24.9 Ac	16.7 ABd
		SP1	1.13 Ba	4.64 Bb	19.8 Ab	26.8 Ab	14.4 Ad	56.3 Ac	77.5 Ac	33.6 Ab	20.4 Ab	25.8 Aa	17.2 Ad
		SP3	1.12 Bab	4.64 Bb	19.7 Ab	26.7 Ab	14.4 Ad	57.9 Ac	79.4 Ac	34.6 Ab	17.6 Bc	20.6 Bc	15.8 Bd
	Spring	FS	2.46 Aa	8.82 Aa	22.3 Aa	29.5 Aa	17.1 Ab	68.1 Ab	88.3 Ab	41.0 Abc	24.3 Aa	29.6 Aa	21.0 Ab
		SP1	1.22 Ba	4.97 Ba	22.4 Aa	29.6 Aa	17.4 Ab	67.1 Ab	86.3 Ab	41.2 Ab	22.6 Ba	26.7 Ba	19.9 Bb
		SP3	1.23 Ba	5.07 Ba	22.6 Aa	30.1 Aa	17.4 Ab	68.1 Ab	87.9 Ab	40.8 Ab	24.5 Aa	30.1 Aa	21.3 Ab
	Summer	FS	1.62 Ac	7.39 Ac	22.9 Aa	29.6 Aa	18.7 Aa	77.7 Aa	95.3 Aa	49.8 Aab	24.3 Aa	26.9 Ab	22.6 ABa
		SP1	0.76 Bb	3.84 Bc	22.9 Aa	28.7 Aa	19.0 Aa	79.3 Aa	94.5 Aa	53.9 Aa	23.5 Aa	26.0 Aa	21.8 Ba
		SP3	0.77 Bc	4.05 Bc	23.0 Aa	29.7 Aa	19.0 Aa	79.2 Aa	95.3 Aa	51.5 Aa	24.5 Aa	26.6 Ab	22.9 Aa
	Autumn	FS	1.69 Abc	6.49 Ad	19.9 Ab	26.0 Ab	15.6 Ac	77.8 Aa	94.5 Aab	51.7 Aa	21.0 Ab	24.0 Ac	19.1 Ac
		SP1	0.98 Bab	3.65 Bd	19.7 Ab	25.0 Ab	16.1 Ac	80.3 Aa	95.7 Aa	56.3 Aa	20.2 ABb	22.1 Bb	18.9 Ac
		SP3	0.96 Bbc	3.62 Bd	19.8 Ab	25.1 Ab	16.1 Ac	78.4 Aa	93.1 Aab	55.5 Aa	19.7 Bb	21.3 Bc	18.6 Ac
3	Winter	FS	1.93 Aa	7.52 Ab	19.7 Ab	26.1 Ab	14.7 Ab	62.9 Ac	82.1 Ac	39.6 Ab	19.2 Ab	22.9 Ab	16.8 Ad
		SP1	1.21 Ba	4.30 Bb	19.7 Ab	25.6 Ab	15.2 Ab	64.3 Ac	82.4 Ac	42.1 Ac	18.5 ABc	20.2 Bb	17.3 Ac
		SP3	1.18 Ba	4.35 Bb	19.7 Ab	25.7 Ab	15.2 Ab	63.5 Ac	81.1 Ac	41.5 Ab	18.1 Bb	19.5 Bc	17.0 Ab
	Spring	FS	1.95 Aa	8.26 Aa	23.1 Aa	30.1 Aa	18.3 Aa	73.9 Aab	93.4 Aab	46.1 Aab	23.3 ABa	25.8 Ba	21.6 Ab
		SP1	1.18 Ba	4.93 Ba	23.2 Aa	29.4 Aa	18.6 Aa	75.1 Ab	93.0 Aab	52.8 Ab	23.1 Ba	24.8 Ba	21.7 Aa
		SP3	1.18 Ba	5.05 Ba	23.3 Aa	30.0 Aa	18.7 Aa	73.9 Ab	91.9 Aab	47.7 Ab	24.2 Aa	27.6 Aa	22.1 Aa
	Summer	FS	1.77 Aab	7.38 Ac	22.8 Aa	29.2 Aa	18.9 Aa	81.9 Aa	97.8 Aa	54.9 Ba	24.0 Aa	25.6 Aa	22.7 Aa
		SP1	1.01 Ba	3.93 Bc	22.5 Aa	28.1 Aa	18.9 Aa	84.7 Aa	97.5 Aa	64.8 Aa	23.3 Aa	24.6 Aa	22.3 Aa
		SP3	1.00 Ba	4.02 Bc	22.8 Aa	28.8 Aa	19.2 Aa	84.2 Aa	97.5 Aa	58.7 ABa	24.0 Aa	25.8 Ab	22.7 Aa
	Autumn	FS	1.58 Ab	6.62 Ad	20.1 Ab	26.6 Ab	15.5 Ab	73.7 Ab	89.4 Ab	51.7 Aa	20.2 Ab	22.1 Ab	18.8 ABc
		SP1	1.01 Ba	3.78 Bd	20.0 Ab	25.6 Ab	15.7 Ab	70.5 Abc	87.2 Abc	52.5 Ab	20.0 ABb	21.1 ABb	19.1 Ab
		SP3	1.00 Ba	3.51 Bd	19.7 Ab	25.0 Ab	15.6 Ab	71.1 Abc	87.3 Ab	48.1 Ab	19.0 Bb	20.4 Bc	18.0 Bb

*Means followed by the same upper case letter are not different ($P<0.05$), comparing positions within each season of the year; and those followed by the same lower case letter are not different ($P<0.05$) in the comparison among seasons of the year.

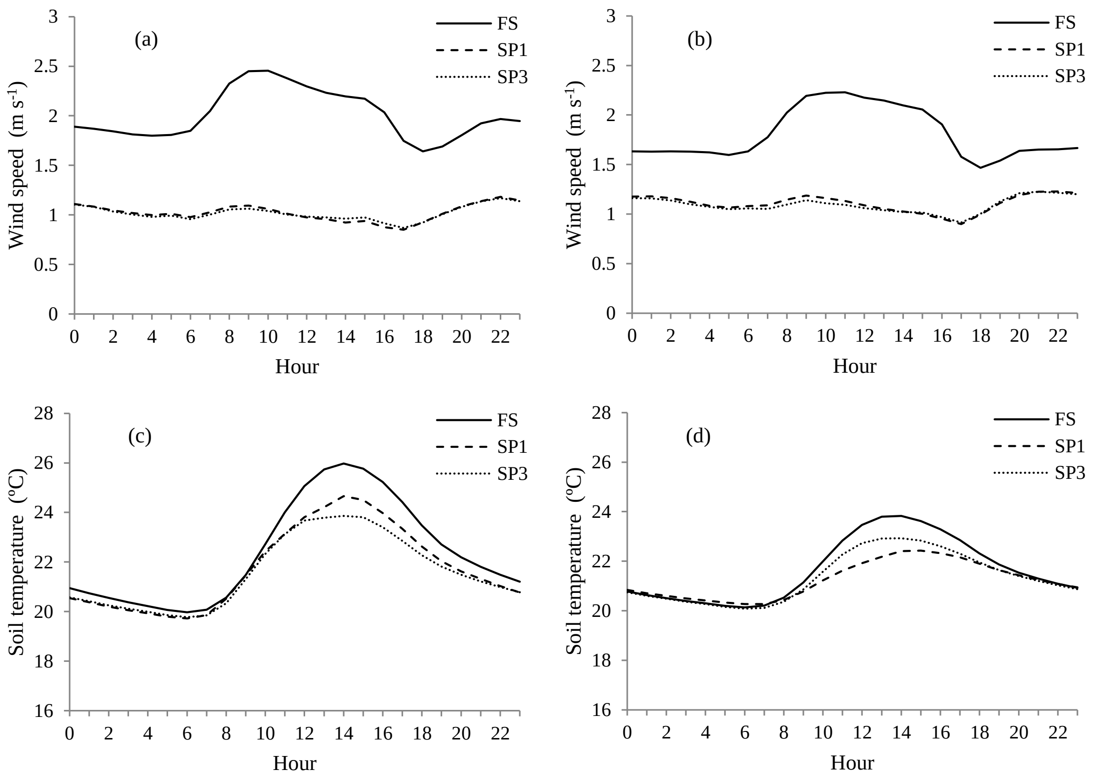

Figure 6. Average hourly wind speed (a, b) and soil temperature (c, d) in the experimental years 2 (a, c,) and 3 (b, d,) at different positions: full sun (FS), below row (SP1), and 7.50 m from the North row (SP3).

Wind speed was always lower in the silvopastoral system due to the trees arrangement in rows and to the short spacing between plants in the row. Such wind speed reduction occurred mainly in the day-time period, especially in the morning, when differences of air temperature promoted by solar radiation caused air movement. Tamang et al. (2010) demonstrated that average wind speed reduction, in the leeside of Cadaghi (*Corymbia torelliana* syn. *Eucalyptus torelliana*) windbreaks with 8 m height, was up to 50% of the open pasture, mainly when the wind direction was perpendicular to the windbreak. Böhm et al. (2014) also showed that wind speed in alley cropping systems, with black locust, decreased till 80% in relation to the open area.

Air temperature and relative humidity were not different between assessed positions, since the design of the system and the tree species employed allowed high canopy porosity and, consequently, enough air movement to suppress such differences. On the other hand, Karki and Goodman (2015) found air temperature 2.3ºC lower in a silvopastoral system with mature loblolly-pine when compared to an open pasture. Pezzopane et al. (2015), assessing a silvopastoral system with rows of Brazilian native trees, oriented North-South, observed higher air temperature in the open area and in the inter-row than at 2 m from tree rows; and lower relative humidity near the trees than at full sun. These results demonstrate that microclimatic changes in silvopastoral systems are affected by their design and tree species employed.

Soil temperature was affected by solar radiation incidence, as well as by wind speed and tree canopy effect on long wave radiation balance. The results obtained in the present study did not agree with those found by Karky and Goodman (2015). These authors observed higher soil temperature at open pasture than in the silvopastoral system, in all months of the year. Amadi et al. (2016), in Saskatchewan, Canada, observed that soil temperature, at a depth of 0.0-0.1 m, was higher in the cropped fields than in the shelterbelts; however it was not true for all periods of the year, e.g. in late summer and early autumn, when the cropped fields were cooled more quickly, their soil temperature was lower than in the shelterbelts, which demonstrates that the local climate affects these relationships.

2.4.2 Potential use of silvopastoral systems to attenuate climate change effects

According to IPCC (2013), temperature increase and reductions in rainfall will be significant in many regions around the world. The protection from solar radiation, in the silvopastoral system, may be very important to mitigate climate change effects in locations where evapotranspiration will increase as function of higher temperature, and rainfall and cloudiness will be decreased. The silvopastoral system design assessed in this study promoted significant decrease in solar radiation incidence, mainly in the distances closer to the tree rows. These changes were more evident during the spring and summer, when solar radiation incidence was higher. In these seasons, high levels of solar radiation, mainly close to noon, affect plants and animals.

Excessively high leaf temperatures can result in stress and in lower photosynthesis (Boyer 1971), affecting plant growth and productivity. Siles et al. (2010) observed that in open sun coffee leaves leaf temperature was higher than air temperature, while in shaded coffee leaf temperature was always lower than air temperature.

Animals’ body temperature is determinant to their thermal comfort (Baliscei et al. 2012), productivity and reproductive efficiency (Garcia et al. 2010). Baliscei et al. (2013) measured black globe temperature, which is strongly correlated with animals’ body temperature, and found lower values in silvopastoral system than in an open area.

The reductions in net radiation and in wind speed, observed in the present study, may be important to reduce evapotranspiration in the plants within a silvopastoral system, since those are factors that affect evapotranspiration (Allen et al 1998).

On the other hand, the wind speed reductions, found in the assessed silvopastoral system, confirm the great capacity of this system to reduce excessive winds or strong gusts, which, according to IPCC (2013), can occur more frequently and more intensely as a consequence of the increase in extreme events caused by climate change, and may cause physical damages to plants (Tamang et al. 2010) and higher stress to animals (Mader et al 1997).

Alterations in air temperature and relative humidity were not significant in the silvopastoral system assessed, which suggest that it is necessary to study others systems designs to protect plants and animals from changes in these variables.

2.5 Conclusions

A silvopastoral system with east-west oriented rows causes shadow movement throughout the year, which promotes more shading at the inter-row of silvopastoral systems, when solar declination is higher; and higher shading at the positions near the trees, when solar declination is close to the local latitude. Net radiation is strongly influenced by incoming solar radiation, and then depends on the factors that affect the shading.

Soil heat flux and soil temperature are also affected by incoming solar radiation, but wind speed and the effect of the canopy, reducing radiation losses, may be determinant for these variables.

Wind speed was always lower in the silvopastoral system, mainly in the diurnal period, due to the trees arrangement in rows and to the short spacing between plants in the row, working as a windbreak.

Air temperature and relative humidity did not differ between open area and silvopastoral system, what was caused by the high canopy porosity, which allowed enough air movement between the areas.

Analyzing the potential of the silvopastoral system to attenuate the climate change effects, the protection from solar radiation may be very important for locations where rainfall and, consequently, cloudiness will be decreased, avoiding stress for plants and animals. The reductions of net radiation and wind speed, observed in this study, may be important to reduce evapotranspiration in the lower layer plants of a silvopastoral system, making the crop water balance less restrictive to their growth. The wind speed reductions confirmed the great capacity of this system to make excessive winds or strong gusts lower.

REFERENCES

Alao, J.S., Shuaibu, R.B., 2013. Agroforestry practices and concepts in sustainable land use systems in Nigeria. J. Hortic. For. 5, 156-159. https://doi.org/10.5897/JHF11.055

Allen, R.G., Pereira, L.S., Raes, D., Smith, M., 1998. Crop evapotranspiration – guidelines for computing crop water requirements. FAO, Rome.

Alvares, C.A., Stape, J.L., Sentelhas, P.C., Gonçalves, J.L.M., Sparovek, G., 2013. Köppen's climate classification map for Brazil. Meteorol. Z. 22, 711-728. https://doi.org/10.1127/0941-2948/2013/0507

Amadi, C.C., Van Rees, K.C.J., Farrell, R.E., 2016. Soil–atmosphere exchange of carbon dioxide, methane and nitrous oxide in shelterbelts compared with adjacent cropped fields. Agric. Ecosyst. Environ. 223, 123-134. https://doi.org/10.1016/j.agee.2016.02.026

Baliscei, M.A., Barbosa, O.R., Souza, W., Costa, M.A.T., Krutzmann, A., Queiroz, E.O., 2013. Microclimate without shade and silvopastoral system during summer and winter. Acta Sci. Anim. Sci. 35, 49-56. https://doi.org/10.4025/actascianimsci.v35i1.15155

Baliscei, M.A., Souza, W., Barbosa, O.R., Cecato, U., Krutzmann, A., Queiroz, E.O., 2012. Behavior of beef cattle and the microclimate with and without shade. Acta Sci. Anim. Sci. 34, 409-415. https://doi.org/10.4025/actascianimsci.v34i4.15055

Böhm, C., Kanzler, M., Freese, D., 2014. Wind speed reductions as influenced by woody hedgerows grown for biomass in short rotation alley cropping systems in Germany. Agrofor. Syst. 88, 579-591. https://doi.org/10.1007/s10457-014-9700-y

Bosi, C., Pezzopane, J.R.M., Sentelhas, P.C., Santos, P.M., Nicodemo, M.L.F., 2014. Productivity and biometric characteristics of signal grass in a silvopastural system. Pesqui. Agropecu. Bras. 49, 449-456. https://doi.org/10.1590/S0100-204X2014000600006

Boyer, J.S., 1971. Nonstomatal inhibition of photosynthesis in sunflower at low leaf water potentials and high light intensities. Plant. Physiol. 48, 532-536.

Filius, A.M., 1982. Economic aspects of agroforestry. Agrofor. Syst. 1, 29-39.

Garcia, A.R., Matos, L.B., Lourenco Junior, J.B., Nahum, B.S., Costa, N.A., 2010. Increased reproductive efficiency of dairy buffaloes due to silvopastoral system adoption in the Eastern Amazon. Rev. Vet. 21, 914-915.

Gomes, L.C., Cardoso, I.M., Mendonca, E.S., Fernandes, R.B.A., Lopes, V.S., Oliveira, T.S., 2016. Trees modify the dynamics of soil CO_2 efflux in coffee agroforestry systems. Agric. For. Meteorol. 224, 30-39. https://doi.org/10.1016/j.agrformet.2016.05.001

IPCC, 2013. Climate Change 2013: The Physical Science Basis. Contribution of Working Group I to the Fifth Assessment Report of the Intergovernmental Panel on Climate Change. Cambridge University Press, Cambridge. https://doi.org/10.1017/CBO9781107415324

Karki, U., Goodman, M.S., 2015. Microclimatic differences between mature loblolly-pine silvopasture and open-pasture. Agrofor. Syst. 89, 319-325. https://doi.org/10.1007/s10457-014-9768-4

King, K.F.S., 1979. Agroforestry and the utilisation of fragile ecosystems. Agrofor. Syst. 2, 161-168.

Lin, B.B., 2010. The role of agroforestry in reducing water loss through soil evaporation and crop transpiration in coffee agroecosystems. Agric. For. Meteorol. 150, 510-518. https://doi.org/10.1016/j.agrformet.2009.11.010

Littell, R.C., Milliken, G.A., Stroup, W.W., Wolfinger, R.D., Schabenberger, O., 2006. SAS for mixed models. SAS Institute, Cary.

Lundgren, B.O., Raintree, J.B., 1982. Sustained agroforestry. In: Nestel B (ed) Agricultural Research for Development: Potentials and Challenges in Asia. ISNAR, The Hague, pp. 37-49.

Mader, T.L., Dahlquist, J.M., Gaughan, J.B., 1997. Wind protection effects and airflow patterns in outside feedlots. J. Anim. Sci. 75, 26-36. https://doi.org/10.2527/1997.75126x

Montagnini, F., Ibrahim, M., Restrepo, E.M., 2013. Silvopastoral systems and climate change mitigation in Latin America. Bois et forêts des tropiques 2, 3-15.

Monteith, J.L., Ong, C.K., Corlett, J.E., 1991. Microclimatic interactions in agroforestry systems. For. Ecol. Manag. 45, 31-44.

Nair, P.K.R., 1993. An introduction to Agroforestry. Kluwer Academic Publishers, Dordrecht.

Nguyen, Q., Hoang, M.H., Öborn, I., Noordwijk, M.V., 2013. Multipurpose agroforestry as a climate change resiliency option for farmers: an example of local adaptation in Vietnam. Clim. Change 117, 241-257. https://doi.org/10.1007/s10584-012-0550-1

Oliveira, T.K., Macedo, R.L.G., Venturin, N., Botelho, S.A., Higashikawa, E.M., Magalhaes, W.M., 2007. Solar radiation in understory of agrosilvopastoral system with eucalypt on different spacings. Cerne 13, 40-50.

Pattanayak, S., Mercer, D.E., 1998. Valuing soil conservation benefits of agroforestry: contour hedgerows in the Eastern Visayas, Philippines. Agric. Econ. 18, 31-46.

Pezzopane, J.R.M., Bosi, C., Nicodemo, M.L.F., Santos, P.M., Cruz, P.G., Parmejiani, R.S., 2015. Microclimate and soil moisture in a silvopastoral system in southeastern Brazil. Bragantia 74, 110-119. https://doi.org/10.1590/1678-4499.0334

Prasad, J.V.N.S., Korwar, G.R., Rao, K.V. et al., 2010. Tree row spacing affected agronomic and economic performance of Eucalyptus-based agroforestry in Andhra Pradesh, Southern India. Agrofor. Syst. 78, 253-267. https://doi.org/10.1007/s10457-009-9275-1

Schroeder, P., 1994. Carbon storage benefits of agroforestry systems. Agrofor. Syst. 27, 89-97.

Siles, P., Harmand, J-M., Vaast, P., 2010. Effects of Inga densiflora on the microclimate of coffee (Coffea arabica L.) and overall biomass under optimal growing conditions in Costa Rica. Agrofor. Syst. 78, 269-286. https://doi.org/10.1007/s10457-009-9241-y

Tamang, B., Andreu, M.G., Rockwood, D.L., 2010. Microclimate patterns on the leeside of single-row tree windbreaks during different weather conditions in Florida farms: implications for improved crop production. Agrofor. Syst. 79, 111-122. https://doi.org/10.1007/s10457-010-9280-4

Vieira, D.L.M., Holl, K.D., Peneireiro, F.M., 2009. Agro-Successional Restoration as a Strategy to Facilitate Tropical Forest Recovery. Restor. Ecol. 17, 451-459. https://doi.org/10.1111/j.1526-100X.2009.00570.x

3. RAINFALL DISTRIBUTION AND SOIL WATER AVAILABILITY IN A FULL SUN PASTURE AND IN A SILVOPASTORAL SYSTEM WITH EUCALYPTUS

ABSTRACT

The aim of this study was to assess two pastoral systems: a full sun pasture system of Piatã palisadegrass, and a silvopastoral system with the same pasture associated with Eucalyptus rows, and their influence on rainfall distribution and soil water availability. The tree rows were oriented near East-West, with 15 m spacing. The treatments considered measurements at 0.00, 3.75, 7.50 and 11.25 m from the trees of the North row, and under full sun. A capacitance probe was used for measuring soil moisture, at all treatments, and three rain gauges for measuring rainfall at full sun, 3.75 and 7.5 m positions. Rainfall distribution was not different ($p<0.05$) between the positions, which suggests that there is a compensation between the rainfall events with low rain intensity and low wind speed, that reduce rainfall below the trees, and the events with high wind speed and wind direction perpendicular to the tree rows, that reduce rainfall at inter-rows. During dry periods, soil water availability until 1-m depth was higher at the inter-row than under the trees, which indicates a faster water uptake by the trees, but, when there was shading at the inter-row, it was lower in the open pasture than at the inter-row, where shading and the windbreak effect promoted lower evapotranspiration. Soil water recharge was higher close to the trees, due to the effect of rainfall interception, increasing the amount of water at this position; whereas the soil water withdraw was faster below the trees, since their roots increased water uptake.

Keywords: Agroforestry; *Urochloa brizantha* cv. BRS Piatã; Soil moisture; Water uptake; Soil water recharge; Throughfall

3.1 Introduction

Silvopastoral systems are a kind of agroforestry system (AFS) in which trees or shrubs are combined with animals and pastures (Nair 1993). These systems improve several aspects for the pasture and animals, such as recovering and sustainability of pasture production, ecological status (Carvalho and Botrel 2002), and animals comfort (Baliscei et al. 2012) and productivity (Garcia et al. 2010).

The main alterations in an AFS are caused by the shade promoted by the trees, but, depending on their arrangement, the trees may also reduce wind speed (Pezzopane et al. 2015). These factors are very important to determine pasture evapotranspiration and soil water availability (Feldhake 2009; Lin 2010).

Several studies have shown the benefits of trees on agroecosystems. According to Nair (1993), the main benefit of an agroforestry system is related to soil conservation, by reducing erosion, maintaining or increasing organic matter, and improving soil structure, porosity, and water holding capacity. Trees may also reduce surface runoff (Benegas et al. 2014), increase infiltrability (Benegas et al. 2014; Sahin et al. 2016); and improve the water use, mainly from deeper soil layers (Gyenge et al. 2002; Pollock et al. 2009), which in summary may increase total plants water consumption (Pezzopane et al. 2015).

On the other hand, agroforestry systems also change rainfall distribution, since tree canopies intercept rainfall, with part of it remaining stored in the leaves and part being redistributed as throughfall and stemflow (Siles et al. 2010). Rainfall interception is affected by leaf area index, structure and shape of the canopy, wind speed, rainfall intensity, and previous rainfall amount, among others. Higher leaf area index and wind speed tend to increase water interception, whereas higher rainfall intensity tends to decrease it (Toba and Ohta 2008).

Considering the capacity of AFS to improve water infiltration, storage, and use, it could be an important strategy to attenuate the drought effects on agricultural systems, which, as reported by IPCC (2013), may be more frequent in several regions of the world, as a function of climate changes. In this context, the aim of this study was to assess two pastoral systems, a full sun pasture system of *Urochloa brizantha* cv. BRS Piatã and a silvopastoral system with the same pasture and rows of Eucalyptus trees, and their influence on rainfall distribution and soil water availability.

3.2 Material and methods

3.2.1 Experimental site

The experiment was carried out in São Carlos, state of São Paulo, Brazil (lat 22°01’ S, long 47°53’ W, alt 860 m), from July 2013 to June 2016. The climate of this location is Cwa (Köppen) with a cool and dry season, from April to September (average air temperature of 19.9ºC and total rainfall of 250 mm), and another warm and wet, from October to March (average air temperature of 23.0ºC and total rainfall of 1100 mm) (Alvares et al. 2013). The soil of the experimental area is an Oxisol, with sandy loam texture and available water capacity, until 1-m depth, between 100 and 110 mm. The trial was composed by an open pasture of *Urochloa* (syn. *Brachiaria*) *brizantha* (Hochst ex A. Rich.) Stapf cv. BRS Piatã, which was the full sun system, and by an adjacent pasture, of the same cultivar, with rows of *Eucalyptus urograndis* (*Eucalyptus grandis x Eucalyptus urophylla*) of the GG100 clonal, which was the silvopastoral system. The trees were planted in April 2011, on the already established pasture, and arranged in simple rows, in a near East-West orientation, with 15 m between rows and 2 m between plants in the rows, totaling 333 trees ha^{-1}. The pasture was grazed by beef cattle of Canchim breed in a rotational grazing, with the resting period of 30 days and the period of occupation of six days. The experimental area totaled 6 ha, being 3 ha in each system, but the assessments were performed only in one paddock, with 0.5 ha, per system. This protocol was adopted because each system was divided into six paddocks, in order to attend the rotational grazing schedule, and the soil moisture measurements were done in the same pasture regrowth or grazing phase for all replications, aiming to allow uniform conditions.

The full sun pasture was considered as a treatment (FS) and in the silvopastoral system, other four treatments were established. The silvopastoral treatments were settled considering the distance from the North row of trees, which was responsible for causing shading in the assessed area in the most of the year, due to solar declination. These treatments were: 0.00 m (SP1); 3.75 m (SP2); 7.50 m (SP3) and 11.25 m (SP4) from the North row (Figure 7).

3.2.2 Rainfall and soil moisture measurements

Three rain gauges (TB4, Hydrological Services Pty Ltd, Warwick Farm, NSW, Australia) were installed in June 2014, at 1.5 m height, being one in the open pasture and two in the silvopastoral system, to measure rainfall continuously, at FS, SP1, and SP3 (Figure 7). These sensors were connected to a datalogger (CR3000, Campbell Scientific, Logan, UT, USA), programmed to record total rainfall every 15 minutes, hour, and day. In this experiment, only throughfall was measured with the rain gauges inside the silvopastoral system, whereas stemflow was considered as part of rainfall interception loss.

To soil moisture measurements, 20 plastic tubes were installed vertically, four in each treatment (Figure 7), in order to allow the access of a portable capacitance probe (Diviner 2000, SENTEK Pty Ltd., Stepney, SA, Australia) to different depths. These measurements were done at least once a week, measuring soil moisture at every 0.1 m until 1.0 m of depth.

The soil water holding capacity was calculated separately for each position of measurement by the difference between field capacity (FC), considered as the highest measured soil moisture (excluding excessively high values obtained after intense rainfalls), and permanent wilting point (PWP), admitted as the lowest soil moisture after a long period without rainfall. After that, the available soil water was calculated by the difference between actual soil moisture and PWP.

Additionally, measurements of photosynthetically active radiation (PAR), at the five treatments; and wind speed and direction, at FS, SP1 and SP3; with linear quantum sensors (Apogee, Logan, UT, USA), and with ultrasonic anemometers (Windsonic, Gill, Lymington, Hampshire, UK), respectively, were performed (Figure 7). These measurements were used to support the discussion about the possible factors that affect rainfall and soil water distribution and variations.

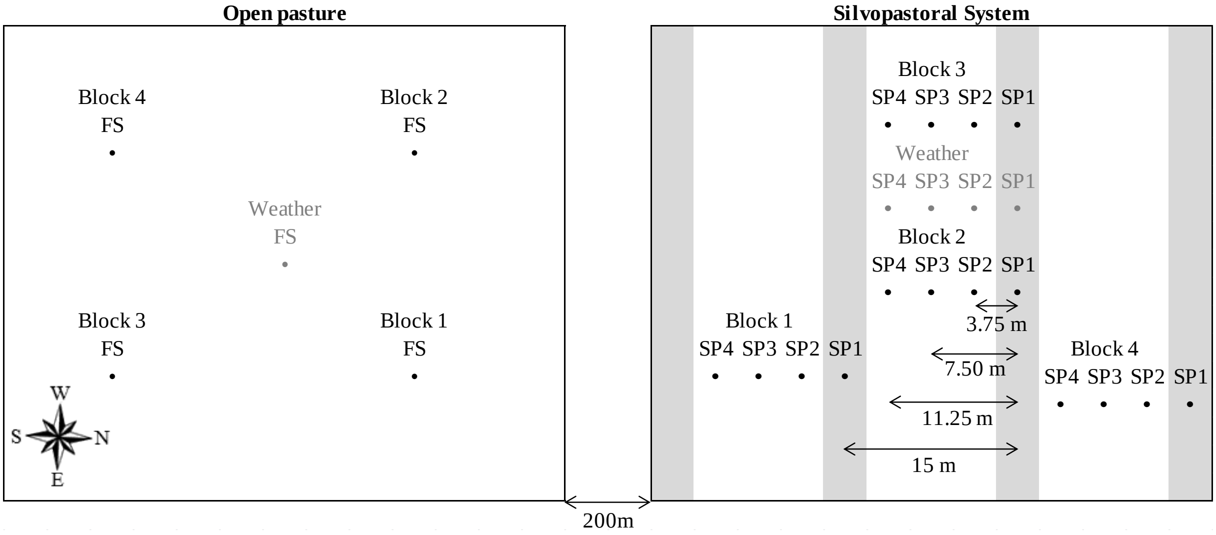

Figure 7. Schematic representation of the experimental paddocks indicating where the data were collected in the open pasture (left) and in the silvopastoral system (right). FS: full sun, SP1: 0.00 m, SP2: 3.75 m, SP3: 7.50 m, SP4: 11.25 m from North row. Gray stripes illustrate the tree rows. Weather: sites where the meteorological variables were measured.

3.2.3 Data analysis

Rainfall distribution was analyzed with a completely randomized design, using the daily totals and considering each rainy day as a replication. These data were analyzed by three methods, the first comparing the positions within each season of the year; the second comparing the positions within four rainfall intensity ranges (lower than 10, from 10 to 30, from 30 to 50 and higher than 50 mm day^{-1}); and the third comparing the positions within seven wind speed ranges (lower than 1.5, from 1.5 to 2.0, from 2.0 to 2.5, from 2.5 to 3.0, from 3.0 to 3.5, from 3.5 to 4.0 and higher than 4.0 m s^{-1}), being the wind speed taken just from the periods during the rains. These data were submitted to an analysis of variance and a

Tukey test with $p \geq 0.05$, for each season or range, using the ANOVA procedure of SAS (Schlotzhauer and Littell 1987).

Additionally, to illustrate cases of rainfall interception in the silvopastoral system, five rainfall events (1/31/2015, 2/8/2015, 8/27/2015, 1/23/2016 and 2/29/2016), with wind speed higher than 3.0 m s^{-1} and wind direction perpendicular to the tree rows (North or South direction), were selected to represent favorable condition for rainfall interception, reducing the amount of rain at SP3; and five rainfall events (12/25/2014, 4/14/2015, 10/10/2015, 10/21/2015 and 10/27/2015), with intensity lower than 3.0 mm day^{-1} and wind speed lower than 2.0 m s^{-1}, were chosen to represent favorable condition for rainfall interception, reducing the amount of rain at SP1.

For the analysis of soil water availability, the experimental design was a randomized complete block with four replications. These data were analyzed as the total profile available soil water and divided into three layers (0-30 cm, 30-60 cm and 60-100 cm), in order to identify differences in root water uptake between positions in different depths. The dataset was submitted to an analysis of variance and a Tukey test ($p \geq 0.05$) for each month. To support the discussion of this analysis, the climatological water balance proposed by Thornthwaite and Mather (1955) was calculated in a ten-day time step for the FS treatment, using the reference evapotranspiration calculated by the Penman-Monteith method (Allen et al. 1998) and considering a soil water holding capacity of 100 mm.

Finally, two different soil water conditions (recharge and withdraw) were selected to illustrate the soil water dynamics in this system. The water recharge events were between 7/8/2014 and 7/11/2014, with a low rainfall (8.9 mm) and between 9/25/2015 and 9/28/2015, with a high rainfall (38.9 mm). The water withdraw events were between 9/14/2015 and 9/25/2015, at the end of the dry season and between 3/28/2016 and 4/18/2016, at the beginning of the dry season.

3.3 Results

3.3.1 Rainfall distribution

Rainfall distribution was not different ($p<0.05$) between the three assessed positions in the silvopastoral system, for all seasons of the two monitored years (Table 6), and for the rain (Table 7) and wind speed (Table 8) intensities during the rainfall events. Observing the absolute total rainfall, the amounts were higher in FS, mainly when compared to SP3 (72.2

mm during 2014/2015 and 181.4 mm during 2015/2016), but not statistically significant (Table 6).

The selected rainfall events showed that, with wind speed higher than 3.0 m s^{-1} and wind direction perpendicular to the tree rows, rainfall was higher at SP1 than at SP3 (Table 9); therefore, with rain intensity lower than 3.0 mm day^{-1} and wind speed lower than 2.0 m s^{-1}, rainfall was lower at SP1 than at SP3 (Table 10); but in general, due to the great variability of the dataset, these conditions did not result in statistical differences.

Table 6. Total rainfall at full sun (FS) and at two positions within a silvopastoral system (SP1: 0.00 m and SP3: 7.50 m from the North row), in each season of the year of two experimental years.

Year	Position	Total rainfall mm				
		Winter	Spring	Summer	Autumn	Total
2014/2015	FS	109.0 a*	377.4 a	645.4 a	286.9 a	1418.6
	SP1	117.9 a	400.5 a	619.5 a	236.8 a	1374.7
	SP3	104.4 a	398.5 a	601.0 a	242.6 a	1346.4
	Average	110.4	392.1	621.9	255.4	
2015/2016	FS	196.1 a	498.2 a	970.5 a	303.8 a	1968.6
	SP1	161.0 a	484.9 a	983.0 a	276.1 a	1905.0
	SP3	175.5 a	445.0 a	890.5 a	276.1 a	1787.2
	Average	177.5	476.0	948.0	285.3	

*Means followed by the same letter are not different in column (P<0.05).

Table 7. Average rainfall at full sun (FS) and at two positions within a silvopastoral system (SP1: 0.00 m and SP3: 7.50 m from the North row), grouped by four rain intensity ranges (lower than 10, from 10 to 30, from 30 to 50 and higher than 50 mm day^{-1}).

Position	Rain intensity range mm day^{-1}			
	<10	10-30	30-50	>50
FS	4.6 a*	17.7 a	36.5 a	84.8 a
SP1	4.2 a	17.1 a	35.9 a	88.2 a
SP3	4.2 a	16.2 a	34.7 a	75.6 a
Average	4.3	17.0	35.7	82.9

*Means followed by the same letter are not different in column (P<0.05).

Table 8. Average rainfall at full sun (FS) and at two positions within a silvopastoral system (SP1: 0.00 m and SP3: 7.50 m from the North row), grouped by seven wind speed ranges (lower than 1.5, from 1.5 to 2.0, from 2.0 to 2.5, from 2.5 to 3.0, from 3.0 to 3.5, from 3.5 to 4.0 and higher than 4.0 m s^{-1}).

Position	Wind speed range $m\ s^{-1}$						
	<1.5	1.5-2.0	2.0-2.5	2.5-3.0	3.0-3.5	3.5-4.0	>4.0
FS	14.6 a*	14.6 a	18.8 a	16.2 a	8.3 a	20.6 a	11.0 a
SP1	13.3 a	13.6 a	18.0 a	16.8 a	9.2 a	21.4 a	10.6 a
SP3	14.8 a	13.9 a	17.0 a	14.3 a	7.5 a	18.8 a	8.3 a
Average	14.3	14.0	17.9	15.7	8.3	20.3	10.0

*Means followed by the same letter are not different in column ($P<0.05$).

Table 9. Rainfall at full sun (FS) and at two positions within a silvopastoral system (SP1: 0.00 m and SP3: 7.50 m from the North row), in five rainfall events with wind speed higher than 3.0 m s^{-1} and wind direction perpendicular to the tree rows (North or South direction).

Position	Date					
	1/31/2015	2/8/2015	8/27/2015	1/23/2016	2/29/2016	Average
FS	8.4	30.2	1.0	7.6	2.3	9.9
SP1	10.4	31.2	0.8	9.9	3.3	11.1
SP3	6.9	19.3	0.3	4.6	1.3	6.5
Average	8.5	26.9	0.7	7.4	2.3	

Table 10. Rainfall at full sun (FS) and at two positions within a silvopastoral system (SP1: 0.00 m and SP3: 7.50 m from the North row), in five rainfall events with rain intensity lower than 3.0 mm day^{-1} and wind speed lower than 2.0 m s^{-1}.

Position	Date					
	12/25/2014	4/14/2015	10/10/2015	10/21/2015	10/27/2015	Average
FS	2.5	1.5	1.0	1.5	1.0	2.1
SP1	0.3	0.3	0.3	0.5	0.3	0.6
SP3	1.3	1.5	1.3	1.5	1.0	2.0
Average	1.4	1.1	0.8	1.2	0.8	

3.3.2 Available soil water

Available soil water (ASW) in the whole profile was higher at SP3 than at SP1in August 2013; in March, April, May and December 2015; and in April 2016. It was higher at SP3 than at FS in June 2014; higher at SP1, SP2 and SP4 than at FS in August 2015; and higher at SP2, SP3 and SP4 than FS in May 2016 (Figure 8a and Table 11).

At the layer between 0 and 30 cm, ASW was more dynamic. It was lower at SP1 than at SP3 from July to October 2013, from March to June 2014, in August and September 2014, and from April to July 2015; lower at FS than at SP3, in August 2013, August 2014 and in May and June 2015; lower at SP1 than at FS, in July and October 2013, and in January, March, April, May, June, September, October and December 2014; lower at FS than at SP2, in August 2015 and May 2016; lower at SP2 than at SP4, in January, February, June, July and August 2014; and lower at SP4 than at SP2 in October 2015 (Table 12).

From 30 to 60 cm depth, ASW was lower at SP1 than at SP3, in March, April and December 2015; lower at FS than at SP3, from May to July 2015; and lower at FS than at the other positions, in August 2015 (Table 13).

At the deepest layer (60-100 cm), ASW was lower at SP2 and SP3 than at SP1, in December 2014; lower at SP1 than at SP3, in March and April 2015; and lower at FS than at SP1, in August and December 2015 (Table 14).

Observing the selected soil water recharge events, the water reposition was higher at SP1 than at the other positions (Figure 9). During the low rainfall event, with 8.9 mm, recharge at SP1 was 7.0 mm, followed by SP2 with 4.6 mm, SP3 with 4.1 mm, FS with 3.5 mm and SP4 with 3.1 mm. On the other hand, during the high rainfall event, with 38.9 mm, recharge was 24.9 mm at SP1, 20.6 mm at FS, 18.1 mm at SP4, 16.7 mm at SP2 and 13.4 mm at SP3, demonstrating high losses by runoff at all positions.

The presented soil water withdraw events demonstrated that water uptake was faster at SP1 than at the other positions (Figure 10). During the initial period of the first withdraw event, between 9/14/2015 and 9/21/2015, it was 43.9 mm at SP1, 26.9 mm at SP2, 24.0 mm at SP4, 22.4 mm at FS and 20.3 mm at SP3; therefore, between 9/21/2015 and 9/25/2015 it was higher at SP4 (24.0 mm), followed by FS, SP2, SP3, and SP1 (16.6, 16.4, 16.2 and 7.7 mm, respectively). Disagreeing with these results, during the first period of the second withdraw event, between 3/28/2016 and 4/8/2016, the water uptake was similar between positions, varying from 21.0 to 24.0 mm; but between 4/8/2016 and 4/18/2016, it was higher at FS, followed by SP2, SP3, SP4 and SP1 (29.4, 21.0, 18.7, 18.1 and 4.3 mm, respectively). Additionally, these withdraw events showed that there were no differences related to the depth of water uptake between positions, indicating that both pasture and tree roots extracted water until 1-m depth easily.

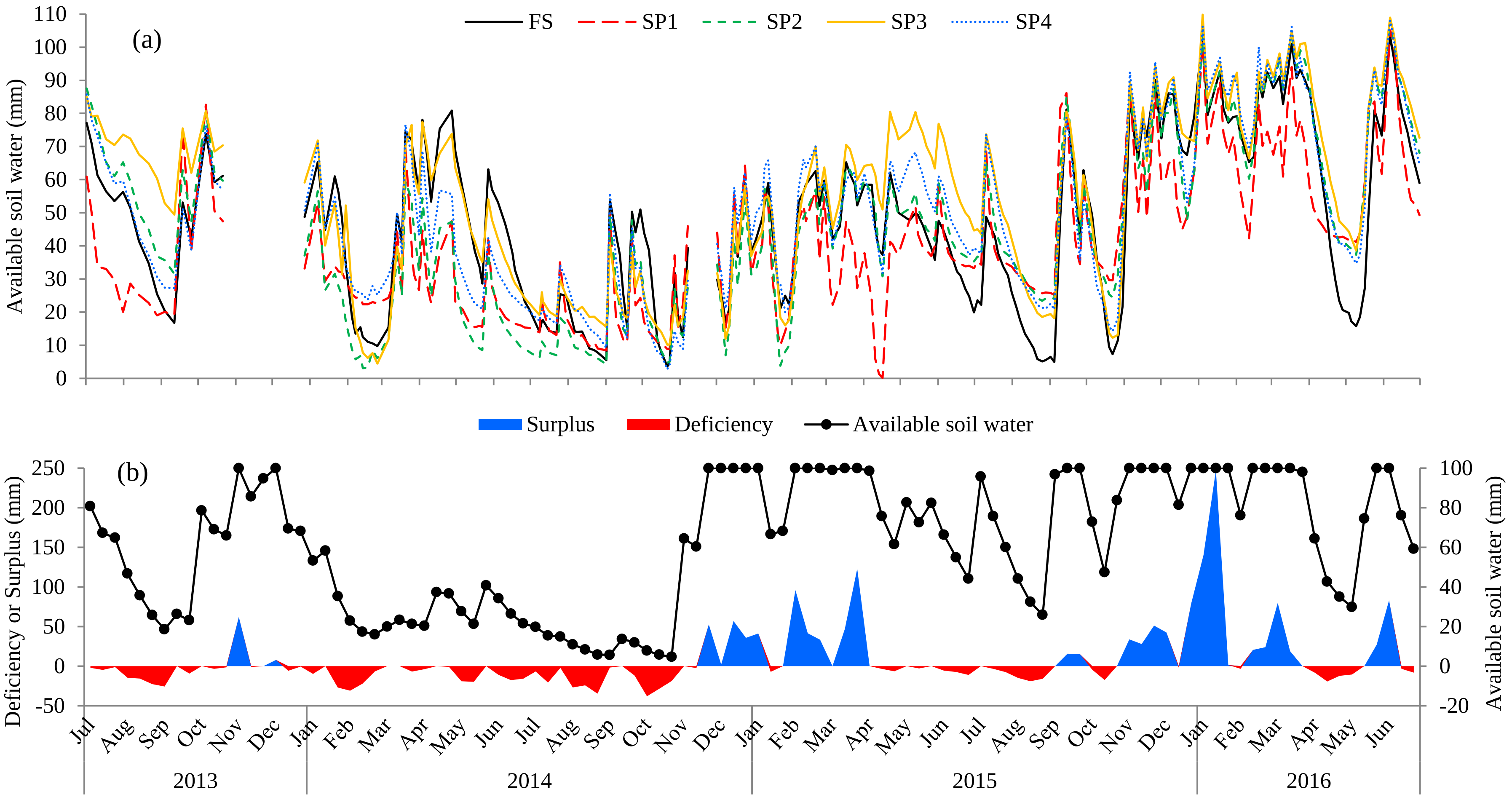

Figure 8. (a) Measured available soil water at the full sun (FS) and at the four positions within the silvopastoral system (SP1: 0.00 m, SP2: 3.75 m, SP3: 7.50 m and SP4: 11.25 m from the North row), in three experimental years. (b) Climatological water balance for the experimental site during the experiment, considering the full sun position.

Table 11. Available soil water from 0 to 1 m depth, at the full sun (FS) and at the four positions within the silvopastoral system (SP1: 0.00 m, SP2: 3.75 m, SP3: 7.50 m and SP4: 11.25 m from the North row), in each month of the three experimental years.

Year	Position	Available soil water mm												
		Jul	Aug	Sep	Oct	Nov	Dec	Jan	Feb	Mar	Apr	May	Jun	Average
2013/2014	FS	62.7 a*	38.3 ab	33.2 a	64.8 a	-	-	51.3 a	13.0 a	53.2 a	70.5 a	46.3 a	35.4 a	46.9
	SP1	39.0 a	23.9 b	38.3 a	60.2 a	-	-	35.0 a	23.5 a	36.1 a	33.9 a	21.9 a	17.3 a	32.9
	SP2	72.9 a	47.7 ab	44.4 a	67.5 a	-	-	30.7 a	6.0 a	37.7 a	39.6 a	17.8 a	12.4 a	37.7
	SP3	76.6 a	66.3 a	60.0 a	73.2 a	-	-	48.5 a	11.0 a	48.9 a	68.6 a	45.2 a	30.4 a	52.9
	SP4	70.1 a	40.7 ab	36.2 a	64.3 a	-	-	48.9 a	26.1 a	51.3 a	51.4 a	28.8 a	24.9 a	44.3
	Average	64.3	43.4	42.4	66.0	-	-	42.9	15.9	45.4	52.8	32.0	24.1	
2014/2015	FS	18.2 a	11.2 a	36.2 a	18.9 a	27.8 a	33.9 a	38.3 a	53.7 a	53.5 ab	57.0 ab	44.5 b	33.8 b	35.6
	SP1	20.1 a	11.4 a	22.4 a	15.4 a	34.2 a	36.9 a	30.7 a	47.4 a	33.5 b	38.3 b	42.7 b	38.6 ab	31.0
	SP2	11.0 a	7.9 a	27.6 a	14.3 a	20.3 a	29.0 a	28.2 a	47.1 a	53.2 ab	57.0 ab	48.1 ab	42.5 ab	32.2
	SP3	23.1 a	19.6 a	26.8 a	16.4 a	25.5 a	32.8 a	33.9 a	54.3 a	59.1 a	69.3 a	72.5 a	58.8 a	41.0
	SP4	22.5 a	17.0 a	29.7 a	10.7 a	19.3 a	40.6 a	42.5 a	58.2 a	53.4 ab	61.1 a	60.0 ab	46.8 ab	38.5
	Average	19.0	13.4	28.6	15.1	25.4	34.6	34.7	52.1	50.5	56.6	53.6	44.1	
2015/2016	FS	34.7 a	11.2 b	47.8 a	26.3 a	77.5 a	77.0 ab	85.6 a	78.8 a	91.2 a	50.5 ab	42.0 b	78.9 a	58.5
	SP1	40.6 a	28.2 a	50.7 a	38.1 a	67.5 a	57.3 b	79.5 a	65.7 a	76.1 a	46.4 b	58.0 ab	71.5 a	56.6
	SP2	44.1 a	27.6 a	53.4 a	35.4 a	72.9 a	71.5 ab	87.9 a	78.4 a	95.3 a	59.2 ab	62.6 a	86.2 a	64.5
	SP3	53.8 a	25.1 ab	53.3 a	29.3 a	79.9 a	80.8 a	91.4 a	83.3 a	97.6 a	66.5 a	64.1 a	89.2 a	67.9
	SP4	49.9 a	25.6 a	48.6 a	27.9 a	80.4 a	74.4 ab	92.6 a	84.7 a	94.3 a	57.7 ab	60.9 a	85.0 a	65.2
	Average	44.6	23.5	50.7	31.4	75.6	72.2	87.4	78.2	90.9	56.1	57.5	82.1	

*Means followed by the same letter are not different in column ($P<0.05$).

Table 12. Available soil water from 0 to 0.3 m depth, at the full sun (FS) and at the four positions within the silvopastoral system (SP1: 0.00 m, SP2: 3.75 m, SP3: 7.50 m and SP4: 11.25 m from the North row), in each month of the three experimental years.

Year	Position	Available soil water mm												
		Jul	Aug	Sep	Oct	Nov	Dec	Jan	Feb	Mar	Apr	May	Jun	Average
2013/2014	FS	26.7 a*	14.2 bc	16.0 ab	25.8 a	-	-	20.9 a	4.1 ab	24.1 a	27.3 a	17.3 a	14.6 a	19.1
	SP1	14.0 b	5.8 c	12.0 b	17.3 b	-	-	10.9 b	5.1 ab	11.9 b	12.3 c	5.4 c	3.7 b	9.8
	SP2	31.3 a	19.2 ab	20.4 a	26.8 a	-	-	11.5 b	2.5 b	18.8 a	18.9 bc	8.1 bc	4.7 b	16.2
	SP3	29.7 a	24.9 a	20.4 a	26.5 a	-	-	17.7 ab	3.8 ab	20.6 a	27.1 a	17.7 a	12.2 a	20.1
	SP4	32.7 a	17.5 ab	19.4 ab	27.2 a	-	-	20.8 a	9.4 a	22.9 a	24.0 ab	13.5 ab	11.0 a	19.8
	Average	26.9	16.3	17.7	24.7	-	-	16.3	5.0	19.7	21.9	12.4	9.2	
2014/2015	FS	9.3 ab	3.7 b	18.0 a	9.5 a	18.8 a	17.6 a	15.0 a	22.1 a	21.0 a	20.3 ab	18.3 bc	14.9 b	15.7
	SP1	8.3 ab	1.8 b	7.2 c	4.9 b	16.3 a	12.6 b	12.1 a	21.3 a	14.3 a	14.8 b	14.8 c	13.2 b	11.8
	SP2	6.0 b	2.7 b	12.0 bc	6.4 ab	13.2 a	14.3 ab	12.5 a	22.5 a	20.3 a	20.8 a	21.1 abc	18.5 ab	14.2
	SP3	10.9 ab	7.4 a	12.5 b	6.6 ab	14.7 a	14.6 ab	11.0 a	21.4 a	19.0 a	22.4 a	26.7 a	22.1 a	15.8
	SP4	11.5 a	7.0 a	13.9 ab	4.5 b	11.2 a	17.4 ab	15.8 a	25.6 a	20.7 a	22.2 a	24.6 ab	18.3 ab	16.1
	Average	9.2	4.5	12.7	6.4	14.8	15.3	13.3	22.6	19.1	20.1	21.1	17.4	
2015/2016	FS	18.2 ab	5.5 b	18.8 a	12.0 ab	27.4 a	27.5 a	28.4 a	28.4 a	31.1 a	13.3 a	14.9 b	24.6 a	20.8
	SP1	12.9 b	7.0 ab	16.6 a	12.8 ab	23.9 a	24.1 a	29.2 a	27.7 a	31.6 a	16.2 a	21.0 ab	25.8 a	20.7
	SP2	19.1 ab	10.3 a	21.8 a	15.4 a	28.3 a	27.8 a	31.4 a	30.9 a	35.0 a	21.4 a	24.8 a	29.8 a	24.7
	SP3	20.8 a	8.2 ab	20.7 a	11.6 ab	27.0 a	28.4 a	30.0 a	28.7 a	32.5 a	19.7 a	21.6 ab	28.2 a	23.1
	SP4	19.8 ab	8.0 ab	19.2 a	10.7 b	27.2 a	27.4 a	31.8 a	30.6 a	32.8 a	18.7 a	20.4 ab	27.8 a	22.9
	Average	18.1	7.8	19.4	12.5	26.8	27.0	30.2	29.3	32.6	17.8	20.5	27.2	

*Means followed by the same letter are not different in column (P<0.05).

Table 13. Available soil water from 0.3 to 0.6 m depth, at the full sun (FS) and at the four positions within the silvopastoral system (SP1: 0.00 m, SP2: 3.75 m, SP3: 7.50 m and SP4: 11.25 m from the North row), in each month of the three experimental years.

Year	Position	Available soil water mm												
		Jul	Aug	Sep	Oct	Nov	Dec	Jan	Feb	Mar	Apr	May	Jun	Average
2013/2014	FS	18.2 a*	11.2 a	8.7 a	17.9 a	-	-	13.9 a	2.9 a	15.8 a	20.9 a	13.2 a	9.5 a	13.2
	SP1	11.2 a	9.5 a	14.8 a	19.4 a	-	-	12.6 a	9.3 a	13.7 a	12.9 a	10.0 a	8.3 a	12.2
	SP2	17.3 a	11.1 a	11.4 a	16.7 a	-	-	7.5 a	1.4 a	10.6 a	10.9 a	4.9 a	3.5 a	9.5
	SP3	20.5 a	18.0 a	17.3 a	19.9 a	-	-	14.1 a	3.5 a	14.9 a	18.8 a	11.9 a	8.0 a	14.7
	SP4	16.1 a	9.0 a	7.9 a	16.7 a	-	-	14.0 a	7.7 a	15.5 a	15.2 a	7.9 a	7.0 a	11.7
	Average	16.7	11.8	12.0	18.1	-	-	12.4	4.9	14.1	15.7	9.6	7.3	
2014/2015	FS	2.9 a	2.5 a	11.7 a	5.0 a	6.9 a	6.7 a	7.4 a	11.4 a	11.5 ab	12.0 ab	7.5 b	5.5 b	7.6
	SP1	7.9 a	6.4 a	10.2 a	6.9 a	12.4 a	8.2 a	6.3 a	11.2 a	7.6 b	9.0 b	9.4 ab	8.2 ab	8.6
	SP2	2.0 a	2.1 a	8.6 a	3.6 a	3.8 a	8.8 a	6.9 a	12.7 a	13.3 ab	13.3 ab	10.3 ab	9.4 ab	7.9
	SP3	5.1 a	5.2 a	7.4 a	4.3 a	6.2 a	9.5 a	9.7 a	17.0 a	18.4 a	19.9 a	20.2 a	16.0 a	11.6
	SP4	5.5 a	4.8 a	9.5 a	3.3 a	6.2 a	10.7 a	10.1 a	13.8 a	14.0 ab	15.4 ab	15.3 ab	11.8 ab	10.0
	Average	4.7	4.2	9.5	4.6	7.1	8.8	8.1	13.2	12.9	13.9	12.5	10.2	
2015/2016	FS	7.1 b	1.5 b	10.9 a	4.8 a	18.7 a	18.5 ab	21.1 a	19.5 a	23.1 a	12.8 a	10.5 a	19.8 a	14.0
	SP1	9.5 ab	6.2 a	12.9 a	8.9 a	17.1 a	12.8 b	18.6 a	15.7 a	18.1 a	10.1 a	13.5 a	16.7 a	13.3
	SP2	11.0 ab	6.5 a	13.5 a	8.2 a	19.1 a	17.6 ab	21.7 a	20.1 a	24.1 a	14.1 a	15.4 a	21.9 a	16.1
	SP3	15.6 a	6.5 a	14.8 a	7.1 a	22.7 a	22.2 a	25.3 a	23.9 a	27.4 a	18.5 a	17.4 a	24.7 a	18.8
	SP4	14.0 ab	6.9 a	13.2 a	7.1 a	21.5 a	19.2 ab	24.1 a	22.4 a	24.5 a	15.3 a	16.3 a	22.7 a	17.3
	Average	11.4	5.5	13.0	7.2	19.8	18.1	22.2	20.3	23.5	14.2	14.6	21.2	

*Means followed by the same letter are not different in column ($P<0.05$).

Table 14. Available soil water from 0.6 to 1 m depth, at the full sun (FS) and at the four positions within the silvopastoral system (SP1: 0.00 m, SP2: 3.75 m, SP3: 7.50 m and SP4: 11.25 m from the North row), in each month of the three experimental years.

Year	Position	Available soil water mm												
		Jul	Aug	Sep	Oct	Nov	Dec	Jan	Feb	Mar	Apr	May	Jun	Average
2013/2014	FS	17.8 a*	12.9 a	8.4 a	21.1 a	-	-	16.5 a	6.0 a	13.2 a	22.2 a	15.7 a	11.4 a	14.5
	SP1	13.8 a	8.6 a	11.5 a	23.5 a	-	-	11.5 a	9.1 a	10.4 a	8.7 a	6.5 a	5.3 a	10.9
	SP2	24.4 a	17.5 a	12.6 a	24.0 a	-	-	11.7 a	2.1 a	8.3 a	9.9 a	4.8 a	4.2 a	11.9
	SP3	26.4 a	23.4 a	22.2 a	26.8 a	-	-	16.8 a	3.7 a	13.4 a	22.6 a	15.6 a	10.1 a	18.1
	SP4	21.3 a	14.2 a	8.9 a	20.4 a	-	-	14.1 a	9.0 a	12.8 a	12.3 a	7.3 a	6.9 a	12.7
	Average	20.7	15.3	12.7	23.2	-	-	14.1	6.0	11.6	15.1	10.0	7.6	
2014/2015	FS	6.0 a	4.9 a	6.5 a	4.4 a	2.1 a	9.6 ab	16.0 a	20.2 a	21.0 ab	24.7 ab	18.7 a	13.5 a	12.3
	SP1	3.9 a	3.2 a	5.0 a	3.6 a	5.6 a	16.1 a	12.2 a	15.0 a	11.5 b	14.6 b	18.4 a	17.2 a	10.5
	SP2	3.1 a	3.1 a	7.0 a	4.3 a	3.2 a	5.9 b	8.9 a	11.9 a	19.6 ab	22.9 ab	16.7 a	14.6 a	10.1
	SP3	7.2 a	7.0 a	6.9 a	5.5 a	4.5 a	8.7 b	13.2 a	15.9 a	21.7 a	27.0 a	25.6 a	20.8 a	13.7
	SP4	5.5 a	5.2 a	6.4 a	2.9 a	1.9 a	12.5 ab	16.6 a	18.7 a	18.7 ab	23.5 ab	20.1 a	16.7 a	12.4
	Average	5.1	4.7	6.4	4.1	3.5	10.6	13.4	16.3	18.5	22.5	19.9	16.5	
2015/2016	FS	9.4 a	4.1 b	18.0 a	9.5 a	31.5 a	31.0 a	36.1 a	30.9 a	36.9 a	24.5 a	16.6 a	34.5 a	23.6
	SP1	18.3 a	15.0 a	21.2 a	16.4 a	26.5 a	20.3 b	31.6 a	22.3 a	26.4 a	20.1 a	23.6 a	29.0 a	22.6
	SP2	14.0 a	10.9 ab	18.0 a	11.8 a	25.5 a	26.2 ab	34.7 a	27.5 a	36.2 a	23.7 a	22.3 a	34.5 a	23.8
	SP3	17.4 a	10.4 ab	17.8 a	10.5 a	30.2 a	30.2 ab	36.1 a	30.7 a	37.7 a	28.4 a	25.2 a	36.3 a	25.9
	SP4	16.1 a	10.8 ab	16.2 a	10.2 a	31.6 a	27.8 ab	36.8 a	31.7 a	36.9 a	23.6 a	24.2 a	34.5 a	25.0
	Average	15.0	10.2	18.3	11.7 a	29.0	27.1	35.1	28.6	34.8	24.1	22.4	33.8	

*Means followed by the same letter are not different in column ($P<0.05$).

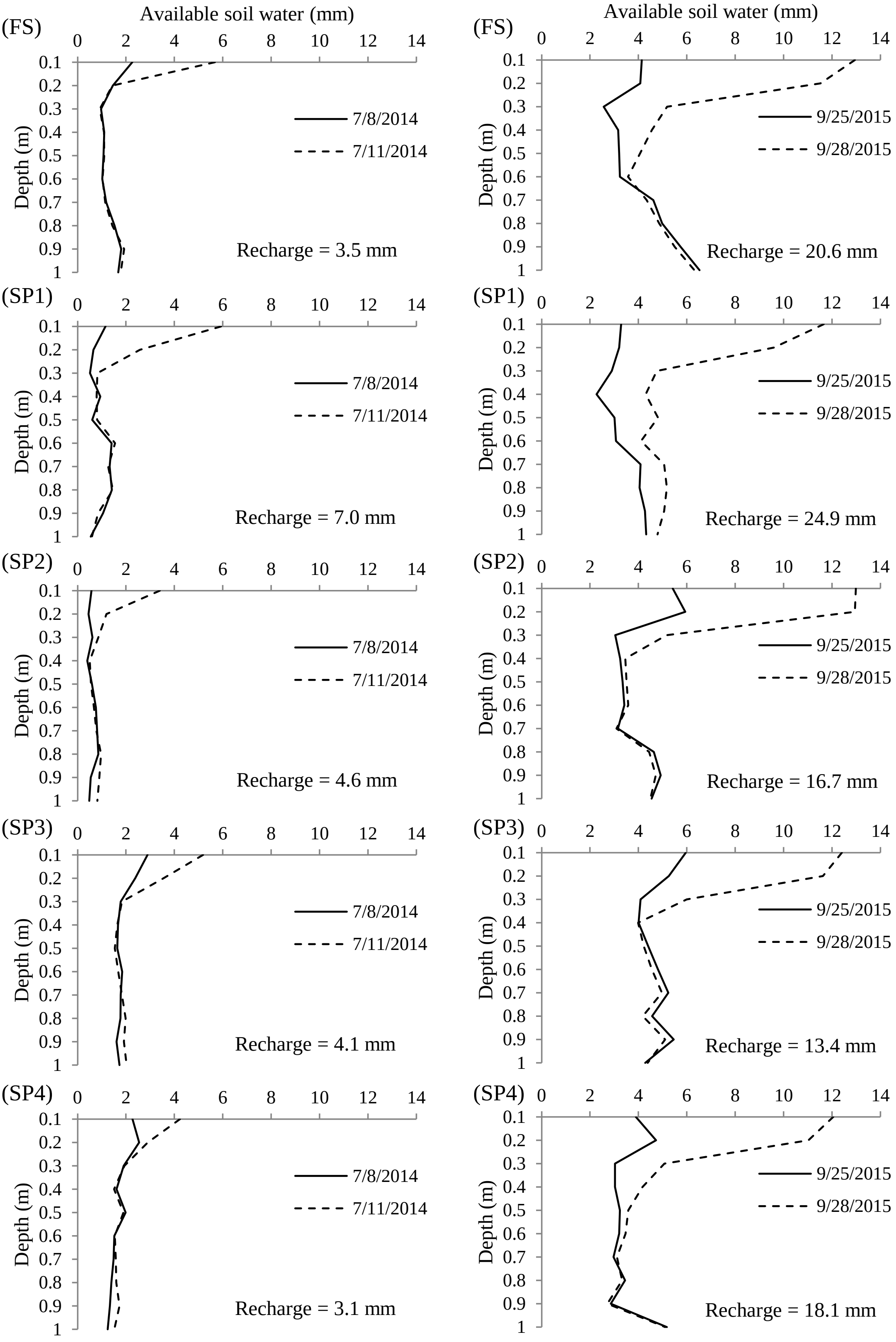

Figure 9. Available soil water at full sun (FS) and at the four positions within the silvopastoral system (SP1: 0.00 m, SP2: 3.75 m, SP3: 7.50 m and SP4: 11.25 m from the North row) during two water recharge events, the first between 7/8/2014 and 7/11/2014 (left), with a low rainfall (8.9 mm); and the second between 9/25/2015 and 9/28/2015 (right), with a high rainfall (38.9 mm).

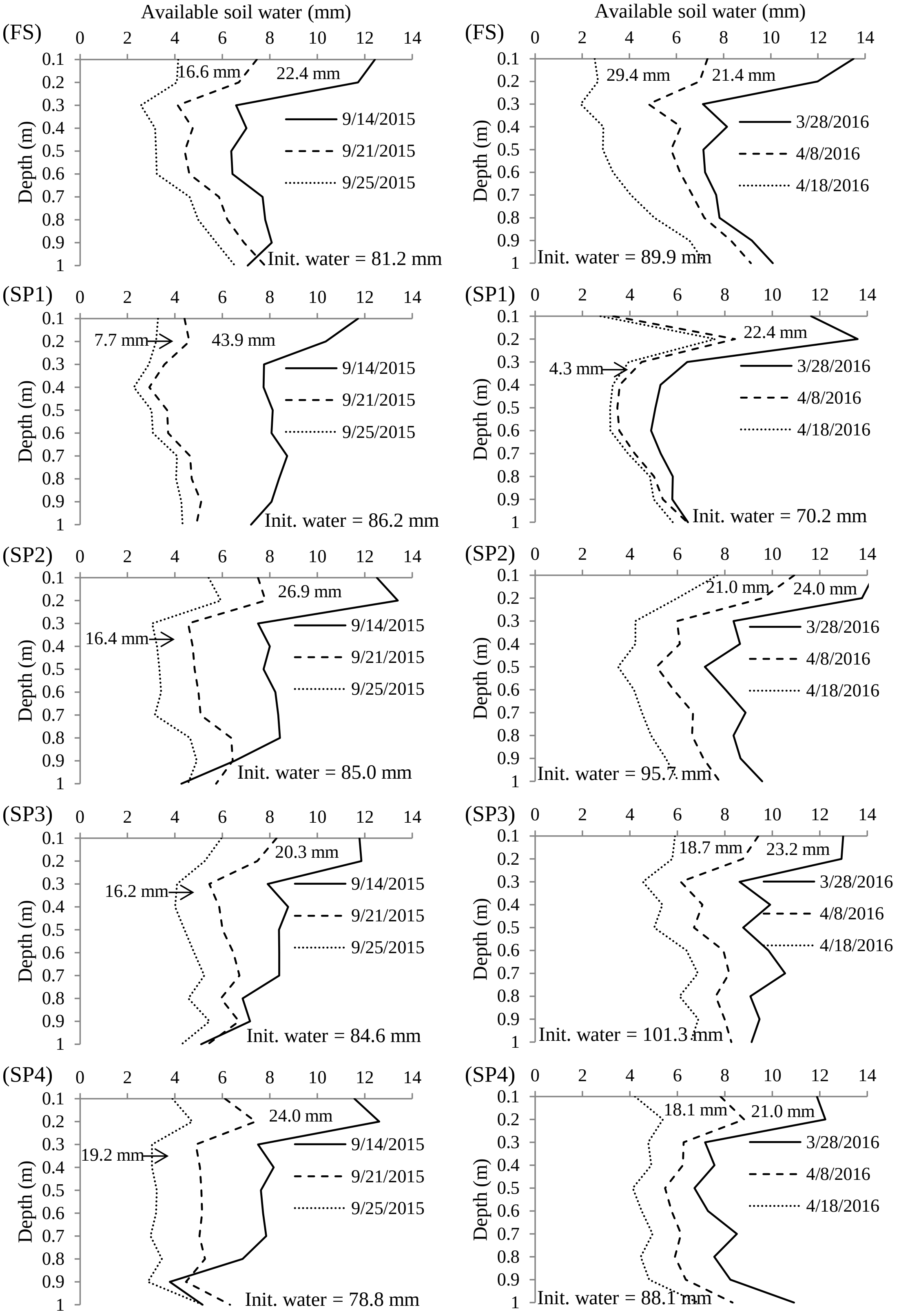

Figure 10. Available soil water at full sun (FS) and at the four positions within the silvopastoral system (SP1: 0.00 m, SP2: 3.75 m, SP3: 7.50 m and SP4: 11.25 m from the North row) during two water withdraw events, the first between 9/14/2015 and 9/25/2015 (left), i.e. end of the dry period; and the second between 3/28/2016 and 4/18/2016 (right), i.e. beginning of the dry period.

3.4 Discussion

Rainfall distribution was not different between positions within seasons of the year (Table 6), due to the great variability observed in the dataset, probably caused by factors as wind speed and direction during the rainfall events, which influenced rain interception in several ways and suppressed the possibility of significant differences; however, the numerical differences in total annual rainfall (Table 6) must be taken into account, since they can affect soil water availability for pasture and trees growth. These results do not agree with those observed by Siles et al. (2010), who observed a higher throughfall in a single coffee plantation than in an agroforestry system composed by coffee and *Inga densiflora*, and by Poppenborg and Hölscher (2009), who obtained a lower throughfall below a cacao agroforestry system than under a single cacao plantation. These differences are mainly caused by the higher different canopy structures and densities of these tree species used.

Rainfall intensity also was not a determining factor for water interception by eucalyptus trees, even under low rain intensity (Table 7). However, rainfall of low intensity (< 3.0 mm day^{-1}) and wind speed lower than 2.0 m s^{-1}, when combined, showed to be important to reduce rainfall amounts below the trees (Table 10). Even with such evidence, more detailed studies are required to confirm it, as done by Toba and Ohta (2008), who assessed an artificial forest with simulated rainfall, in order to determine the influences of forest structure and rainfall conditions on interception loss.

Analyzing wind speed influence on rainfall distribution, the results allowed to observe that this factor isolated was not important (Table 8), but when more focus is given to wind speed higher than 3.0 m s^{-1} and direction perpendicular to the eucalyptus rows, the results indicated decrease in rainfall amounts at the inter-row (Table 9). This influence was exemplified by Poppenborg and Hölscher (2009), who observed higher throughfall at the canopy side exposed to prevailing winds, in a cacao agroforest, demonstrating that most of the water was intercepted by the leaves at this side, reducing rainfall at the opposite side. Therefore more studies about the influence of wind speed associated with wind direction must be carried out to explain in detail these relationships for trees arranged in rows.

In general, ASW was lower at SP1 than at SP3 (Tables 11, 12, 13 and 14) when drying periods occurred (Figure 8), which were important for faster water uptake at SP1. This faster water uptake near the trees was also observed by Pezzopane et al. (2015), in a silvopastoral system with *Urochloa decumbens* and Brazilian native trees, by Wilson (1998), in a green panic pasture arborized with *Eucalyptus argophloia*, and by Tian et al. (2017), in an intercropping system with loblolly pine and switchgrass.

When lower ASW was observed at FS than at SP3 (Tables 11, 12, 13 and 14), the most determinant factor was the highest pasture evapotranspiration at FS, which was determined by the higher solar radiation and wind speed at this position than within the silvopastoral system. This lower evapotranspiration within agroforestry systems was also observed by Lin (2010), in an arborized coffee plantation, and by Feldhake (2009), in a silvopastoral system. These authors attributed these alterations mainly to the differences in the incoming solar radiation, however, Feldhake (2009) also observed influence of wind speed on evapotranspiration when pasture was exposed to prevailing winds.

Specifically at the first layer (0-30 cm), ASW was more dynamic due to the faster water uptake by the plants, in the first days of a drying period, and the easier water recharge, even with low rainfall. When SP1 reached lower ASW than FS, intense drying periods occurred, which increased the importance of the trees water uptake, despite the higher pasture evapotranspiration at FS (Table 12 and Figure 8). In August 2015 and May 2016, ASW was lower at FS than at SP2 due to intense drying periods, combined with higher incoming solar radiation at FS, increasing water consumption by the pasture. When differences were observed between SP2 and SP4, rainfall interception or higher solar radiation at one or at the other positions were the main factors, since the root depth and density should be the same at both positions in the inter-row.

During the selected soil water recharge events, recharge was higher at SP1 due to the rainfall perpendicular to the rows (near South direction), with high wind speed, and its interception by the tree canopy, increasing rainfall at SP1 and decreasing it at the other silvopastoral positions (Figure 9). In the low rainfall event, recharge was 3.5 mm at FS due to the rainfall interception by the pasture (Figure 9), which had more biomass than at the silvopastoral positions. During the high rainfall event, rainfall interception was more important, since the wind speed was high (4.6 m s^{-1}) and the wind direction was perpendicular to the rows, effects that were confirmed by the measured throughfall, which was 45.2 mm at SP1 and 35.3 mm at SP3. These increases on recharge at SP1 may also be a consequence of improvements on soil structure and porosity, caused by tree roots, which can promote higher water infiltration and lower runoff. Pezzopane et al. (2015) also observed higher soil water recharge at the position below the trees than at the inter-row positions, with recharge until 70 cm depth, at the first one, and until 60 cm depth at the other positions, after a rainfall event of 90 mm.

During the soil water withdraw events, water consumption was faster at SP1 (Figure 10) due to the effect of the tree roots, which increased total root density at this position and, consequently, root water uptake, as also showed by Pezzopane et al. (2015). In the first withdraw event, this relationship was more evident, since the initial water content was similar at all positions, but in the second withdraw event, the soil at SP1 had lower initial water content, which promoted similar water consumption between 3/28/2016 and 4/8/2016 (Figure 10), due to the higher difficulty for water absorption at SP1, caused by the higher pressure of water retention at this position.

3.5 Conclusions

Silvopastoral systems promote alterations on rainfall distribution and soil water availability due to the rainfall interception and water uptake by the trees.

Throughfall amounts are reduced below the trees, under rainfall of low intensity and low wind speed; and reduced at the inter-row, under rainfall with high wind speed and wind direction perpendicular to the tree rows.

Available soil water until 1-m depth is affected by water uptake by the trees, decreasing it near the trees, and by shading and the windbreak effect, reducing evapotranspiration within the silvopastoral system.

Soil water recharge tends to be higher close to the trees, mainly when rainfall interception increases throughfall at this position or due to improvements on soil structure and porosity, which increase water infiltration and decrease runoff.

Soil water withdraw is faster below the trees, which is caused by the higher roots density and, consequently, more water absorption at this position.

REFERENCES

Allen, R.G., Pereira, L.S., Raes, D., Smith, M., 1998. Crop evapotranspiration – guidelines for computing crop water requirements. FAO, Rome.

Alvares, C.A., Stape, J.L., Sentelhas, P.C., Goncalves, J.L.M., Sparovek, G., 2013. Köppen's climate classification map for Brazil. Meteorol. Z. 22, 711-728. https://doi.org/10.1127/0941-2948/2013/0507

Baliscei, M.A., Souza, W., Barbosa, O.R., Cecato, U., Krutzmann, A., Queiroz, E.O., 2012. Behavior of beef cattle and the microclimate with and without shade. Acta Sci. Anim. Sci. 34, 409-415. https://doi.org/10.4025/actascianimsci.v34i4.15055

Benegas, L., Ilstedt, U., Roupsard, O., Jones, J., Malmer, A., 2014. Effects of trees on infiltrability and preferential flow in two contrasting agroecosystems in Central America. Agric. Ecosyst. Environ. 183, 185-196. https://doi.org/10.1016/j.agee.2013.10.027

Carvalho, M.M., Botrel, M.A., 2002. Arborização de pastagens: um caminho para a sustentabilidade de sistemas de produção animal a pasto. In: Forragicultura e pastagens: temas em evidência. UFLA, Lavras.

Feldhake, C.M., 2009. Forage evapotranspiration and photosynthetically active radiation interception in proximity to deciduous trees. Agric. Water Manag. 96, 1170-1174. https://doi.org/10.1016/j.agwat.2009.02.011

Garcia, A.R., Matos, L.B., Lourenco Junior, J.B., Nahum, B.S., Costa, N.A., 2010. Increased reproductive efficiency of dairy buffaloes due to silvopastoral system adoption in the Eastern Amazon. Rev. Vet. 21, 914-915.

Gyenge, J.E., Fernández, M.E., Dalla Salda, G., Schlichter, T.M., 2002. Silvopastoral systems in Northwestern Patagonia II: water balance and water potential in a stand of *Pinus ponderosa* and native grassland. Agrofor. Syst. 55, 47-55. https://doi.org/10.1023/A:1020269432671

IPCC, 2013. Climate Change 2013: The Physical Science Basis. Contribution of Working Group I to the Fifth Assessment Report of the Intergovernmental Panel on Climate Change. Cambridge University Press, Cambridge. https://doi.org/10.1017/CBO9781107415324

Lin, B.B., 2010. The role of agroforestry in reducing water loss through soil evaporation and crop transpiration in coffee agroecosystems. Agric. For. Meteorol. 150, 510-518. https://doi.org/10.1016/j.agrformet.2009.11.010

Nair, P.K.R., 1993. An introduction to Agroforestry. Kluwer Academic Publishers, Dordrecht.

Pezzopane, J.R.M., Bosi, C., Nicodemo, M.L.F., Santos, P.M., Cruz, P.G., Parmejiani, R.S. 2015. Microclimate and soil moisture in a silvopastoral system in southeastern Brazil. Bragantia 74, 110-119. https://doi.org/10.1590/1678-4499.0334

Pollock, K.M., Mead, D.J., McKenzie, B.A., 2009. Soil moisture and water use by pastures and silvopastures in a sub-humid temperate climate in New Zealand. Agrofor. Syst. 75, 223-238. https://doi.org/10.1007/s10457-008-9172-z.

Poppenborg, P., Hölscher, D., 2009. The influence of emergent trees on rainfall distribution in a cacao agroforest (Sulawesi, Indonesia). Flora 204, 730-736. https://doi.org/10.1016/j.flora.2008.10.003

Sahin, H., Anderson, S.H., Udawatta, R.P., 2016. Water infiltration and soil water content in claypan soils influenced by agroforestry and grass buffers compared to row crop management. Agrofor. Syst. 90, 839-860. https://doi.org/10.1007/s10457-016-9899-x

Schlotzhauer, S.D., Littell, R.C., 1987. SAS System for Elementary Statistical Analysis, NC: SAS Institute Inc, Cary.

Siles, P., Vaast, P., Dreyer, E., Harmand, J-M., 2010. Rainfall partitioning into throughfall, stemflow and interception loss in a coffee (Coffea arabica L.) monoculture compared to an agroforestry system with Inga densiflora. J. Hydrol. 395, 39-48. https://doi.org/10.1016/j.jhydrol.2010.10.005

Thornthwaite, C.W., Mather, J.R. 1955. The water balance. Centerton, New Jersey.

Tian, S., Cacho, J.F., Youssef, M.A., Chescheir, G.M., Fischer, M., Nettles, J.E., King, J.S., 2017. Switchgrass growth and pine-switchgrass interactions in established intercropping systems. GCB Bioenergy 9, 845-857. https://doi.org/10.1111/gcbb.12381

Toba, T., Ohta, T., 2008. Factors affecting rainfall interception determined by a forest simulator and numerical model. Hydrol. Process. 22, 2634-2643. https://doi.org/10.1002/hyp.6859

Wilson, J.R., 1998. Influence of planting four tree species on the yield and soil water status of green panic pasture in subhumid southeast Queensland. Trop. Grassl. 32, 209-220.

4. APSIM NEXT GENERATION TROPICAL PASTURE MODEL AND ITS PARAMETERIZATION FOR PIATÃ PALISADEGRASS

ABSTRACT

The APSIM modelling framework has some deficiencies for simulating tropical pastures, which requires improvements in this model for simulating such species. The aim of this study was to develop a state-of-the-art tropical pasture model in the APSIM modeling framework and to parameterize and test it for simulating Piatã palisadegrass growth, under cutting and rotational grazing managements. For this purpose, four field experiments were conducted to investigate cutting management under irrigated and rainfed conditions and grazing management under rainfed conditions with high and low N supply. Two experiments were used for the model parameterization and with the remaining two used for its testing. The forage mass simulations performed in this study showed good agreement between observed and estimated data (R^2 between 0.82 and 0.97, d between 0.92 and 0.98, and NSE ranging from 0.72 to 0.92) for the various managements and environmental conditions. Important aspects of the APSIM-Tropical Pasture required to simulate the experimental data included initial growth simulations after pasture sowing, growth partitioning and senescence during flowering, and the reallocation and retranslocation of plant dry matter and nitrogen. The simulations for grazing systems were important in identifying the main needs for estimating their related processes and interactions such as to account for biomass losses during and after grazing due to the damage caused by animals. Even considering the promising performance of the APSIM-Tropical Pasture, it already needs to be tested in other locations, climate conditions, soils, and grazing or cutting intensities, to prove its accuracy and reach enough confidence.

Keywords: *Urochloa brizantha* cv. Piatã; Forage; Management; Cutting; Rotational grazing; Tropical grass

4.1. Introduction

Grasslands comprise about 80% of the agricultural lands around the world, representing a great range of ecosystems (Steinfeld et al. 2006; Wright et al. 2006). In Brazil, around 196 million hectares are occupied by pastures (FAO 2014). Tropical grasses are used as summer season forage in subtropical areas and as perennial forage in tropical regions, mainly due to their high yields (Tsuruta et al. 2015). The majority of cultivated pasture areas in Brazil is currently established with grasses of the Urochloa (syn Brachiaria) genus, which has shown excellent adaptation to most of the Brazilian environmental conditions, promoted by their C_4 metabolism.

Crop models are highly useful tools for understanding the agricultural systems and the interactions between their components, such as weather, soil, genotypes, among others. Specifically for pastures, crop modeling may assist in forage management, production, and efficiency (Lara et al. 2012). Forage simulation models may also allow better control over the feed demand and supply at the farm level, and help farmers to plan activities and make decisions (Barioni et al. 2003). Among the several types of crop models, the mechanistic ones are those based on the understanding and systematization of the main plant physiological processes and the interactions with other processes in the agroecosystem (Andrade et al. 2015). This kind of approach has being applied for tropical pastures simulation by the following models: ALMANAC (Agricultural Land Management Alternative with Numerical Assessment Criteria), Century, Orchidee Grassland Management, CROPGRO Perennial Forage, APSIM (Agricultural production systems simulator), and STICS (*Simulateur mulTIdisciplinaire pour les Cultures Standard*), all of them with satisfactory performance.

The ALMANAC model was used by Kiniry et al. (2007) for simulating growth and yield of bermudagrass (*Cynodon dactylon*) and bahiagrass (*Paspalum notatum*); Century was used for simulating several tropical grasslands (Parton et al. 1993); Orchidee was tested for *Panicum maximum* (Coltri et al. 2014); the CROPGRO Perennial Forage model of DSSAT (Decision Support System for Agrotechnology Transfer) was created for bahiagrass (Rymph et al. 2004) and adapted for bermudagrass (Alderman 2008), Xaraés palisadegrass (*Urochloa brizantha* cv. Xaraés) (Pedreira et al. 2011), Tanzânia guineagrass (*Panicum maximum* cv. Tanzânia) (Lara et al. 2012), Marandu palisadegrass (*U. brizantha* cv. Marandu) (Pequeno et al. 2014) and Convert HD 364 brachiariagrass (*U. hybrid* cv. Mulato II) (Pequeno et al. 2017); the APSIM was initially parameterized for *Panicum coloratum* cv. Bambatsi, and Araújo et al. (2013) adapted it for *Panicum maximum* cv. Mombaça; and recently, the STICS model was used for simulating Piatã palisadegrass (*U. brizantha* cv. Piatã) growth under continuous stocking (Santos 2016).

The APSIM modelling framework consists of a mechanistic model composed of modules developed to simulate biophysical processes in agroecosystems (Keating et al. 2003; Holzworth et al. 2014). APSIM provides models for over thirty crops, pastures and tree species through its plant modules, as well as soil processes related to water (SoilWat), N and soil organic matter (SoilN), and surface organic matter (SurfaceOM) (Probert et al. 1998), while also providing a flexible agricultural management capability that enables the user to set crop rotations and management (Moore et al. 2014). The APSIM modules available for simulating pasture growth and yield are the *AgPasture* model (Johnson et al. 2008), which simulates mixed pastures of C_3 and C_4 grasses and legumes; *Lucerne* (Robertson et al. 2002), which is employed to simulate lucerne (*Medicago sativa*) and recently was adapted by Ojeda et al. (2016) for simulating switchgrass; and *Growth*, which simulates trees and tropical pastures growth.

The APSIM-Growth has some deficiencies for simulating tropical pastures, which are mainly related to the absence of capability to change partitioning and senescence between phenological phases, the specific leaf area that cannot be calculated considering environmental factors, and the absence of a storage organ. Then, improvements are required in this model for simulating these species. However, the first adaptation of a mechanistic model for grazing systems was performed by Santos (2016), however, these models never were adapted for tropical grasses under rotational grazing. In this context, the aim of this study was to develop a state-of-the-art tropical pasture model in the APSIM Plant Modelling Framework and to parameterize and test this model for simulating Piatã palisadegrass growth under cutting and rotational grazing management.

4.2. Material and methods

4.2.1. Model structure

The APSIM-Tropical Pasture model described here was developed for APSIM Next Generation (Holzworth et al. 2014; Holzworth et al. 2015) using the APSIM Plant Modelling Framework, described by Brown et al. (2014), which allows the model developer to choose, from a library of commonly-used functions or algorithms for plant modeling. The model is then built with the calculations necessary for the crop of interest and configured into a model description using the eXtensible Markup Language (XML). The role of the APSIM-Tropical Pasture in an APSIM simulation is to perform the calculations of growth, resource use and organic matter flows for the pasture and to send their results to the other models within the simulation.

APSIM-Tropical Pasture aims to be a generic pasture model that may be used for simulating the growth of all tropical grass species including the effects of cutting or grazing based managements on the pasture growth and productivity, needing few adjustments and a calibration of its parameters for each species or cultivar. The main equation for growth within APSIM-Tropical Pasture is:

$$G = RUE \times RI \times \min(Ft, Fn, Fvpd) \times Fw \quad (1)$$

where: G is the daily pasture growth (g m^{-2}), RUE is the whole plant´s solar radiation use efficiency (g MJ^{-1}), which represents the ratio between dry matter accumulation (root + shoot growth) and total incoming solar radiation intercepted, RI (MJ). RI is calculated through the Beer-Lambert law, using the leaf area index (LAI) estimated by the model and an extinction coefficient (k). Ft is the temperature factor, which is determined by the cardinal temperatures, varying linearly from 0 to 1 between the minimum base temperature (Tb) and the first optimum temperature (TO_1), remaining constant (= 1) between the TO_1 and the second optimum temperature (TO_2), and then decreasing linearly from 1 to 0 between TO_2 and the maximum base temperature (TB). Fn is the nitrogen factor, which is determined by a linear interpolation from the minimum (LNC_{min}) to the optimum (LNC_{opt}) leaf nitrogen concentration. Fvpd is the vapor pressure deficit (VPD) factor, which works similarly to Fn, and Fw is the water stress factor determined by the ratio between water supply and plant water demand. Specifically, Ft, Fn, and Fvpd are regulated by a minimum function, which imposes the Liebig’s minimum law, meaning that only the most limiting factor is used for the growth calculations.

APSIM-Tropical Pasture considers four sub-models related to the following plant organs: leaf, stem, root and storage organ. The leaf sub-model calculates specific leaf area (SLA), LAI (multiplying SLA by leaf mass), RI and photosynthesis (Equation 1), which will estimate the dry matter (DM) to be partitioned among the organs. Additionally, this sub-model has a leaf kill function for frost, regulated by daily minimum temperature; and the leaf senescence and leaf detachment (addition of dead leaves to surface organic matter) calculations. The stem, root, and storage organ sub-models also have their senescence and detachment calculations, such as the leaf sub-model, and have a N demand to assimilate the DM provided during partitioning. The root sub-model calculates root depth, starting from the sowing depth and then considering a fixed root front velocity until a given value of maximum root depth is achieved; root length density for each soil layer, based on root depth, root biomass and a specific root density provided by the user; and has capabilities that allow to determine maximum daily N uptake and modify water uptake, based on LAI, and N uptake, based on root length density and soil water. The storage organ sub-model describes the crown of bunch grasses, but may consider stolon or rhizome for species that have these organs.

APSIM-Tropical Pasture also has a DM and N arbitrator which calculates partitioning of DM and N within the plant. The four organ sub-models calculate demands for structural and non-structural biomass and N which is partitioned by the arbitrator from daily growth and N uptake. Non-structural N is reallocated from senescening parts of organs to satisfy unmet demands. The root and storage organ sub-models have another capability that allows DM and N retranslocation, i.e. both can work as storage organs and provide non-structural DM and N to supply the demand of other organs. Furthermore, the organs provide functions to modify partitioning, senescence, reallocation and retranslocation based on several factors, such as plant age, daylength, among others, which may be associated with phenological phases; and SLA calculations that take into account water deficit and shading effects.

Additionally, APSIM-Tropical Pasture has a cutting management capability, which allows the user to set the residual leaf and stem mass after a cutting or a grazing event using a management scripting language (Moore et al. 2014).

The rest of the calculations required to simulate a pasture system are provided by the APSIM modeling framework. The simulations of water, N, and surface organic matter processes are performed using the standard SoilWat, SoilN and SurfaceOM modules of APSIM (Probert et al. 1998), and potential evapotranspiration is calculated by the MicroClimate module (Snow and Huth 2004), using the Penman-Monteith equation (Allen et al. 1998).

4.2.2. Parameterization for Piatã palisadegrass

The data used to parameterize the model were collected in two field experiments carried out at Embrapa Pecuária Sudeste, in São Carlos, state of São Paulo, Brazil (21°57'42" S, 47°50'28" W, 860 m), in pastures of *Urochloa* (syn. *Brachiaria*) *brizantha* (Hochst ex A. Rich.) Stapf cv. BRS Piatã. The climate of this site is Cwa (Köppen) with a cool and dry season from April to September (average air temperature of 19.9ºC and total rainfall of 250 mm), and a warm and wet season from October to March (average air temperature of 23.0ºC and total rainfall of 1100 mm) (Alvares et al. 2013).

4.2.2.1. Experiment 1:

This experiment was conducted under cutting management with both irrigated and rainfed conditions. Sowing was in February 2011 (after soil preparation and corrections of chemical attributes) in 5 x 5 m plots, with four replications. Nine growth cycles were performed from April 2011 to July 2012. For every cycle the final forage was assessed, with the grass uniformly cut down to 0.2 m above the soil surface (stubble height). Each plot was fertilized with 30 kg ha^{-1} of N at the beginning of each cycle, totaling approximately 240 kg ha^{-1} per year. Growth cycles ranged from 35 days in the summer to 55 days in the winter, according to the meteorological conditions of each cycle, which are presented in Table 15.

Table 15. Average air temperature (Tavg), average incoming solar radiation (SR), and total rainfall (RF), during each cycle of the experiments used in the APSIM-Tropical Pasture model parameterization and test.

	Weather variable	Cycle										
		1	2	3	4	5	6	7	8	9	10	11
Exp. 1	Tavg (ºC)	17.2	17.7	20.7	20.3	22.0	21.7	22.5	19.8	17.4	-	-
	SR (MJ m^{-2} d^{-1})	14.0	14.0	18.2	20.9	21.5	18.8	19.4	15.1	11.8	-	-
	RF (mm cycle^{-1})	75.0	12.4	63.6	176.0	299.0	450.6	81.8	238.0	236.0	-	-
Exp. 2	Tavg (ºC)	25.0	22.5	21.1	20.2	19.5	17.9	20.4	22.4	23.3	22.6	22.3
	SR (MJ m^{-2} d^{-1})	24.5	19.4	14.0	15.0	12.7	11.3	17.1	16.3	18.9	17.8	16.4
	RF (mm cycle^{-1})	176.0	226.8	283.8	59.4	63.6	60.5	5.3	175.5	184.2	236.3	603.7
Exp. 3	Tavg (ºC)	19.1	15.8	18.7	19.0	20.8	23.3	22.1	22.9	24.6	-	-
	SR (MJ m^{-2} d^{-1})	15.7	12.7	14.4	16.2	18.1	22.2	17.9	18.6	19.9	-	-
	RF (mm cycle^{-1})	36.6	26.4	61.6	220.0	115.8	164.0	336.2	313.0	272.2	-	-
Exp. 4	Tavg (ºC)	23.8	22.6	22.2	17.9	-	-	-	-	-	-	-
	SR (MJ m^{-2} d^{-1})	20.9	18.4	19.0	11.4	-	-	-	-	-	-	-
	RF (mm cycle^{-1})	148.3	213.6	7.1	249.4	-	-	-	-	-	-	-

Sprinkler irrigation was applied, with a variable irrigation schedule, taking into account the accumulated difference between reference evapotranspiration (ETo) and rainfall. Irrigation was commenced when the readily available water (RAW) was completely consumed and ceased when soil moisture reached field capacity. The RAW considered was 20 mm, representing 33.3% of the soil water holding capacity (SWHC) to 0.6 m depth.

Photosynthetically active radiation (PAR) interception in the irrigated plots was measured at least eight times per cycle, using a ceptometer (AccuPAR LP-80, Decagon Devices, Pullman, WA, USA), which recorded incoming PAR above pasture canopy and transmitted PAR at 0.2 m above the soil surface (stubble height).

During each growth cycle, four forage collections were performed, being taken two subsamples per plot for quantifying the biomass accumulation (above 20 cm), using a 0.25 m^2 (0.5 x 0.5 m) quadrat. The forage collected was immediately weighed and subsamples of each plot were mixed. From this two ~0.2 kg green mass samples were taken, one sample designed to perform morphological separation (leaf, stem and dead material) and another to determine the dry matter (DM). The percentage of DM from the morphological fractions was calculated by weighing both subsamples before and after drying them in an oven at 65ºC until they reached a constant weight. Having the weight of the green mass harvested in 0.25 m^2, the pasture DM productivity was estimated from the fractions in this area, and then extrapolated to 1 ha (kg ha^{-1}).

Once the morphological separation was performed, the fractions representing the leaves were used to determine the leaf area with a leaf area meter, model LI-3100C (Li-Cor, Lincoln, Nebraska, USA). Using leaf area and the area of ground from where forage was harvested (0.25 m^{2}), the leaf area index (LAI) was determined.

As stubble mass and its morphological composition were not assessed in this experiment, these data were taken from an irrigated experiment carried out between 2009 and 2010 in the same area (Cruz 2010), described in the model test section as experiment 3. For the irrigated plots the same stubble values were considered for the corresponding period, but for the rainfed plots, these data were estimated considering null accumulation during the dry period, and the same accumulation of the irrigated plots in the wet periods. Crown mass was determined by dividing the stubble stem mass by 2, so it was considered as the stem mass below 10 cm.

4.2.2.2. Experiment 2:

This experiment was conducted under grazing management and rainfed conditions, during 11 growth cycles, from December 2014 to January 2016. The pasture was grazed by beef cattle in rotational grazing. The resting period was 30 days and the period of occupation was six days. Soil fertilization comprised as the application of 50 kg ha^{-1} of N in the 1st, 2nd, 3rd, and 4th cycles, immediately after grazing. The meteorological conditions of each growth cycle are presented in Table 15.

Each growth cycle had five pasture assessments at approximately 0, 9, 16, 23 and 30 days after grazing. These assessments were obtained by cutting the forage at 10 cm above the ground. To determine the forage biomass and biometric characteristics below 10 cm, four assessments were done, one in each season of the year, cutting the pasture until the ground level. Additionally, to determine the reproductive and the vegetative periods, apical meristems were analyzed at the end of each resting period, being collected 10 representative tillers per plot, cut longitudinally and observed with a magnifying glass to be classified as vegetative or reproductive, so, when there was at least one reproductive tiller per plot, the period was considered reproductive.

In each harvesting, leaf mass, stem mass, dead material mass, LAI, and SLA were quantified, following the same procedures above described for the experiment 1. Crown mass was considered as the measured stem mass below 10 cm.

4.2.2.3. Parameterization process

The first step of the model parameterization process determined the minimum base temperature (Tb), k, RUE, and standard SLA, using the data from the irrigated plots of experiment 1.

Tb was determined using Arnold's (1959) least variability method. For this method, degree-days were accumulated (ADD) for each growth cycle, considering the period from a cut until when PAR interception reached 95% (Moreno et al. 2014), with Tb ranging from 0 to 20^{o}C, and calculations for each 0.1^{o}C increase. The temperature that minimized the cycle deviation (SDday), in days, was considered as the pasture's Tb. Based on this criterion five growth cycles were used (cycles 1, 2, 3, 5 and 6).

The total degree-days accumulated (ADD) during the growth period was calculated based on daily degree-days (DD_i) obtained by the following equations (Pereira et al. 2002):

$$DD_i = (\frac{T\max_i + T\min_i}{2} - Tb) \qquad \text{for Tmin > Tb} \quad (2)$$

$$DD_i = \frac{(T\max_i - Tb)^2}{2(T\max_i - T\min\ )} \qquad \text{for Tb > Tmin} \quad (3)$$

where: $Tmax_i$ is the daily maximum air temperature and $Tmin_i$ the daily minimum air temperature, in ^{o}C.

Once this study was conducted under field conditions where the maximum mean temperature was 23.7^{o}C, it was not possible to determine the optimal (TO_1 and TO_2) and the maximum base temperatures (TB), therefore, these values were taken from Pequeno et al. (2014), who obtained TO_1 = 30.2ºC, TO_2 = 40ºC and TB = 45ºC for *Urochloa brizantha* cv. Marandu.

Light extinction coefficient and PAR use efficiency were determined using the pasture growth data from the irrigated plots of the first experiment and only from periods when growth and partitioning were not affected by initial plant development or flowering (the end of the cycle 3, the whole cycles 4 and 8, and the beginning of the cycles 5 and 6).

Light extinction coefficient (k), for each pasture assessment, was determined by adapting the Beer-Lambert law:

$$k = -\left[\frac{\ln\left(1 - \frac{I}{100}\right)}{LAI}\right] \quad (4)$$

where: I is the radiation interception (%) and LAI is the leaf area index, both measured at the stubble height.

PAR use efficiency was determined as the slope of the linear regression between forage dry mass and the corrected amount of PAR intercepted ($ParI_{corr}$), which was calculated by:

$$ParI_{corr} = ParI \times Ft \quad (5)$$

where: ParI is the amount of PAR intercepted and Ft a temperature factor calculated using the four cardinal temperatures.

As PAR interception was measured at the stubble height (20 cm), it was necessary to do a correction for the interception by the leaves below this height. For that the Beer-Lambert law was applied:

$$I = Io' \times (1 - e^{-k \times LAI'}) \quad (6)$$

where: Io' is the PAR transmitted by the canopy above the stubble height, LAI' is the LAI below the stubble height and k is the same extinction coefficient previously determined for the canopy above the stubble height.

To determine the aboveground RUE, as only PAR interception was measured, PAR use efficiency was multiplied by 0.5, considering that the proportion of PAR from the total incoming radiation was 50%. To calculate the whole plant RUE, the aboveground RUE was divided by 0.8, considering that 20% of total accumulation was used for root growth.

Standard SLA was calculated as the average of the SLA values (ratio between LAI and leaf mass) obtained from the irrigated plots of the Experiment 1 and only from periods when the growth and partitioning were not affected by initial plant development or flowering.

The second parameterization step added the pasture management operations (sowing, fertilization, irrigation and cutting events) into the APSIM-Tropical Pasture. The management practices were specified using a specific scripting language (Moore et al., 2014). Sowing was performed considering a population of 225 plants m^{-2}, with a sowing depth of 10 cm and row spacing of 20 cm.

The third parameterization step was to adjust the parameters of the growth simulations for each organ under cutting management, and subsequently, changing the partitioning and senescence parameters for the grazing management experiment.

Specifically, in pastures under grazing, there are forage mass losses after a grazing event which occur due to physical damage caused by the animals. Therefore, it was necessary to use the cutting management capability to set the biomass losses after grazing. The losses were set on the first day after grazing and their values were adjusted to achieve the best simulation for the last productivity data of each cycle.

Concomitantly with this process, the soil water and nitrogen simulations were calibrated. For soil water, assessments were obtained twice a week, in the two parameterization experiments, using a portable capacitance probe (Diviner 2000, SENTEK Pty Ltd., Stepney, SA, Australia) to measure soil moisture at every 0.1 m until 1.0 m of depth. These were used to adjust all the SoilWat model parameters for each experiment. Soil nitrogen content was not measured during the experiments. Adjustments were done based on the effect of simulated soil nitrogen on pasture growth calculations, being necessary to create a Leaching Control Tool to decrease NO_3 leaching in 95% from the value simulated by the model, since the SoilWat model overestimated leaching for the soil of the experimental site, which showed to be inadequate to the pasture growth.

Initial nitrate, ammonium, organic carbon contents and soil pH were assumed to be the same for all the experiments. Initial nitrate content was 86.5 kg ha^{-1}, initial ammonium content was 59.6 kg ha^{-1}, initial organic carbon was 13.8 kg m^{-2} in which 7.7 kg m^{-2} were inert, and soil pH ranged from 5.5 in the surface layer to 6.3 in the deeper layer. Initial surface organic matter was different between experiments: Experiments 1 and 3 had 10 kg ha^{-1}, due to the soil tillage performed before sowing; Experiment 2 had 1000 kg ha^{-1}, as it had an established pasture; Experiment 4 had a value equal to the last one of the simulation of Experiment 2 as they were conducted sub sequentially in the same area.

The daily meteorological data used for the simulations (incoming solar radiation, maximum and minimum air temperatures, rainfall, wind speed and relative humidity) were taken from an automatic weather station installed near the experiments, under standard conditions (Allen et al. 1998).

4.2.3. Model testing

Data of forage mass obtained from two experiments with Piatã palisadegrass, conducted in the same location where the parameterization experiments were carried out, were used to test the model efficiency to simulate the pasture growth.

4.2.3.1. Experiment 3

This experiment was carried out in the same area of the Experiment 1, from February 2009 to March 2010. Sowing was in February 2009 in 5 x 2 m plots, with four replications. From April 2009 to March 2010, nine growth cycles were performed, lasting from 28 to 36 days and with forage collection at the final day. Every cycle, after the forage assessment, the plots had the grass uniformly cut down to the stubble height (0.25 m), when a new growth cycle was initiated, with each plot being fertilized with 30 kg ha^{-1} of N, totaling approximately 300 kg ha^{-1} per year. The meteorological conditions of each cycle are presented in Table 15.

Sprinkler irrigation was applied in this experiment with a variable irrigation schedule taking into account the soil moisture measured with a capacitance probe. Irrigation was commenced when 25% of the soil water holding capacity (SWHC) to 0.6 m depth was consumed and was applied to return the soil moisture to field capacity.

The forage collections were performed using samples above the stubble height, to quantify canopy mass; and samples below the stubble height until the ground level, to assess stubble mass. These samples were submitted to the same procedures considered in the Experiment 1.

4.2.3.2. Experiment 4

This experiment was conducted under grazing management and rainfed conditions, in the same area used for Experiment 2 and comprised four growth cycles, from January to June 2016. In this experiment, forage assessments were taken only at 0 and 30 days after grazing. The pasture management and forage collection procedures were the same of Experiment 2. Soil fertilization was applied only in the 3rd cycle, with 50 kg ha^{-1} of N, immediately after grazing. The meteorological conditions of each cycle are presented in the Table 15.

4.2.4. Statistical analysis of model performance

Several statistical indexes were used to evaluate the model performance for estimating pasture growth in relation to the environmental conditions observed throughout the field experiments, previously described. These statistics were:

a) linear regression between observed (O) and estimated (E) values of each variable, and the respective coefficient of determination (R^2);

b) Willmott (1981) agreement index (d), which quantifies model´s accuracy:

$$d = 1 - \frac{\sum_{i=1}^{n}(O_i - E_i)^2}{\sum_{i=1}^{n}(|E_i - \bar{O}| + |O_i - \bar{O}|)^2} \tag{7}$$

c) Nash-Sutcliffe efficiency (NSE), which describes the model accuracy and, as suggested by Moriasi et al. (2007), means satisfactory model performance when its values are higher than 0.5, and good performance when greater than 0.65:

$$NSE = 1 - \frac{\sum_{i=1}^{n}(E_i - O_i)^2}{\sum_{i=1}^{n}(O_i - \bar{O})^2} \tag{8}$$

d) Mean error (ME), as an indicator of bias in the simulations

$$ME = \left(\frac{1}{n}\right)\sum_{i=1}^{n}(E_i - O_i) \tag{9}$$

e) Mean absolute error (MAE)

$$MAE = \left(\frac{1}{n}\right)\sum_{i=1}^{n}|E_i - O_i| \tag{10}$$

f) Root mean square error (RMSE)

$$RMSE = \sqrt{\left[\left(\frac{1}{n}\right)\sum_{1=i}^{n}(O_i - E_i)^2\right]} \tag{11}$$

4.3. Results

4.3.1. APSIM-Tropical Pasture Parameterization

The minimum base temperature (Tb) found for Piatã palisadegrass was 8.9ºC, the light extinction coefficient (k) was 0.65, the standard SLA was 0.02 m^2 g^{-1}, and the PAR use efficiency was 2.31 g MJ^{-1} (Figure 11), which resulted in whole plant radiation use efficiency (RUE) of 1.44 g MJ^{-1}.

The APSIM-Tropical Pasture calibration for Piatã palisadegrass resulted in a range of parameters (Tables 16, 17, 18, 19 and 20) that optimized growth predictions considering all managements (irrigated and rainfed, low and high nitrogen supply, cutting and grazing) and environmental conditions (dry and wet seasons, warm and cool periods) assessed in the two parameterization experiments. Among the leaf sub-model parameters (Table 16); k (0.65), RUE (1.44 g MJ^{-1}), Ft, Fn (with LNC_{opt} = 0.021 g g^{-1} and LNC_{min} = 0.005 g g^{-1}), Fw, standard

SLA (0.02 m^2 g^{-1}) and its age and water factors are the most important for growth calculations. The main parameters for root growth were root front velocity (20 mm day^{-1}), root senescence rate (0.001 day^{-1}), the maximum and minimum root N concentrations (0.003 and 0.001 g g^{-1}, respectively), and specific root length (100 m g^{-1}) (Table 17). The most important parameters for stem and crown growth were maximum and minimum N concentrations (0.003 and 0.001 g g^{-1}, respectively) (Table 18). Additionally, partitioning and senescence parameters also were essential for growth simulations, mainly to show the differences caused by pasture development and management (Tables 19 and 20).

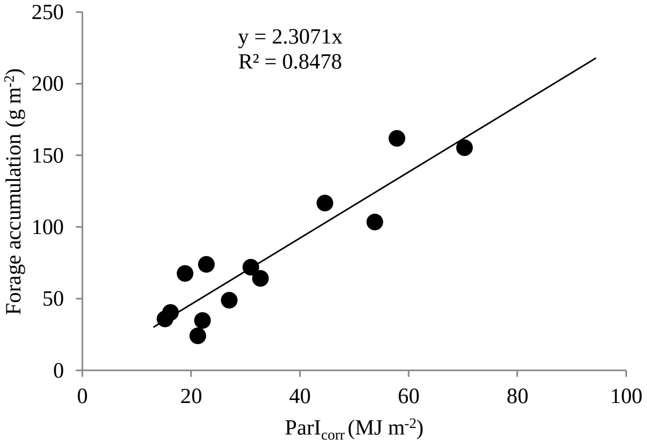

Figure 11. Linear regression between forage accumulation and intercepted PAR corrected by temperature (ParI$_{corr}$), in order to determine PAR use efficiency (regression slope).

Dry matter partitioning was considered the same for cut and grazed pasture during the initial growth period, since initial growth was not assessed in the experiment with grazing (Table 19). These values were regulated by pasture age, from sowing to when the pasture was 0.71 years old, with the partitioning fractions varying to age 0.7 years. Partitioning of dry matter production to root growth was 33% for early growth to build the root system but this decreased from 0.2 years until the age 0.71 years, when the pasture was considered completely established and partitioning values were equal to those obtained for adult plants (Table 19). Partitioning during vegetative and reproductive periods (after the age 0.71 years) was regulated by daylength (Table 19). The assessments of apical meristems performed in the Experiment 2 indicated that meristems were induced to flowering when daylength was increased to 13 h and remained flowering until daylength was reduced to 11 h. Partitioning into root was suppressed during this reproductive period, since the stem elongation during flowering increased the dry matter demand for stem and crown growth. However, analysis of the effects of cutting and grazing management on partitioning demonstrated that the cut pasture presented more dry matter going to crown than the grazed pasture, which was a consequence of the higher senescence resulting from the removal of the majority of the apical meristems and the consequent death of tillers under cutting management. For grazed pasture, in vegetative periods after a dry season, when a great part of the crown tissues died, there was more dry matter going to crown and less to leaf (Table 19), in order to grow new tillers.

Senescence was differentiated between pasture management systems for aboveground organs, but it was the same for the root system (Table 20). For the pasture under cutting management, senescence of leaf, stem, and crown was increased during the reproductive phase (Table 20). For pasture under grazing, senescence of all organs remained the same during all the phenological phases (Table 20), since the animals tend to do not remove a great part of the apical meristems, avoiding a massive death of tillers.

Table 16. Leaf sub-model parameters calibrated for Piatã palisadegrass.

Parameter	Unit	Value
Initial plant weight	g plant^{-1}	0.01
Initial plant leaf mass	g plant^{-1}	0.01
Leaf structural fraction	0-1	0.9
Light extinction coefficient (k)	-	0.65
Leaf maximum N concentration	g g^{-1}	0.021
Leaf minimum N concentration	g g^{-1}	0.005
Leaf N reallocation factor	day^{-1}	0.5
Leaf detachment time	days	30
Whole plant rad. use effic. (RUE)	g MJ^{-1}	1.44
Temperature factor (Ft)	x: temperature (ºC)	x: 8.9, 30.2, 40.0, 45.0
	y: Ft value	y: 0.0, 1.0, 1.0, 0.0
Vapour press. def. factor (Fvpd)	x: VPD (kPa)	x: 0.0, 10.0, 50.0
	y: Fvpd value	y: 1.0, 1.0, 1.0
Nitrogen factor (Fn)	x: N conc. (g g^{-1})	x: 0.005, 0.021
	y: Fn value	y: 0.0, 1.0
Water deficit factor (Fw)	x: supply/demand	x: 0.0, 1.0
	y: Fw value	y: 0.0, 1.0
Leaf kill function for frost	x: min. temp. (ºC)	x: 0.0, 2.0
	y: factor value	y: 0.0, 1.0
Standard SLA	m^2 g^{-1}	0.020
Age factor on SLA	x: pasture age (years)	x: 0.0, 0.3, 0.7
	y: SLA (m^2 g^{-1})	y: 0.015, 0.018, 0.020
Water factor on SLA	x: Fw	x: 0.0, 0.8, 1.0
	y: factor value	y: 0.0, 0.4, 1.0

The values of forage mass losses after grazing adjusted for each cycle of the experiment with pasture under grazing, considered only losses of leaf and stem, assuming that crown (stem below 10 cm) did not loss biomass due to grazing damages. The biomass losses tended to be higher in the summer cycles, when forage mass was higher (Table 21). These values ranged from 200 kg ha^{-1} in the 9th cycle to 1800 kg ha^{-1} in the 2nd cycle, whereas leaf mass losses ranged from 100 kg ha^{-1} in the 9th cycle to 800 kg ha^{-1} in the 1st cycle, and stem mass losses from 100 kg ha^{-1} in the 4th and 9th cycles to 1500 kg ha^{-1} in the 2nd cycle (Table 21).

Table 17. Root sub-model parameters calibrated for Piatã palisadegrass.

Parameter	Unit	Value
Root front velocity	mm day^{-1}	20
Root senescence rate	Fraction (0-1) day^{-1}	0.001
Root maximum N concentration	g g^{-1}	0.003
Root minimum N concentration	g g^{-1}	0.001
Maximum daily N uptake	g plant^{-1}	6.0
Maximum root depth	mm	10000
Root structural fraction	0-1	0.8
Water uptake (KL) modifier	x: LAI	x: 0.0, 3.0, 10.0
	y: factor value	y: 1.0, 1.0, 1.0
NO_3 uptake modifier (KNO3)	x: Root length dens.	x: 0.0, 0.003
	y: NO_3 uptake	y: 0.03, 0.03
NH_4 uptake modifier (KNH4)	x: Root length dens.	x: 0.0, 0.003
	y: NH_4 uptake	y: 0.0, 0.0
N uptake soil water factor	x: Root.RWC	x: 0.0, 0.5, 1.0
	y: factor value	y: 1.0, 1.0, 1.0
Initial root mass	g plant^{-1}	0.02
Specific root length	m g^{-1}	100
Root nitrogen demand switch	(0-1)	1.0

Table 18. Stem and crown sub-models parameters calibrated for Piatã palisadegrass.

Parameter	Unit	Value
Stem N reallocation factor	0-1	0.0
Stem N retranslocation factor	0-1	0.0
Stem DM retranslocation factor	0-1	0.0
Stem maximum N concentration	g g^{-1}	0.003
Stem minimum N concentration	g g^{-1}	0.001
Initial stem mass	g m^{-2}	0.0
Stem structural fraction	0-1	1.0
Stem detachment rate	Fraction (0-1) day^{-1}	0.01
Stem DM conversion efficiency	0-1	1.0
Stem nitrogen demand switch	(0-1)	1.0
Crown N reallocation factor	0-1	0.0
Crown maximum N concentration	g g^{-1}	0.003
Crown minimum N concentration	g g^{-1}	0.001
Initial crown mass	g m^{-2}	0.0
Crown structural fraction	0-1	0.5
Crown detachment rate	Fraction (0-1) day^{-1}	0.01
Crown DM conversion efficiency	0-1	1.0
Crown nitrogen demand switch	(0-1)	1.0

Table 19. Dry matter partitioning between organs for Piatã palisadegrass under cutting and grazing managements, in different pasture ages, daylength values and phenological phases.

Age (years)	Daylength (hours)	Phenological phase	Partitioning fraction (0-1)							
			Cutting				Grazing			
			Leaf	Root	Stem	Crown	Leaf	Root	Stem	Crown
0.00		Initial growth	0.50	0.33	0.09	0.08	-	-	-	-
0.20			0.50	0.33	0.09	0.08	-	-	-	-
0.30			0.55	0.25	0.10	0.10	-	-	-	-
0.40			0.55	0.25	0.10	0.10	-	-	-	-
0.71			0.55	0.20	0.15	0.10	-	-	-	-
> 0.71		Vegetative	0.55	0.20	0.15	0.10	0.55	0.20	0.25	0.00
> 0.71		Vegetative*	-	-	-	-	0.35	0.20	0.25	0.20
> 0.71	13.0	Reproductive	0.55	0.00	0.25	0.20	0.55	0.00	0.43	0.02
> 0.71	12.5		0.55	0.00	0.25	0.20	0.55	0.00	0.43	0.02
> 0.71	12.5	Reproductive	0.55	0.00	0.35	0.10	0.55	0.00	0.43	0.02
> 0.71	11.0		0.55	0.00	0.35	0.10	0.55	0.00	0.43	0.02
> 0.71		Vegetative	0.55	0.20	0.15	0.10	0.55	0.20	0.25	0.00
> 0.71		Vegetative*	-	-	-	-	0.35	0.20	0.25	0.20

* Regrowth after a dry period when part of the crown tissues died.

Table 20. Senescence parameters for Piatã palisadegrass under cutting and grazing managements, in different daylength values and phenological phases.

Daylength (hours)	Phenological phase	Cutting				Grazing			
		Senescence Rate (d^{-1})				Senescence Rate (d^{-1})			
		LRT*(d)	Root	Stem	Crown	LRT*(d)	Root	Stem	Crown
10.6	Vegetative	80	0.001	0.005	0.005	80	0.001	0.005	0.005
13.0		80	0.001	0.005	0.005	80	0.001	0.005	0.005
13.0	Reproductive	80	0.001	0.005	0.005	80	0.001	0.005	0.005
11.4		80	0.001	0.005	0.005	80	0.001	0.005	0.005
11.4	Reproductive	56	0.001	0.015	0.015	80	0.001	0.005	0.005
11.0		56	0.001	0.015	0.015	80	0.001	0.005	0.005
11.0	Vegetative	56	0.001	0.015	0.015	80	0.001	0.005	0.005
10.7		56	0.001	0.015	0.015	80	0.001	0.005	0.005
10.7	Vegetative	80	0.001	0.005	0.005	80	0.001	0.005	0.005
10.6		80	0.001	0.005	0.005	80	0.001	0.005	0.005

* Leaf senescence is calculated using a leaf residence time (LRT) in days.

Good agreement between observed and estimated data was observed for all vegetative variables in all the assessed pasture managements (Table 22). Forage live mass simulations presented good precision (R^2 between 0.82 and 0.93), good accuracy (d between 0.92 and 0.98, and NSE from 0.72 to 0.91) and low errors (Table 22 and Figure 13). Dry matter partitioning between the aboveground organs also was satisfactorily simulated, with good precision and accuracy between observed and estimated data (R^2 between 0.72 and 0.97, d between 0.89 and 0.99, and NSE from 0.65 to 0.94) in most of the managements, except for crown growth in the Experiment 2, which even in this case presented a reasonable performance (R^2 = 0.64, d = 0.86, and NSE = 0.53) (Table 22). LAI simulations were efficient mainly for irrigated pasture under cutting management (R^2 = 0.78, d = 0.89, and NSE = 0.55) and for rainfed pasture under grazing (R^2 = 0.81, d = 0.93, and NSE = 0.70); however for rainfed pasture under cutting management the model´s performance was only regular (R^2 = 0.62, d = 0.88, and NSE = 0.48) (Table 22), what in the end did not affect substantially forage mass simulations. The SLA simulations presented a regular precision and accuracy (R^2 between 0.47 and 0.66, d between 0.82 and 0.90, and NSE from 0.39 to 0.61) (Table 22), which was caused by the great variability of SLA data; however the time series of SLA showed that this approach was able to capture the environment effects on SLA satisfactorily, both for cut and grazed pastures (Figure 14).

Table 21. Forage mass losses after grazing adjusted for each cycle of the Experiment 2 used for the APSIM-Tropical Pasture parameterization for Piatã palisadegrass under grazing and rainfed conditions.

Cycle	Grazing end date	Forage mass losses after grazing (kg ha^{-1})		
		Leaf	Stem	Total
1	12/26/2014	800	100	900
2	1/30/2015	300	1500	1800
3	3/6/2015	200	1000	1200
4	4/14/2015	300	100	400
5	5/19/2015	300	600	900
6	6/23/2015	300	500	800
7	7/29/2015	300	400	700
8	9/3/2015	200	300	500
9	10/9/2015	100	100	200
10	11/13/2015	500	500	1000
11	12/21/2015	600	800	1400

Time series of observed and estimated data are shown for the parameterization experiments, under cutting management and irrigated (Figure 12a) or rainfed (Figure 12b) conditions, and under grazing management and rainfed conditions (Figure 12c). The model was able to capture several trends across all conditions. Growth differences during initial development were satisfactorily simulated under cutting management and irrigated and rainfed conditions, as presented in the first three growth cycles of the Experiment 1 (Figure 12a and 12b). The effect of reproductive periods on pasture growth was also well represented by the model as showed in the simulations for the cycles 5, 6, 7 and 8 of the Experiment 1 (Figure 12a and 12b) and 1, 2, 3, 10 and 11 of the Experiment 2 (Figure 12c). Similarly, the simulations followed the impact of water deficit on pasture growth, as showed mainly in the cycles 2 and 3 of the Experiment 1 (Figure 12a and 12b) and in the cycles 6 and 7 of the Experiment 2 (Figure 12c). Nitrogen effects on growth were well captured by the model, with good simulations for high N supply (cycles 1, 2, 3, 4 of the Experiment 2) and low N supply (from the 5th to the 11th cycle of the Experiment 2) (Figure 12c), despite the uncertainties in initial N content and organic matter pools and in N leaching. The assumed values of forage mass losses after grazing allowed good growth simulations under grazing, mainly for the last forage mass value of each cycle, therefore the observed values of the first three assessments after cutting suggest that the speed of these losses was higher in the cycles conducted during the warm and wet seasons (e.g. cycles 1 and 2) and lower in those conducted during the cool and dry seasons (e.g. cycles 5, 6 and 7) (Figure 12c), showing that these losses do not occur in the first days after grazing for all environmental conditions.

4.3.2. APSIM-Tropical Pasture Test

The test of APSIM-Tropical Pasture for growth simulations for the Experiment 3, where pastures were irrigated and with cutting management, resulted in very good performance (Figure 15a and 16a), with $R^2 = 0.94$, $d = 0.98$, NSE = 0.92, ME = 328.1 kg ha^{-1}, MAE = 542.8 kg ha^{-1} and RMSE = 724.4 kg ha^{-1}, confirming the capability of this model to simulate this kind of system. The results of the comparison between observed and estimated forage live mass for pasture grown under rainfed conditions and grazing were also very good, considering the great variability and difficulties to assess grazed pastures (Figure 15b and 16b). The statistical results prove such performance, as follows: $R^2 = 0.97$, $d = 0.97$, NSE = 0.88, ME = -395.2 kg ha^{-1}, MAE = 395.2 kg ha^{-1} and RMSE = 494.3 kg ha^{-1}.

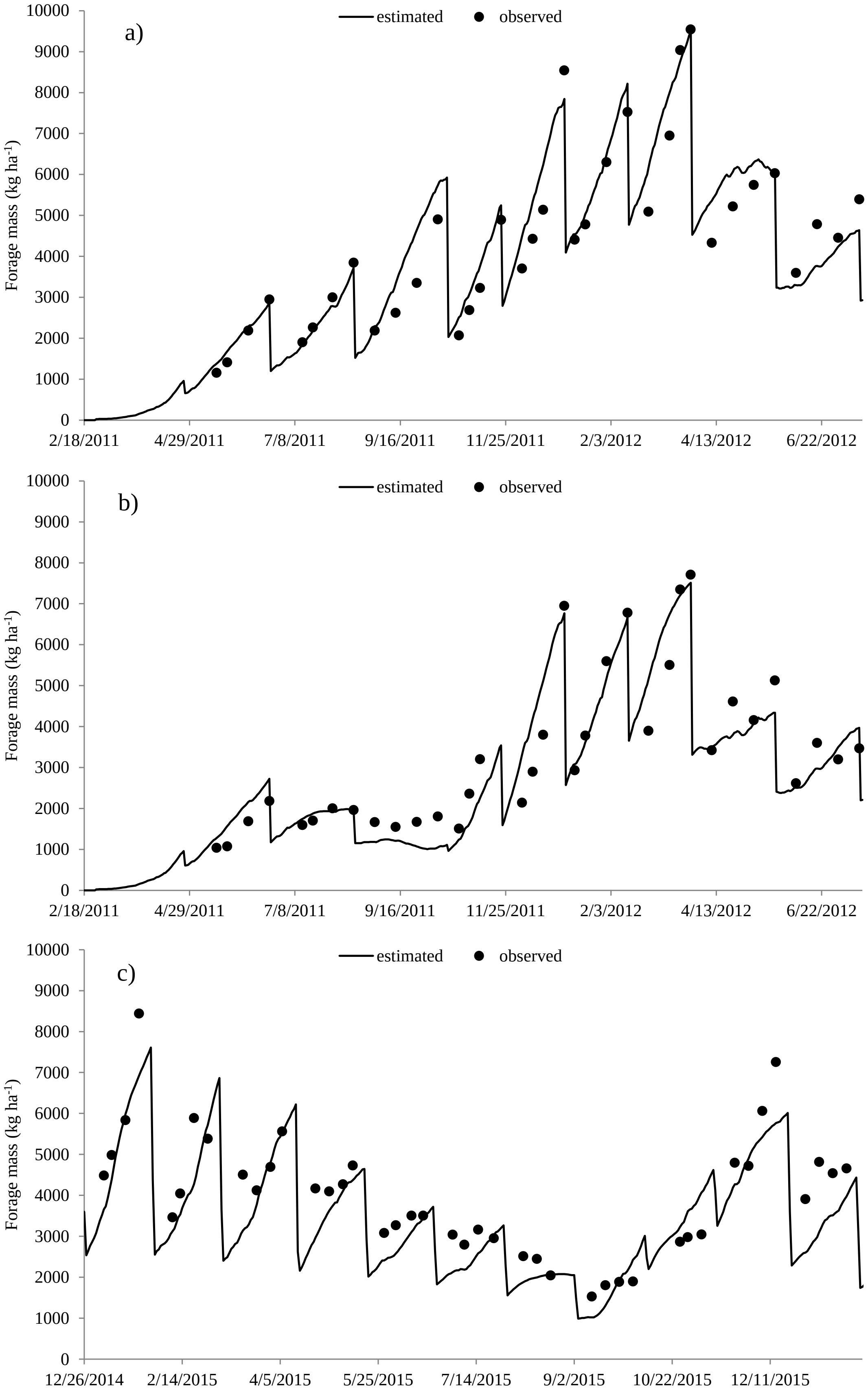

Figure 12. Time series of observed and estimated forage live mass for the experiments used in the APSIM-Tropical Pasture parameterization for Piatã palisadegrass under cutting management and irrigated (a) and rainfed (b) conditions; and under grazing management and rainfed (c).

Table 22. Statistical indexes for the simulations of forage live mass (FLM), leaf mass (Leaf), stem mass (Stem) and crown mass (Crown) (kg ha^{-1}); and of leaf area index (LAI) and specific leaf area (SLA) (m^2 g^{-1}), for the two experiments used in the APSIM-Tropical Pasture parameterization for Piatã palisadegrass and its comparison with observed data. R^2 = coefficient of determination, d = agreement index, NSE = Nash-Sutcliffe efficiency, ME = mean error (kg ha^{-1}), MAE = mean absolute error (kg ha^{-1}), RMSE = root mean square error (kg ha^{-1}).

Variable	Experiment 1 (Cutting management and irrigated)					
	R^2	d	NSE	ME	MAE	RMSE
FLM	0.93	0.98	0.91	277.7	495.8	620.3
Leaf	0.83	0.94	0.77	221.1	373.4	440.3
Stem	0.90	0.97	0.89	51.1	179.1	288.2
Crown	0.94	0.98	0.94	5.5	122.3	151.6
LAI	0.78	0.89	0.55	0.6	0.7	0.9
SLA	-	-	-	-	-	-
	Experiment 1 (Cutting management and rainfed)					
	R^2	d	NSE	ME	MAE	RMSE
FLM	0.89	0.97	0.88	45.8	493.2	632.2
Leaf	0.72	0.92	0.69	12.5	390.4	467.0
Stem	0.88	0.97	0.88	20.3	168.1	245.3
Crown	0.97	0.99	0.96	12.9	67.7	103.3
LAI	0.62	0.88	0.48	0.2	0.7	0.9
SLA	0.66	0.90	0.61	0.4	1.7	2.1
	Experiment 2 (Grazing management and rainfed)					
	R^2	d	NSE	ME	MAE	RMSE
FLM	0.82	0.92	0.72	-458.3	623.7	771.3
Leaf	0.85	0.94	0.73	-116.4	232.7	297.8
Stem	0.73	0.89	0.65	-236.7	365.0	503.5
Crown	0.64	0.86	0.53	-107.4	177.4	226.5
LAI	0.81	0.93	0.70	-0.1	0.5	0.6
SLA	0.47	0.82	0.39	-0.1	1.3	1.7

4.4. Discussion

The APSIM-Tropical Pasture model showed to be able to simulate tropical pastures growth in several managements and environmental conditions, such as with or without irrigation, low and high nitrogen supply, cutting and grazing managements, dry and wet seasons, warm and cool periods. This capacity must allow many future parameterizations for several tropical pasture species with high importance for livestock and production of energy from biomass. Therefore the model can be improved in many aspects to simulate with better accuracy the pastoral systems composed by these species and their interactions with the managements employed, mainly grazing, which promotes a range of new interactions between animals and pasture; and must be tested in several locations, for different tropical pasture species, and with a wider range of climates, soils and management practices.

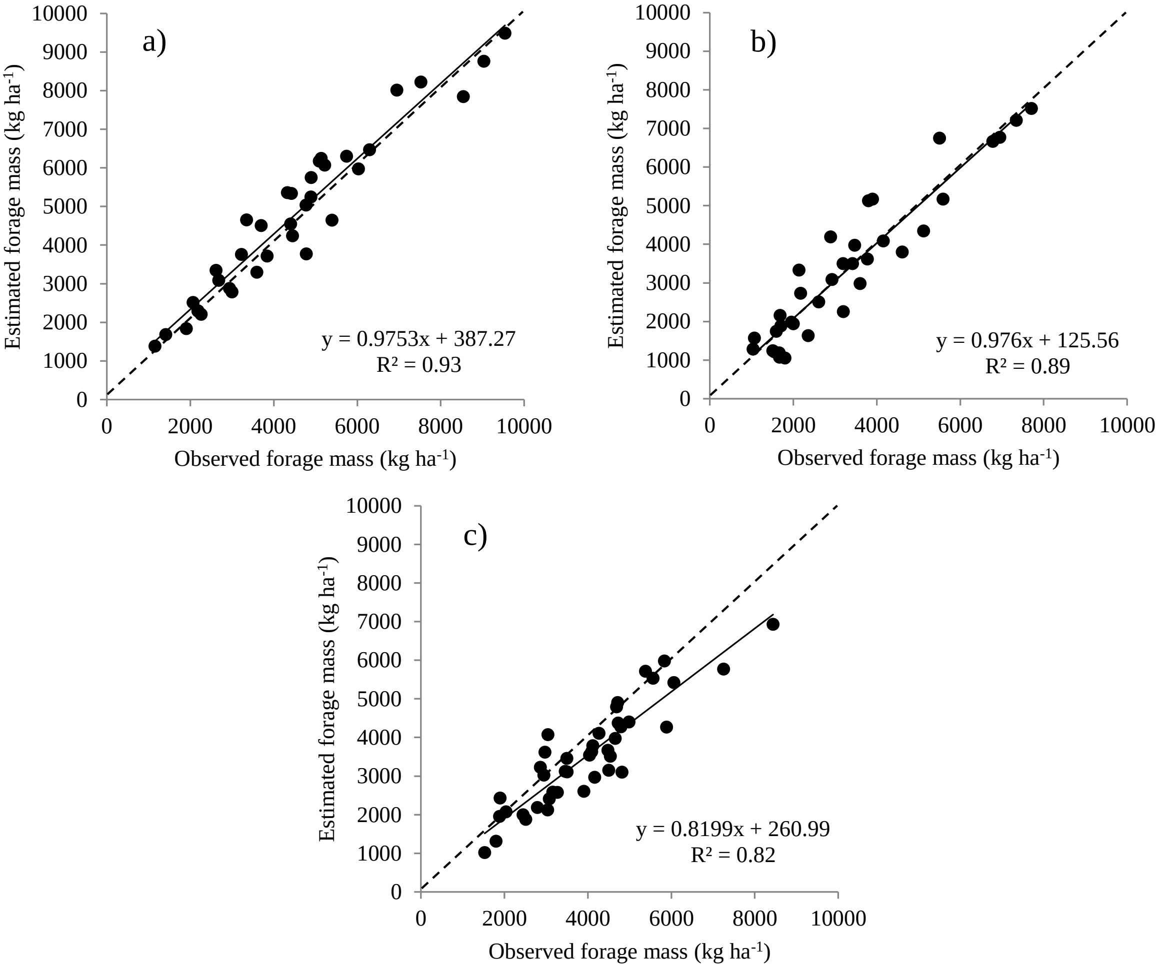

Figure 13. Relationships between observed and estimated forage live mass for the experiments used in the APSIM-Tropical Pasture parameterization for Piatã palisadegrass under cutting management, irrigated (a) and rainfed (b), and under grazing management and rainfed conditions (c).

The Piatã palisadegrass forage mass simulations showed a good agreement between observed and estimated data, achieving statistical results similar to the best parameterizations for tropical pastures available in the literature (Lara et al. 2012; Pedreira et al. 2011; Pequeno et al. 2014; Pequeno et al. 2017), confirming the model efficacy. The results for irrigated pasture under cutting management (R^2 = 0.93 and 0.94, d = 0.98, NSE = 0.91 and 0.92, ME = 277.7 and 328.1 kg ha^{-1}, MAE = 495.8 and 542.8 kg ha^{-1} and RMSE = 620.3 and 724.4 kg ha^{-1}) where similar to the those obtained by Pedreira et al. (2011) for Xaraés palisadegrass (d = 0.84 and RMSE = 538 kg ha^{-1}), by Lara et al. (2012) for Tanzânia guineagrass (d = 0.98 and RMSE = 494.2 kg ha^{-1}), by Pequeno et al. (2014) for Marandu palisadegrass (d = 0.91 and 0.96 and RMSE = 464 and 523 kg ha^{-1}) and by Pequeno et al. (2017) for Convert HD 364 brachiariagrass (d = 0.88 and 0.96 and RMSE = 619 and 532 kg ha^{-1}), all of them using the CROPGRO-Perennial Forage model for simulations. On the other hand, the results for rainfed pasture under cutting management (R^2 = 0.89, d = 0.97, NSE = 0.88, ME = 45.8 kg ha^{-1}, MAE = 493.2 kg ha^{-1} and RMSE = 632.2 kg ha^{-1}) were also similar to those obtained by Pequeno et al. (2014) for Marandu palisadegrass (d = 0.93 and 0.96 and RMSE = 526 and 501 kg ha^{-1}) and by Pequeno et al. (2017) for Convert HD 364 brachiariagrass (d = 0.89 and 0.93 and RMSE = 571 and 738 kg ha^{-1}), also using the CROPGRO-Perennial Forage model.

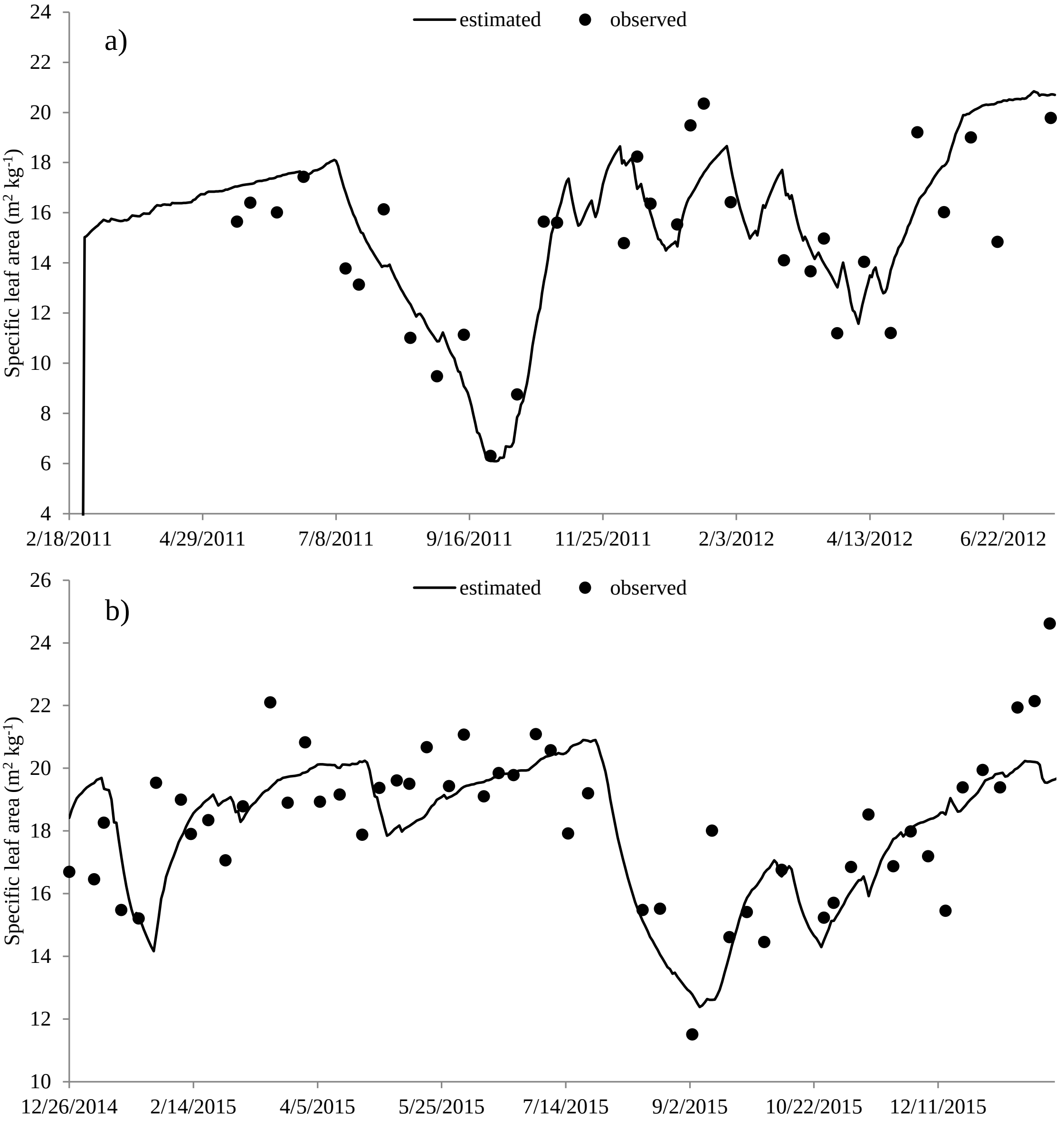

Figure 14. Time series of observed and estimated specific leaf area for the experiments used in the APSIM-Tropical Pasture parameterization for Piatã palisadegrass under cutting (a) or grazing (b) management and under rainfed conditions.

Santos (2016) simulated Piatã palisadegrass growth under continuous stocking with the STICS model and achieved R^2 = 0.48 and RMSE = 1020 kg ha^{-1}, while the present simulations for the same species under rotational grazing resulted in R^2 = 0.82 and 0.97, d = 0.92 and 0.97, NSE = 0.72 and 0.98, ME = -458.3 and -395.2 kg ha^{-1}, MAE = 623.7 and 395.2 kg ha^{-1} and RMSE = 771.3 and 494.3 kg ha^{-1}. Comparing the results observed in this study with those from Araújo et al. (2013), who simulated Mombaça guineagrass using the APSIM-Growth model, it is possible to confirm that the APSIM-Tropical Pasture model improved the simulations of tropical pastures in the APSIM modelling framework.

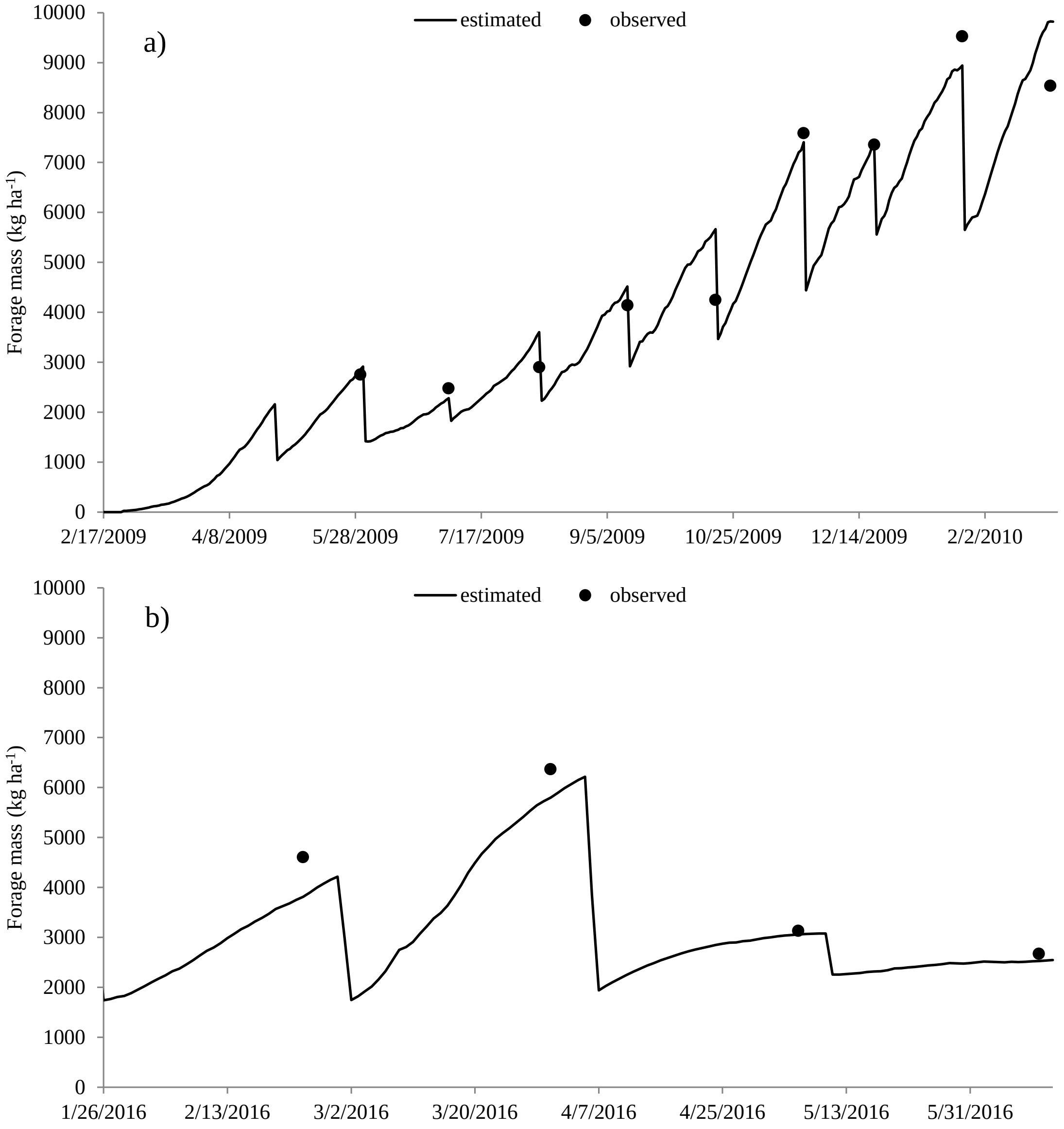

Figure 15. Time series of observed and estimated forage live mass for the experiments used in the APSIM-Tropical Pasture testing for Piatã palisadegrass under cutting management and irrigated (a), and under grazing management and rainfed (b).

The improvements promoted by APSIM-Tropical Pasture on tropical pastures modeling were due to the model capabilities that allowed: better initial growth simulations;

simulations of growth partitioning and senescence considering the effects of flowering, which was never before implemented in a tropical pasture model; and N reallocation and retranslocation simulations. The simulations for grazing systems also were an important initiative to identify the main needs for simulating its related processes and interactions, clarifying some calculations that must be implemented in tropical pasture models and encouraging future studies to improve the understanding of these systems.

Partitioning and senescence were strongly influenced by management and phenological phases, so they need good estimates of the beginning and ending of the reproductive period and of the flowering effects on these processes. For Piatã palisadegrass, the environmental factors that determine the induction of meristems to flowering are not completely clear, so in this study was assumed that daylength regulated this process, but more studies should be carried out to make the simulation of this process more precise. Additionally, more detailed experiments should be performed to assess the variation of apical meristems height during different pasture development phases and the removal of these meristems by cutting or grazing in different stubble heights or stubble mass amounts, in order to explain better the tiller death dynamics and its effect on partitioning and senescence.

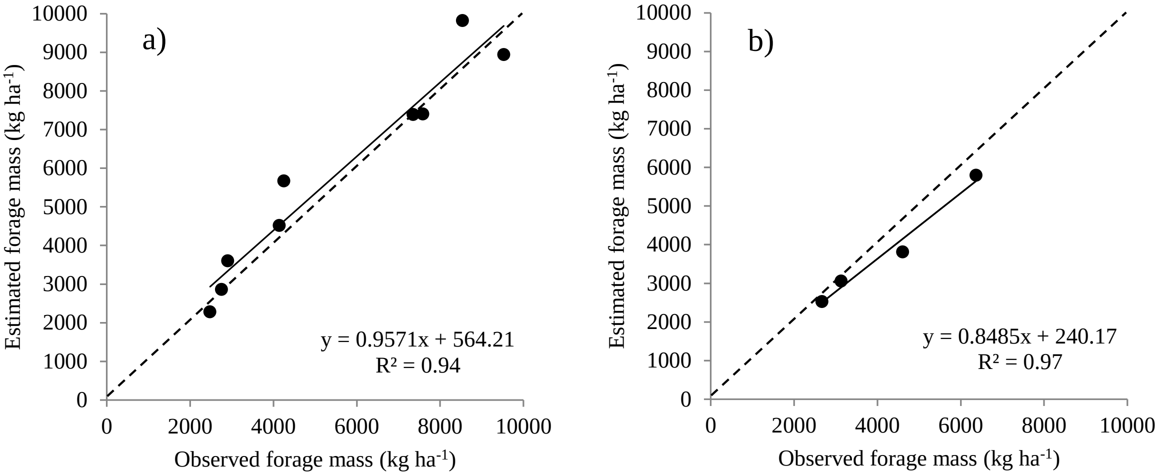

Figure 16. Relationships between observed and estimated forage live mass for the experiments used in the APSIM-Tropical Pasture testing for Piatã palisadegrass under irrigated cutting management (a) and under rainfed grazing management (b).

The DM and N arbitrator needs improvements on the reallocation and retranslocation processes, firstly by enabling the arbitration of the amounts of DM that are structural and non-structural, which is not implemented yet. Subsequently, the arbitration of reallocation and retranslocation also must be improved by inserting a capability for DM reallocation and retranslocation, as well as calculations that allow controlling to where the DM and N recycled from senescent organs will be reallocated, and the DM and N coming from storage organs will be translocated. New studies about source/sink relationships during different phenological phases will help to explain these processes for tropical pastures. The simulations for the cycles 10 and 11 of the Experiment 2 (Figure 12c) highlighted the need of a good capability for DM retranslocation, since they were not accurate probably due to the need of some DM retranslocation from the storage organs to attend the demand for stem elongation during flowering, which seems to be an effect of the low N supply during these cycles.

Currently, the stubble mass and morphology are not simulated by APSIM-Tropical Pasture, since the cutting management capability allows setting the amounts of leaf, stem, and crown in the stubble remained after each cut or grazing event. It seems to be a good tool for tropical pastures simulation, but efforts must be done for developing studies about stubble dynamics throughout the pasture development and ways to simulate it under cutting and grazing managements. Specifically for pastures under grazing, forage mass losses during and after grazing, caused by animals physical damages, are very important for the success of simulations, so it is important to develop tools to simulate these losses, based on factors such as: forage mass during grazing, stocking rate, among others. Such tool must be able to transfer lost forage mass to the surface organic matter and to calculate the speed of the losses after grazing, which, as suggested by the observed values from Experiment 2, may be higher during the warm and wet season and lower during the cool and dry season (Figure 12c).

Improvements must be performed in the N leaching and surface organic matter simulations, since these variables were not well simulated for the soil conditions under study. Therefore, more studies should be carried out for explaining these processes for tropical soils and for supporting new improvements in the model.

4.5. Conclusions

The APSIM-Tropical Pasture model is able to simulate tropical pasture growth under various management and environmental conditions, such as drought and good water supply, low and high nitrogen fertilization, and cutting and grazing systems.

Several requirements for future work have been identified during this study. The environmental factors that induce flowering are not completely clear for Piatã palisadegrass, so this presents a problem for applying a model for this species at a large scale.

The pasture simulations under grazing must be improved to account for biomass losses during and after grazing due to the damage caused by animals. Finally, the model must be tested for more locations, climate conditions, soils, and grazing or cutting intensities, in order to improve its accuracy and achieve enough confidence to be applied for planning and decision-making in pastoral systems.

REFERENCES

Alderman, P.D., 2008. Simulating the regrowth dynamics of Tifton 85 bermudagrass as affected by nitrogen fertilization. MSc Thesis – University of Florida, Gainesville. 115 p.

Allen, R.G., Pereira, L.S., Raes, D., Smith, M., 1998. Crop evapotranspiration – guidelines for computing crop water requirements. FAO, Rome.

Alvares, C.A., Stape, J.L., Sentelhas, P.C., Goncalves, J.L.M., Sparovek, G., 2013. Köppen’s climate classification map for Brazil. Meteorol. Z. 22, 711-728. https://doi.org/10.1127/0941-2948/2013/0507

Andrade, A.S., Santos, P.M., Pezzopane, J.R.M., Araujo, L.C., Pedreira, B.C., Pedreira, C.G.S., Marin, F.R., Lara, M.A.S., 2015. Simulating tropical forage growth and biomass accumulation: an overview of model development and application. Grass Forage Sci. 71, 54-65. https://doi.org/10.1111/gfs.12177

Araujo, L.C., Santos, P.M., Rodriguez, R., Pezzopane, J.R.M., Oliveira, P.P.A., Cruz, P.G., 2013. Simulating Guineagrass production: empirical and mechanistic approaches. Agron. J. 105, 61–69. https://doi.org/10.2134/agronj2012.0245

Arnold, C.Y., 1959. The development and significance of the base temperature in a linear heat unit system. Proc. Am. Soc. Hortic. Sci. 74, 430–445.

Barioni, L.G., Martha Jr, G.B., Ramos, A.K.B., Veloso, R.F., Rodrigues, D.C., Vilela, L., 2003. Planejamento e gestão do uso de recursos forrageiros na produção de bovinos em pastejo, in: Peixoto, A.M., et al. (Eds.), Anais do 20th Simpósio sobre Manejo de Pastagem, FEALQ, Piracicaba, pp. 105-153.

Brown, H.E., Huth, N.I., Holzworth, D.P., Teixeira, E.I., Zyskowski, R.F., Hargreaves, J.N.G., Moot, D.J., 2014. Plant modelling framework: software for building and running crop models on the APSIM platform. Environ. Model. Softw. 62, 327-350. https://doi.org/10.1016/j.envsoft.2014.09.005

Coltri, P.P., Viovy, N., Chang, J., Araújo, L.C., Barioni, L.G., Santos, P.M., Pezzopane, J.R.M., 2014. Evaluating the new Orchidee-GM (Grassland Management) model to tropical area in Brazil, in: Livestock, climate change and food security conference, Conference Abstract Book, INRA, Paris, pp.96.

Cruz, P.G., 2010. Produção de forragem em *Brachiaria brizantha*: adaptação, geração e avaliação de modelos empíricos e mecanicistas para estimativa do acúmulo de forragem. PhD Thesis - University of São Paulo, Piracicaba. 102 p.

FAO, 2014. FAOSTAT. http://www.fao.org/faostat/en/#data/RL (accessed 18 August 2017).

Holzworth, D.P., Huth, N.I., Devoil, P.G., Zurcher, E.J., Herrmann, N.I., Mclean, G., Chenu, K., Oosterom, E.J., Snow, V., Murphy, C., Moore, A.D., Brown, H., Whish, J.P.M., Verral, S., Fainges, J., Bell, L.W., Peake, A.S., Poulton, P.L., Hochman, Z., Thorburn, P.J., Gaydon, D.S., Dalgliesh, N.P., Rodriguez, D., Cox, H., Chapman, S., Doherty, A., Teixeira, E., Sharp, J., Cichota, R., Vogeler, I., Li, F.Y., Wang, E., Hammer, G.L., Robertson, M.J., Dimes, J.P., Whitbread, A.M., Hunt, J., Van Hees, H., Mcclelland, T., Carberry, PS., Hargreaves, J.N.G., Macleod, N., Mcdonald, C., Harsdorf, J., Wedgwood, S., Keating, B.A., 2014. APSIM - Evolution towards a new generation of agricultural systems simulation. Environ. Model. Softw. 62, 327-350.

Holzworth, D., Huth, N.I., Fainges, J., Herrmann, N.I., Zurcher, E., Brown, H., Snow, V., Verral, S., Cichota, R., Doherty, A., DeVoil, P., McLean, G., Brider, J., 2015. APSIM Next Generation: The final frontier?, in: 21st International Congress on Modelling and Simulation, Proceedings of the 21st International Congress on Modelling and Simulation, Gold Coast, pp. 347–353. http://www.mssanz.org.au/modsim2015 (accessed 19 August 2017).

Johnson, I.R., Chapman, D.F., Snow, V.O., Eckard, R.J., Parsons, A.J., Lambert, M.G., Cullen, B.R., 2008. DairyMod and EcoMod: biophysical pasture simulation models for Australia and New Zealand. Aust. J. Exp. Agric. 48, 621-631. https://doi.org/10.1071/EA07133

Keating, B.A., Carberry, P.S., Hammer, G.L., Probert, M.E., Robertson, M.J., Holzworth, D., Huth, N.I., Hargreaves, J.N.G., Meinke, H., Hochman, Z., Mclean, G., Verburg, K., Snow, V., Dimes, J.P., Silburn, M., Wang, E., Brown, S., Bristow, K.L., Asseng, S., Chapman, S., Mccown, R.L., Freebairn, D.M., Smith, C.J., 2003. An overview of APSIM, a model designed for farming systems simulation. Eur. J. Agron. 18, 267–288. https://doi.org/10.1016/S1161-0301(02)00108-9

Kiniry, J.R., Burson, B.L., Evers, G.W., Williams, J.R., Sanchez, H., Wade, C., Featherston, J.W., Greenwade, J., 2007. Coastal Bermudagrass, Bahiagrass, and native range simulation at diverse sites in Texas. Agron. J. 99, 450–461. https://doi.org/10.2134/agronj2006.0119

Lara, M.A.S., Pedreira, C.G.S., Boote, K.J., Pedreira, B.C., Moreno, L.S.B., Alderman, P.D., 2012. Predicting growth of *Panicum maximum*: an adaptation of the CROPGRO - perennial forage model. Agron. J. 104, 600–611. https://doi.org/ 10.2134/agronj2011.0272

Moore, A., Holzworth, D., Herrmann, N., Brown, H., deVoil, P., Snow, V., Zurcher, E., Huth, N., 2014. Modelling the manager: representing rule-based management in farming systems simulation models. Environ. Model. Softw. 62, 327-350. https://doi.org/10.1016/j.envsoft.2014.09.001

Moreno, L.S.B., Pedreira, C.G.S., Boote, K.J., Alves, R.R., 2014. Base temperature determination of tropical *Panicum spp.* grasses and its effects on degree-day-based models. Agric. For. Meteorol. 186, 26-33. https://doi.org/10.1016/j.agrformet.2013.09.013

Moriasi, D.N., Arnold, J.G., Van Liew, M.W., Bingner, R.L., Harmel, R.D., Veith, T.L., 2007. Model evaluation guidelines for systematic quantification of accuracy in watershed simulations. Trans. Am. Soc. Agric. Biol. Eng. 50, 885-900.

Ojeda, J.J., Volenec, J.J., Brouder, S.M., Caviglia, O.P., Agnusdei, M.G., 2016. Evaluation of Agricultural Production Systems Simulator as yield predictor of *Panicum virgatum* and *Miscanthus x giganteus* in several US environments. GCB Bioenergy 9, 796-816. https://doi.org/10.1111/gcbb.12384

Parton, W.J., Scurlock, J.M.O., Ojima, D.S., Gilmanov, T.G., Scholes, R.J., Schimel, D.S., Kirchner, T., Menaut, J-C., Seastedt, T., Garcia Moya, E., Apinan Kamnalru, T., Kinyamario, J.I., 1993. Observations and modeling of biomass and soil organic matter dynamics for the grassland biome worldwide. Glob. Biogeochem. Cycles 7, 785–809.

Pedreira, B.C., Pedreira, C.G.S., Boote, K.J., Lara, M.A.S., Alderman, P.D., 2011. Adapting the CROPGRO perennial forage model to predict growth of *Brachiaria brizantha*. Field Crop. Res. 120, 370–379. https://doi.org/10.1016/j.fcr.2010.11.010

Pequeno, D.N.L., Pedreira, C.G.S., Boote, K.J., 2014. Simulating forage production of Marandu palisade grass (*Brachiaria brizantha*) with the CROPGRO-Perennial Forage model. Crop Pasture Sci. 65, 1335–1348. https://doi.org/10.1071/CP14058

Pequeno, D.N.L., Pedreira, C.G.S., Boote, K.J., Alderman, P.D., Faria, A.F.G., 2017. Species-genotypic parameters of the CROPGRO Perennial Forage Model: Implications for comparison of three tropical pasture grasses. Grass Forage Sci. (in press). https://doi.org/10.1111/gfs.12329

Pereira, A.R., Angelocci, L.R., Sentelhas, P.C., 2002. Agrometeorologia: Fundamentos e aplicações práticas. Agropecuária, Guaíba.

Probert, M.E., Dimes, J.P., Keating, B.A., Dalal, R.C., Strong, W.M., 1998. APSIM's water and nitrogen modules and simulation of the dynamics of water and nitrogen in fallow systems. Agric. Syst. 56, 1-18. https://doi.org/10.1016/S0308-521X(97)00028-0

Robertson, M.J., Carberry, P.S., Huth, N.I., Turpin, J.E., Probert, M.E., Poulton, P.L., Bell, M., Wright, G.C., Yeates, S.J., Brinsmead, R.B., 2002. Simulation of growth and development of diverse legume species in APSIM. Aust. J. Agric. Res. 53, 429-446. https://doi.org/10.1071/AR01106

Rymph, S.J., Boote, K.J., Irmak, A., Mislevy, P., Evers, G.W., 2004. Adapting the CROPGRO model to predict growth and composition of tropical grasses: developing physiological parameters. Soil Crop Sci. Soc. Fla. Proc. 63, 37–51.

Santos, D.C., 2016. Características do capim-piatã e desempenho de bovinos em sistemas silvipastoris no cerrado brasileiro. PhD Thesis - Federal University of Goiás, Goiânia.

Snow, V.O., Huth, N.I., 2004. The APSIM MICROMET Module. HortResearch Internal Report, HortResearch, Auckland.

Steinfeld, H., Gerber, P., Wassenaar, T., Castel, V., Rosales, M., de Haan, C., 2006. Livestock’s long shadow: environmental issues and options. FAO, Rome.

Tsuruta, S-I., Shimoda, K., Kouki, K., Ebina, M., 2015. The Present Status of C4 Tropical Grasses Breeding and Molecular Approaches. JARQ 49, 203-215. https://doi.org/10.6090/jarq.49.203

Willmott, C.J., 1981. On the validation of models. Phys. Geogr. 2, 184–194.

Wright, I.A., Jones, J.R., Davies, D.A., Davidson, G.R., Vale, J.E., 2006. The effect of sward surface height on the response to mixed grazing by cattle and sheep. Anim. Sci. 82, 271-276. https://doi.org/10.1079/ASC200517

5. TWO-DIMENSIONAL MODEL FOR ESTIMATING SOLAR RADIATION TRANSMISSION IN SILVOPASTORAL SYSTEM WITH EUCALYPTUS IN ROWS

ABSTRACT

Models for simulating radiation transmission by eucalyptus trees in agroforestry systems are not available in literature, which is a main concern when the purpose is to simulate plants growth in an intercropping system. Based on that, the aim of this study was to develop a two-dimensional model for simulating radiation transmission by eucalyptus trees arranged in rows in a silvopastoral system. This radiation transmission model is applicable for trees arranged in rows, considering the row as a wall, without significant spaces between tree canopies; and its calculations are based on a view point and its relationships with the sun and the row. Such model comprises three sub-models: shading model, which calculates the sun positioning, the relationships sun-row-view point and determines if there is shading on the point of interest; LAI distribution model, which calculates the LAI in four vertical layers and in six horizontal layers and give as result the LAI that is projecting shade; and radiation transmission calculations. For the model testing, quantum sensors were installed in four positions within the silvopastoral system (0.00, 3.75, 7.50 and 11.25 m from the North row) and at full sun to measure PAR from December 2014 to June 2016. The model developed in this study was efficient (R^2 between 0.61 and 0.92, d from 0.87 to 0.97, NSE between 0.48 and 0.88) for estimating PAR transmission. The model can be improved in future studies by estimating the distance crossed by the light beam within the canopy and by refining the leaf area distribution in the canopy. Tests should be performed in several locations, for different latitudes and agroforestry arrangements.

Keywords: Agroforestry; Photosynthetically active radiation; Solar radiation interception; Tree canopy; Shading; Leaf area index

5.1. Introduction

Since the classic study of Monsi and Saeki (1953), many models have been proposed for estimating solar radiation transmission through canopies. Such models were developed initially for estimating solar radiation transmission in homogeneous crops or forestry canopies, and more recently for discontinuous canopies (intercropping, agroforestry or forest systems), isolated tree crowns, crops arranged in rows, among others (Abraha and Savage 2010; Annandale et al. 2004; Chen et al. 1994; Dupraz 2012; Duursma and Mäkelä 2007; Oyarzun et al. 2007; Sinoquet and Bonhomme 1992; Talbot and Forrester 2014; Wang and Jarvis 1990; Zhao et al. 2003).

In general, these approaches have taken into account calculations of solar radiation beam angle, canopy shape, leaf area density, radiation extinction coefficient, leaf angle distribution, canopy reflectivity and measurements or estimates of incoming solar radiation as reference data (Monsi and Saeki 1953; Oyarzun et al. 2007; Sinoquet and Bonhomme 1992; Wang and Jarvis 1990).

Monsi and Saeki (1953) proposed that the solar radiation intensity decreases exponentially through the leaf layers. Wang and Jarvis (1990) developed the MAESTRO model, recently incorporated to MAESPA (Duursma and Medlyn 2012), to calculate solar radiation absorption, photosynthesis and transpiration of tree crowns, using as reference the model of Norman and Welles (1983) and the model of Grace et al. (1987). MAESTRO is divided into seven submodels, with four of them describing solar radiation interception by tree canopies. The first submodel calculates the sun position and, consequently, the hour angle and the azimuthal angles of the sun during the day and the daylength. The second model partitions the incoming solar radiation into PAR and NIR fractions and determines sky cloudiness and hourly fractions of sunshine duration. The third submodel calculates the mean leaf area density and the fractions of the leaf area in different angles at each grid point in the tree crown, the sub-volume at each grid point and the diffuse radiation extinction coefficients for them. Finally, the fourth submodel calculates the hourly and daily amounts of PAR, NIR and thermal radiation absorbed by the target tree. Charbonnier et al. (2013) also employed MAESTRO to simulate competition for light in a coffee agroforestry system.

Sinoquet and Bonhomme (1992) developed a two-dimensional model to estimate radiative transfer through crop canopies in mixed and row intercropping systems. This model describes canopy structure, radiation interception within mixed zones, radiation course within the canopy, incoming solar radiation interception, radiation scattering and radiation balance.

Chen et al. (1994) used an approach based on fractal geometry for modeling the canopy, which allows the simulation of the three-dimensional radiation regime in a heterogeneous canopy.

Oyarzun et al. (2007) proposed a simple model to estimate radiation interception by fruit-tree orchards. The model considers trees as prismatic-shaped porous bodies and the intercepted solar radiation by the orchard is computed based on geometric relationships between the stand structure, the sun position, and the length of the shadow cast by the trees, taking daily incoming solar radiation as reference. Similarly, Zhao et al. (2003) created a model to estimate the shortwave radiation distribution in an agroforestry system planted in regular arrays, but they assumed trees with spherical crowns.

These references demonstrate that there are many efforts for describing solar radiation transmission and absorption by plant canopies for both conventional agricultural and agroforestry systems, but it is still necessary to clarify several aspects related for many different plant associations or system arrangements to incorporate such knowledge to crop simulation models. In this context, models were not developed specifically for estimating radiation transmission by eucalyptus trees in agroforestry systems, so the aim of this study was to develop a two-dimensional model for simulating radiation transmission by eucalyptus trees arranged in rows in a silvopastoral system.

5.2. Material and methods

5.2.1. Model development

The new radiation transmission model is applicable only for systems with trees arranged in rows; with trees spacing, in the row, short enough to suppress spaces between the tree canopies, working as a wall; and its calculations are based on a view point and its relationships with the sun and the row (Figure 17). For this model, the canopy shape does not matter, but the base of the canopy must be its widest part. Such model comprises three sub-models: shading model, LAI distribution model and radiation transmission calculations.

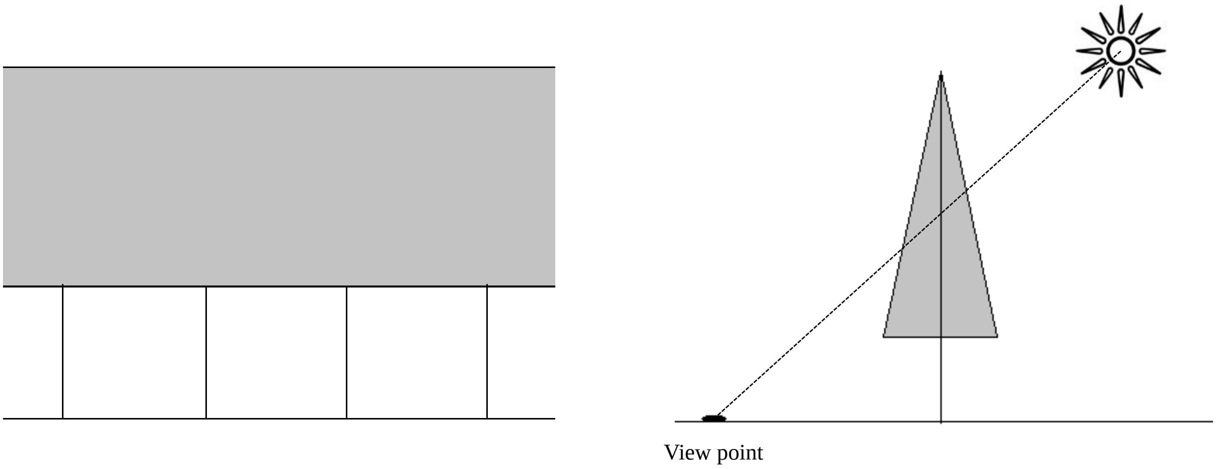

Figure 17. Schematic representation of the model´s assumptions: longitudinal canopy view, without spaces, working as a wall (left) and transversal canopy view in relation to the position of the sun (right).

5.2.1.1. Shading model

The shading sub-model calculates the sun positioning, the relationships sun-row-view point and determines if there is shading on the point of interest. The input data for this sub-model are: day of year (DY), local hour, latitude (φ) and longitude (λ), in decimal, time-zone standard meridian (Tm), distance from the North row (DR), row spacing (RS), tree height (TH), canopy beginning height (Cbh), canopy width (CW), canopy width to North (CWN), row orientation (RO) in degrees (ranging from 90º to -89.9º, being that 0º is E-W, 90º is N-S, 45º is NW-SE and -45º is NE-SW), ground slope (GS) in degrees, slope orientation (SO) in degrees (ranging from 90º to -90º and following the same distribution rule of RO), and slope direction (Sd) in degrees (ranging from 180º to -180º, being that 0º is N, -90º is E, 90º is W and 180º is S).

The equations from Equation 1 to Equation 9 were used for determining sun positioning. For this, local hour correction (Eq. 12), solar declination (δ) (Eq. 13), hour angle (h) (Eq. 14), zenith angle (z) (Eq. 15), hour angle at sunrise (h_s) (Eq. 16), zenith angle at noon (z_{12}) (Eq. 17), solar elevation angle (ê) (Eq. 18), solar azimuth from North (α_N) (Eq. 19) and solar azimuth from South (α_S) (Eq. 20) were calculated.

$$\text{If } \lambda > \text{Tm then } LH_{corr} = Hour + \left[\frac{(|\lambda - Tm|)}{15}\right] \qquad \text{If } \lambda \leq \text{Tm then } LH_{corr} = Hour - \left[\frac{(|\lambda - Tm|)}{15}\right] \tag{12}$$

$$\delta = 23.45 \times sin\left[\frac{360}{365} \times (DY - 80)\right] \tag{13}$$

$$h = (LH_{corr} - 12) \times 15 \tag{14}$$

$$z = cos^{-1} \times (\sin\varphi \times \sin\delta + \cos\varphi \times \cos\delta \times \cos h) \tag{15}$$

$$h_s = cos^{-1} \times (-\tan\varphi \times \tan\delta) \tag{16}$$

$$z_{12} = |\delta - \varphi| \tag{17}$$

$$\hat{e} = 90 - z \tag{18}$$

$$\alpha_N = cos^{-1}\left[\frac{(\sin\delta - \sin\varphi\times\cos z)}{(\cos\varphi\times\sin z)}\right] \tag{19}$$

If $h=0$ then
- If $z_{12}<0$ then $\alpha_N = 180^{\circ}$
- If $z_{12}\geq 0$ then $\alpha_N = 0^{\circ}$

If $h\neq 0$ then
- If $h<0$ then α_N = negative
- If $h\geq 0$ then α_N = positive

$$\alpha_S = cos^{-1}\left[\frac{\sin\varphi\times\cos z - \sin\delta}{(\cos\varphi\times\sin z)}\right] \tag{20}$$

If $h=0$ then
- If $z_{12}<0$ then $\alpha_S = 0^{\circ}$
- If $z_{12}\geq 0$ then $\alpha_S = 180^{\circ}$

If $h\neq 0$ then
- If $h<0$ then α_S = negative
- If $h\geq 0$ then α_S = positive

The equations between Eq. 21 and Eq. 24 were used for calculating the sun-row-view point relationships, which consist in determine where the radiation beam, coming from the sun, is crossing the canopy to reach the view point. For this, the following calculations were performed: lateral displacement angle ($\widehat{dl}$) (Eq. 21), which means the angle between the transect line and the light beam line (Figure 18); lateral displacement (dl) (Eq. 22), which represents the distance between the transect line and the light beam line, on the row line and in the horizontal level (Figure 19), considering DRN_{corr} and DRS_{corr} as the distances from the North and the South rows, respectively, corrected by ground slope; distance from the row on the light beam line (DR_{lb}) (Eq. 23), which consists in the distance between the view point and the row on the light beam line, in the horizontal level (Figure 20); and tree height projecting shade (THshade) (Eq. 24), which calculates the canopy height that is projecting shade on the view point (Figure 21).

$$\text{North row: } \widehat{dl}_N = \alpha_N + RO \tag{21}$$

$$\text{South row: } \widehat{dl}_S = RO - \alpha_S$$

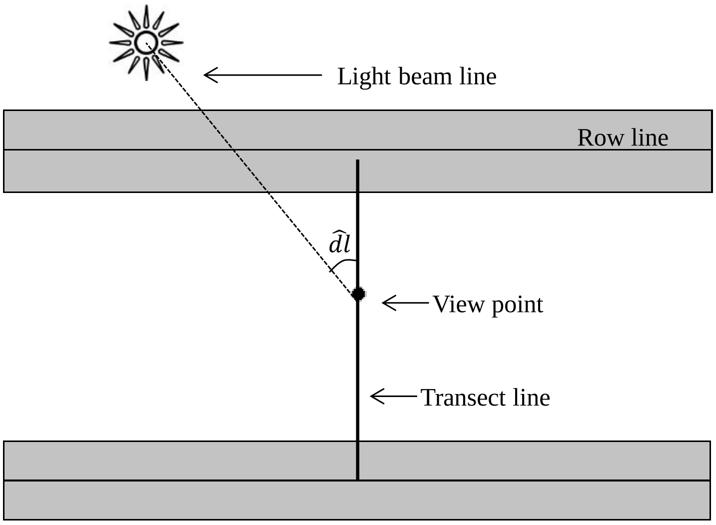

Figure 18. Schematic representation of a superior view of an inter-row with the angle between the transect line and the light beam line ($\widehat{dl}$). Gray strips represent tree rows.

$$\text{If } |\widehat{dl}_N| \leq 90^{\circ} \text{ then } \; dl = \tan \widehat{dl}_N \times DRN_{corr} \tag{22}$$

$$\text{If } |\widehat{dl}_N| > 90^{\circ} \text{ then } \; dl = \tan \widehat{dl}_S \times DRS_{corr}$$

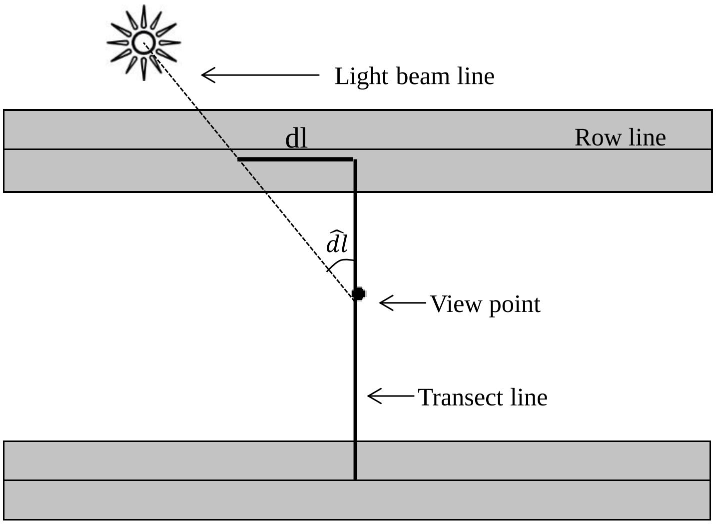

Figure 19. Schematic representation of a superior view of an inter-row with the lateral displacement (dl) from the transect line to the light beam line, on the row line. Gray strips represent tree rows.

$$\text{If } |\widehat{dl}_N| \leq 90^{\circ} \text{ then } \; DR_{lb} = \sqrt{dl^2 + DRN_{corr}{}^2} \tag{23}$$

$$\text{If } |\widehat{dl}_N| > 90^{\circ} \text{ then } DR_{lb} = \sqrt{dl^2 + DRS_{corr}{}^2}$$

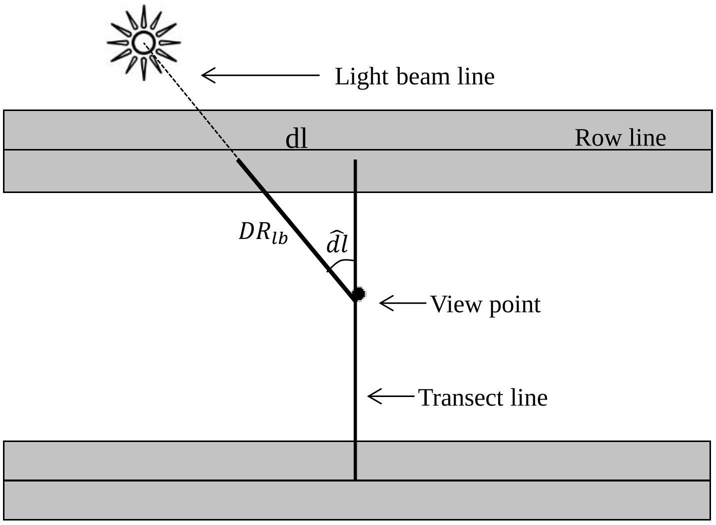

Figure 20. Schematic representation of a superior view of an inter-row with the distance between the view point and the row line, on the light beam line (DR_{lb}). Gray strips represent tree rows.

$$THshade = \tan \hat{e} \times DR_{lb} \tag{24}$$

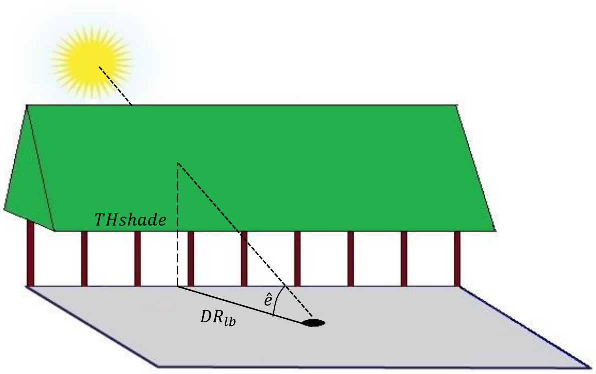

Figure 21. Schematic representation of a tree row indicating the height where the light beam crosses the canopy (THshade).

Additionally, it was necessary to do corrections for ground slope, calculating the row with lower ground level or row at the slope direction (Eq. 25), slope variation by each degree of the azimuth angle (SV) (Eq. 26), slope at light beam line (S_{lbl}) (Eq. 27), slope parallel to the rows (S_p) (Eq. 28), slope at transect line (S_t) (Eq. 29), distance from the North row corrected for slope (DRN_{corr}) (Eq. 30), row spacing corrected for slope (RS_{corr}) (Eq. 31), distance from the South row corrected for slope (DRS_{corr}) (Eq. 32), light beam angle (horizontal) at which slope effect on tree height is inverted ($\widehat{Lb}_{inv}$) (Eq. 33), additional tree height caused for slope (TH_{add}) (Eq. 34) (Figure 22), tree height corrected for ground slope (TH_{corr}) (Eq. 35), and tree height projecting shade corrected for slope ($THshade_{corr}$) (Eq. 36).

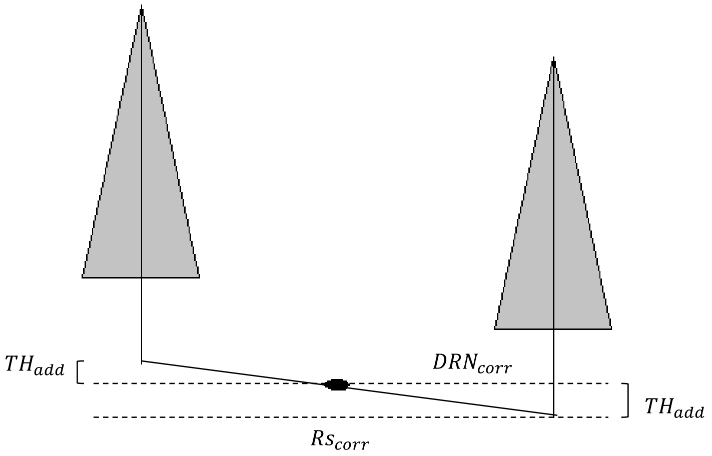

Figure 22. Schematic representation of two rows, one with a positive additional height (TH_{add}) (left) and the other with a negative additional height (right), caused by ground slope.

$$\text{If } |Sd + RO| > 90^{\circ} \text{ then South row} \qquad (14)$$

$$\text{If } |Sd + RO| \leq 90^{\circ} \text{ then North row}$$

$$SV = \frac{GS}{90} \qquad (15)$$

$$S_{lbl} = |[(|SO| - |\alpha_N|) \times SV]| \qquad (16)$$

$$S_p = |[(|SO| - RO - 90) \times SV]| \qquad (17)$$

$$S_t = GS - S_p \qquad (18)$$

$$DRN_{corr} = \cos S_t \times DRN \qquad (19)$$

$$RS_{corr} = \cos S_t \times RS \qquad (20)$$

$$DRS_{corr} = RS_{corr} - DRN_{corr} \qquad (21)$$

If Sd < 0 then $\widehat{Lb}_{inv} = Sd + 90$ (22)

If Sd ≥ 0 then $\widehat{Lb}_{inv} = Sd - 90$

$$TH_{add} = \tan S_p \times |dl| \tag{23}$$

If Row lower ground level = North then
- If $|\alpha_N| > \widehat{Lb}_{inv}$ then TH_{add} is positive
- If $|\alpha_N| \leq \widehat{Lb}_{inv}$ then TH_{add} is negative

If Row lower ground level = South then
- If $|\alpha_N| > \widehat{Lb}_{inv}$ then TH_{add} is negative
- If $|\alpha_N| \leq \widehat{Lb}_{inv}$ then TH_{add} is positive

$$TH_{corr} = TH + TH_{add} \tag{24}$$

$$THshade_{corr} = THshade + TH_{add} \tag{25}$$

When the corrections for ground slope were done, it was necessary to do the corrections for canopy beginning height (Cbh) and canopy width (CW), being the first important when the light beam is crossing the row above the canopy beginning height, and the last when the light beam misses the canopy vertical line, but is intercepted by the lateral branches (Figure 23). These corrections are for shade coming from the row ahead (Figure 24) or from the back row (Figure 25).

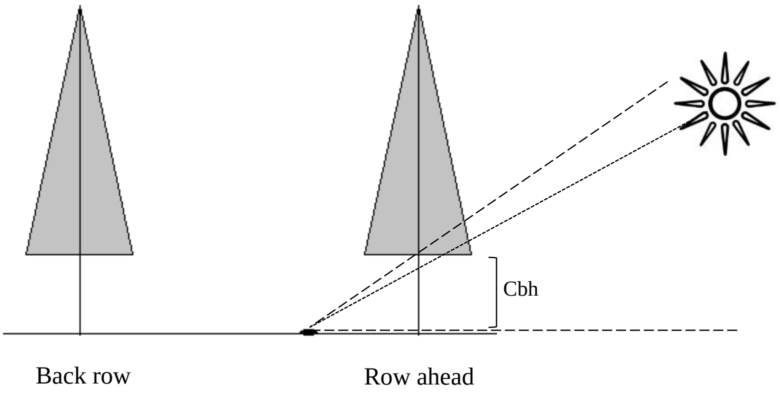

Figure 23. Schematic representation of the row ahead and the back row, defined by the sun position.

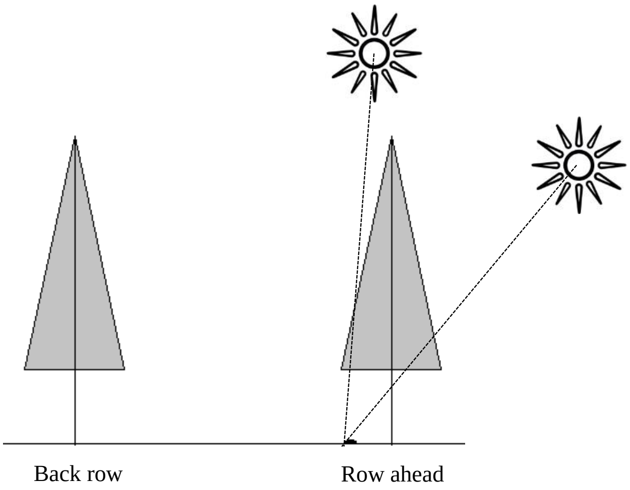

Figure 24. Schematic representation of two sun positions with shading from the lateral branches of the row ahead.

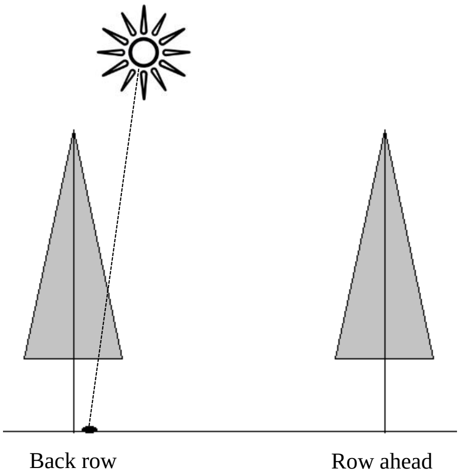

Figure 25. Schematic representation of a sun position with shading coming from the back row.

The calculations necessaries for these corrections were: canopy beginning height corrected by slope (Cbh_{corr}) (Eq. 37), distance from the position (or view point) to the point where the light beam reaches the Cbh_{corr} ($D_{posi\text{-}pointahead}$) (Eq. 38) (Figure 26), distance from the row ahead to the point where light beam reaches Cbh_{corr} ($D_{rowahead\text{-}pointahead}$) (Eq. 39), width projecting shade from row ahead ($TWshade_{ahead}$) (Eq. 40), distance from the position to the canopy boundary of the back row ($D_{posi\text{-}bound}$) (Eq. 41), distance from the back row to its boundary ($D_{backrow\text{-}bound}$) (Eq. 42), distance from the back row to the position ($D_{backrow\text{-}posi}$) (Eq. 43), distance from the position to the point where light beam line reaches Cbh_{corr} ($D_{posi\text{-}pointback}$) (Eq. 44), distance from the back row to the point where light beam line reaches

Cbh$_{corr}$ (D$_{backrow\text{-}pointback}$) (Eq. 45), and width projecting shade from the back row (TWshade$_{back}$) (Eq. 46).

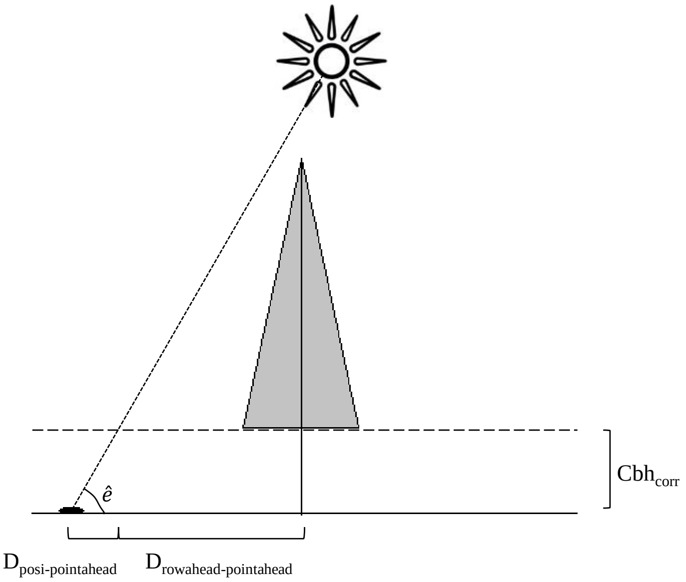

Figure 26. Schematic representation of a condition when the light beam reaches the canopy beginning line out of the canopy, i.e., without shading.

$$Cbh_{corr} = Cbh + TH_{add} \tag{37}$$

$$D_{posi-pointahead} = \frac{Cbh_{corr}}{\tan \hat{e}} \tag{38}$$

$$D_{rowahead-pointahead} = DR_{lb} - D_{posi-pointahead} \tag{39}$$

$$\begin{aligned} &\text{If } \left|\widehat{dl}_N\right| > 90^{\circ} \text{ then } \quad TWshade_{ahead} = D_{rowahead-pointahead} \times \cos \widehat{dl}_S \\ &\text{If } \left|\widehat{dl}_N\right| \leq 90^{\circ} \text{ then } \quad TWshade_{ahead} = D_{rowahead-pointahead} \times \cos \widehat{dl}_N \end{aligned} \tag{40}$$

$$\begin{aligned} &\text{If } \left|\widehat{dl}_N\right| > 90^{\circ} \text{ then } \quad D_{posi-bound} = \frac{(CW_S - DRN_{corr})}{\cos \widehat{dl}_S} \\ &\text{If } \left|\widehat{dl}_N\right| \leq 90^{\circ} \text{ then } \quad D_{posi-bound} = \frac{(CW_N - DRN_{corr} - RS_{corr})}{\cos \widehat{dl}_N} \end{aligned} \tag{41}$$

$$\begin{aligned} &\text{If } \left|\widehat{dl}_N\right| > 90^{\circ} \text{ then } \quad D_{backrow-bound} = \frac{CW_S}{\cos \widehat{dl}_S} \\ &\text{If } \left|\widehat{dl}_N\right| \leq 90^{\circ} \text{ then } \quad D_{backrow-bound} = \frac{CW_N}{\cos \widehat{dl}_N} \end{aligned} \tag{42}$$

$$D_{backrow-posi} = D_{backrow-bound} - D_{posi-bound} \tag{43}$$

$$D_{posi-pointback} = \frac{Cbh}{\tan \hat{e}} \tag{44}$$

$$D_{backrow-pointback} = D_{backrow-posi} + D_{posi-pointback} \tag{45}$$

$$\begin{array}{l}\text{If } \left|\widehat{dl}_N\right| > 90^{\circ} \text{ then } \; TWshade_{back} = D_{backrow-pointback} \times \cos \widehat{dl}_S \\ \text{If } \left|\widehat{dl}_N\right| \leq 90^{\circ} \text{ then } \; TWshade_{back} = D_{backrow-pointaback} \times \cos \widehat{dl}_N\end{array} \tag{46}$$

Finally, having THshade$_{corr}$, TWshade$_{ahead}$ and TWshade$_{back}$, it was possible to do the final test for shading, which is comprised of 4 subtests: for height projecting shade (Eq. 47), for sunset and sunrise (Eq. 48), for lateral branches from the row ahead (Eq. 49) and for lateral branches from the back row (Eq. 50).

$$\begin{array}{l}\text{If } \; THshade_{corr} < Cbh_{corr} \text{ then } 0 \\ \text{If } \; THshade_{corr} \geq Cbh_{corr} \text{ then } \left\langle \begin{array}{l} \nearrow \text{If } \; THshade_{corr} > TH_{corr} \text{ then } 0 \\ \searrow \text{If } \; THshade_{corr} \leq TH_{corr} \text{ then } 1 \end{array} \right.\end{array} \tag{47}$$

$$\begin{array}{l}\text{If } \; |h| > hs \text{ then } 1 \\ \text{If } \; |h| \leq hs \text{ then} \left\langle \begin{array}{l} \nearrow \text{If } THshade_{corr} < 0 \text{ then } 1 \\ \searrow \text{If } \; THshade_{corr} \geq 0 \text{ then } 0 \end{array} \right.\end{array} \tag{48}$$

$$\begin{array}{l}
\text{If } \; TWshade_{ahead} < 0 \text{ then } \left\langle \begin{array}{l}
\nearrow \text{If } \left|\widehat{dl}_N\right| > 90^{\circ} \text{ then} \left\langle \begin{array}{l} \nearrow \text{If } |TWshade_{ahead}| > CW_S \text{ then } 0 \\ \searrow \text{If } |TWshade_{ahead}| \leq CW_S \text{ then } 1 \end{array} \right. \\
\searrow \text{If } \left|\widehat{dl}_N\right| \leq 90^{\circ} \text{ then} \left\langle \begin{array}{l} \nearrow \text{If } |TWshade_{ahead}| > CW_N \text{ then } 0 \\ \searrow \text{If } |TWshade_{ahead}| \leq CW_N \text{ then } 1 \end{array} \right.
\end{array} \right. \\
\text{If } \; TWshade_{ahead} \geq 0 \text{ then } \left\langle \begin{array}{l}
\nearrow \text{If } \left|\widehat{dl}_N\right| > 90^{\circ} \text{ then} \left\langle \begin{array}{l} \nearrow \text{If } |TWshade_{ahead}| > CW_N \text{ then } 0 \\ \searrow \text{If } |TWshade_{ahead}| \leq CW_N \text{ then } 1 \end{array} \right. \\
\searrow \text{If } \left|\widehat{dl}_N\right| \leq 90^{\circ} \text{ then} \left\langle \begin{array}{l} \nearrow \text{If } |TWshade_{ahead}| > CW_S \text{ then } 0 \\ \searrow \text{If } |TWshade_{ahead}| \leq CW_S \text{ then } 1 \end{array} \right.
\end{array} \right.
\end{array} \tag{49}$$

$$\begin{array}{lll} & \nearrow & \text{If } |TWshade_{back}| > \text{CW}_\text{S} \text{ then } 0 \\ \text{If } \left|\widehat{dl}_N\right| > 90^{\text{o}} \text{ then} & & \\ & \searrow & \text{If } |TWshade_{back}| \leq \text{CW}_\text{S} \text{ then } 1 \\ & \nearrow & \text{If } |TWshade_{back}| > \text{CW}_\text{N} \text{ then } 0 \\ \text{If } \left|\widehat{dl}_N\right| \leq 90^{\text{o}} \text{ then} & & \\ & \searrow & \text{If } |TWshade_{back}| \leq \text{CW}_\text{N} \text{ then } 1 \end{array} \tag{50}$$

After these calculations, if the sum of the four results is 0 there is no shade, and if the sum is ≥ 1 there is shade.

5.2.1.2. LAI distribution model

The LAI distribution sub-model calculates the LAI in four vertical layers (Figure 27) and in six horizontal layers (Figure 28) and give as result the LAI that is projecting shade, using the $\text{THshade}_{\text{corr}}$, $\text{TWshade}_{\text{ahead}}$ and $\text{TWshade}_{\text{back}}$, calculated by the shading model. The input data for this sub-model are the average LAI considering the canopy projection area, and the fraction of leaf area in each vertical or horizontal layer (f).

The vertical LAI distribution is determined by leaf area per linear meter of row (LA) (Eq. 51); average LAI by vertical canopy area (LA_v) (Eq. 52), which represents the LA equally distributed in the area that is seen when the canopy is observed laterally; LAI in the low layer (LAI_{low}) (Eq. 53), considering the inferior 1/3 of the canopy; LAI in the intermediate layer (LAI_{int}) (Eq. 54), considering the middle 1/3 of the canopy; LAI in the high layer (LAI_{high}) (Eq. 55), considering the superior 1/3 of the canopy minus the top layer; LAI in the top layer (LAI_{top}) (Eq. 56), considering the 5% superior of the canopy; and LAI at the height projecting shade (LAI_{TH}), which is determined matching the height projecting shade with its correspondent LAI (Eq. 57). A top layer is considered due to the conic format of the canopy at this layer, which promotes spaces without leaves and decrease in the total LAI. Additionally, as the present model is two-dimensional, a correction by the lateral displacement angle ($\widehat{dl}$) is necessary, since as higher is this angle as higher will be the distance that the radiation beam must cross trough the canopy (Figure 28). For this, LAI correction factor by lateral displacement (f_{dlh}) (Eq. 58) and LAI corrected by lateral displacement ($\text{LAIcorr}_{\text{TH}}$) (Eq. 59) must be calculated.

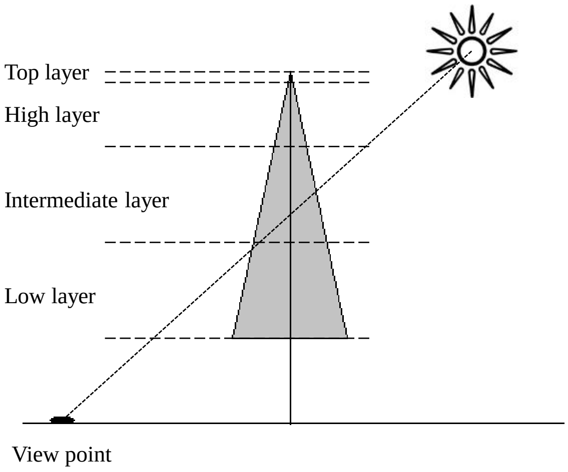

Figure 27. Schematic representation of the four vertical layers of the tree canopy.

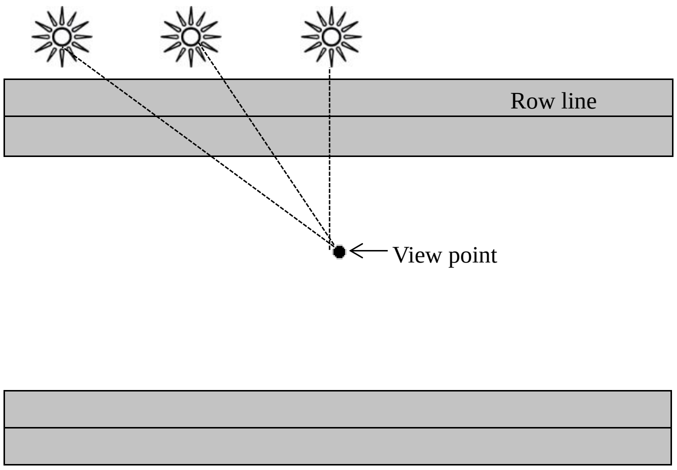

Figure 28. Schematic representation of the effect of lateral displacement on the distance that light beam must cross through the canopy.

$$LA = LAI \times CW \tag{51}$$

$$LAI_v = \frac{LA}{(TH-Cbh)} \tag{52}$$

$$LAI_{low} = \frac{LA \times f_{low}}{\left[\frac{(TH-Cbh)}{3}\right]} \tag{53}$$

$$LAI_{intm} = \frac{LA \times f_{intm}}{\left[\frac{(TH-Cbh)}{3}\right]} \tag{54}$$

$$LAI_{high} = \frac{LA \times f_{high}}{\left\{\left[\frac{(TH-Cbh)}{3}\right]-\left[\frac{(TH-Cbh)}{20}\right]\right\}} \tag{55}$$

$$LAI_{top} = \frac{LA \times f_{top}}{\left[\frac{(TH-Cbh)}{20}\right]} \quad (56)$$

If $THshade_{corr} < Cbh_{corr}$ or $THshade_{corr} > TH_{corr}$ then no shade (57)
If $THshade_{corr} \geq Cbh_{corr}$ and $THshade_{corr} \leq TH_{corr}$ then match with its correspondent LAI

$$\text{If } \left|\widehat{dl}_N\right| > 90^{o} \text{ then } f_{dlh} = \left|\left(\left|\widehat{dl}_S\right| - 90\right)^{-0.15}\right| \quad (58)$$
$$\text{If } \left|\widehat{dl}_N\right| \leq 90^{o} \text{ then } f_{dlh} = \left|\left(\left|\widehat{dl}_N\right| - 90\right)^{-0.15}\right|$$

$$LAIcorr_{TH} = \frac{LAI_{TH}}{f_{dlh}} \quad (59)$$

The horizontal LAI distribution is determined calculating the LAI fraction in each horizontal layer (f) (Eq. 60) (Figure 29), and the LAI at the canopy width projecting shade (LAI_{TW}) (Eq. 61). A correction factor for lateral displacement (f_{dlw}) (Eq. 62) and for zenith angle must be performed (f_z) (Eq. 63), this last one because, when the zenith angle increases, the distance that the light beam must cross within the canopy decreases (Figure 30). Finally, the LAI corrected by lateral displacement and zenith angle ($LAIcorr_{TW}$) is calculated (Eq. 64).

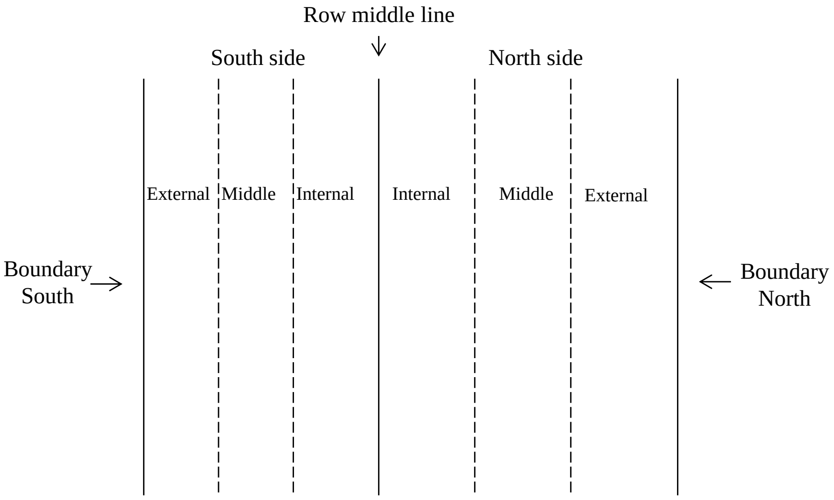

Figure 29. Schematic representation of the six horizontal layers of a row.

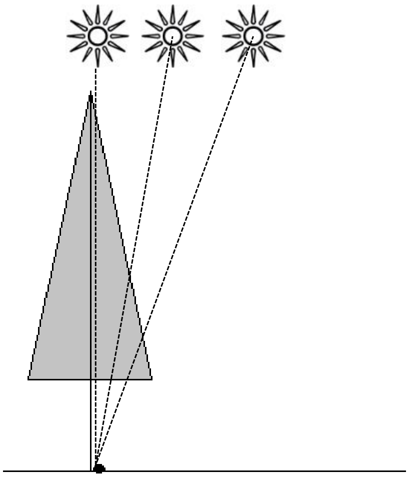

Figure 30. Schematic representation of the zenith angle effect on the distance that light beam must cross through the canopy.

$$LAI_{layer} = \frac{LA \times f_{layer}}{\left[\frac{CW_N or\,(CW - CW_N)}{3}\right]} \qquad (60)$$

If TWshade > CW of the correspondent side, then no shade. (61)

If TWshade $\leq$ CW of the correspondent side, then matches with its correspondent LAI.

For the external layer: $f_Z = z^{-0.18}$

For the middle layer: $f_Z = z^{-0.22}$ (62)

For the internal layer: $f_Z = z^{-0.60}$

If $\left|\widehat{dl}_N\right| > 90^{\circ}$ then $f_{dlw} = \left|\left(\left|\widehat{dl}_S\right| - 90\right)^{-0.5}\right|$ (63)

If $\left|\widehat{dl}_N\right| \leq 90^{\circ}$ then $f_{dlw} = \left|\left(\left|\widehat{dl}_N\right| - 90\right)^{-0.5}\right|$

$$LAIcorr_{TW} = \frac{LAI_{TW} \times f_z}{f_{dlw}} \qquad (64)$$

All the calculations above are done for the row 1, but to calculate the total LAI projecting shade, it is necessary also to consider the shading coming from the adjacent rows (rows 2 and 3) (Figure 31). For this, all the calculations by shading and LAI distribution sub-models must be repeated, for each adjacent row, only changing the input data: distance from the row (DR) and row spacing (RO) (Eq. 65, 66, 67 and 68). After that, LAI projecting shade for each row (LAI_{shade}) (Eq. 69), considering the horizontal LAI distribution only when there is no shading promoted by the canopy vertical line, and the total LAI projecting shade ($LAIshade_{Total}$) (Eq. 70) are calculated.

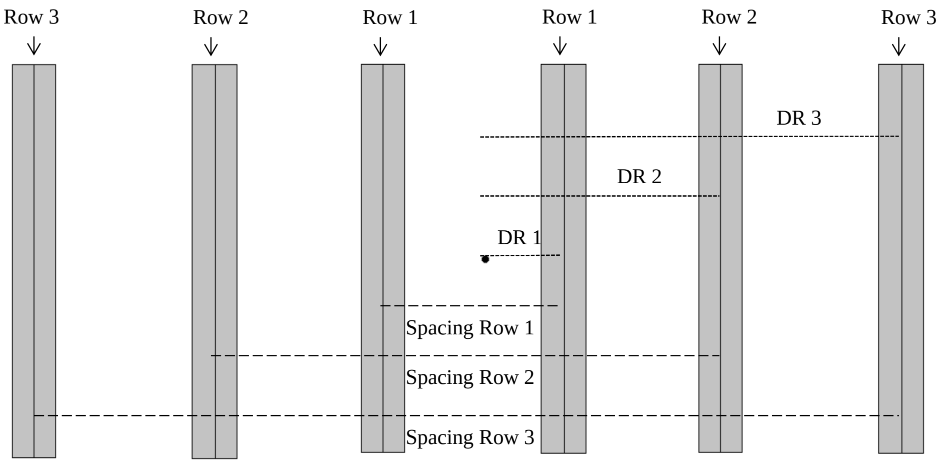

Figure 31. Schematic representation of the distance from the row (DR) and the spacing of the rows 1, 2 and 3.

$$DR_{row2} = DR_{row1} + RS_{row1} \tag{65}$$

$$RS_{row2} = RS_{row1} \times 3 \tag{66}$$

$$DR_{row3} = DR_{row1} + (RS_{row1} \times 2) \tag{67}$$

$$RS_{row3} = RS_{row1} \times 5 \tag{68}$$

If light beam crosses the vertical canopy line then $LAI_{shade} = LAIcorr_{TH}$ (69)
If light beam crosses the lateral branches but not the vertical line then $LAI_{shade} = LAIcorr_{TW}$

$$LAI_{shade_{Total}} = LAI_{shade_{row1}} + LAI_{shade_{row2}} + LAI_{shade_{row3}} \tag{70}$$

5.2.1.3. Radiation transmission calculations

The calculations of radiation transmission are done using as input data the x coefficient for leaf angle distribution and measured data of external daily total incoming radiation (MJ m^{-2} day^{-1}), which is distributed for every 15 minutes based on the extra-terrestrial radiation curve. For this, the following calculations are required: daylength (N), in hours (Eq. 71); extra-terrestrial solar radiation for every 15 minutes (Qo), in W m^{-2} (Eq. 72); average Q_0 in the diurnal period (Qo_{avg}), in W m^{-2} (Eq. 73); multiplier for Qg distribution along the day ($mult_{Qo}$) (Eq. 74); average external radiation along the day ($Qgext_{avg}$), in W m^{-2} (Eq. 75); external solar radiation (Qg_{ext}), in W m^{-2} (Eq. 76); fraction of diffuse radiation at full sun ($fdif_{ext}$) (Eq. 77); external diffuse radiation ($Qdif_{ext}$), in W m^{-2} (Eq. 78); diffuse radiation transmissivity (t_{dif}), determined through the model of Gou et al. (2017), using an extinction coefficient for z = 45°, and the LAI from the average LAI vertical; transmitted diffuse radiation ($Qdif_t$), in W m^{-2} (Eq. 79); extinction coefficient for ellipsoidal leaf angle distribution (k) (Eq. 80), based on Campbell and Norman (1998); direct radiation transmissivity (t_{dir}) (Eq. 81); external direct radiation ($Qdir_{ext}$), in W m^{-2} (Eq. 82); transmitted direct radiation ($Qdir_t$), in W m^{-2} (Eq. 83); transmitted radiation at every 15 minutes (Qt), in W m^{-2} (Eq. 84) and, finally, daily total transmitted radiation (Qt_{day}), in MJ m^{-2} day^{-1} (Eq. 85).

$$N = \frac{2 \times hs}{15} \tag{71}$$

$$Q_0 = 1367 \times \left[1 + 0.033 \times \left(\frac{360}{365} \times DY\right)\right] \times (\sin\varphi \times \sin\delta + \cos\varphi \times \cos\delta \times \cos h) \tag{72}$$

If $Q_0 < 0$ then $Q_0 = 0$

$$Q_{0_{avg}} = \frac{\sum Q_0}{N \times 4} \tag{73}$$

$$mult_{Q_0} = \frac{Q_0}{Q_{0_{avg}}} \tag{74}$$

$$Q_{g_{ext\,avg}} = \frac{Q_{g_{day}} \times 10^6}{N \times 3600} \tag{75}$$

$$Q_{g_{ext}} = Q_{g_{ext\,avg}} \times mult_{Q_0} \tag{76}$$

$$\text{If } Q_{g_{ext}} \leq 0 \text{ then } f_{dif_{ext}} = 0 \tag{77}$$

$$\text{If } Q_{g_{ext}} > 0 \text{ then } f_{dif_{ext}} = 11 \times Q_{g_{ext}}{}^{-0.675}$$

$$\text{If } f_{dif_{ext}} > 1 \text{ then } Q_{dif_{ext}} = Q_{g_{ext}} \times 1 \quad (78)$$
$$\text{If } f_{dif_{ext}} \leq 1 \text{ then } Q_{dif_{ext}} = Q_{g_{ext}} \times f_{dif_{ext}}$$

$$Q_{dif_t} = Q_{dif_{ext}} \times t_{dif} \quad (79)$$

$$k = \frac{\sqrt{x^2+(\tan z)^2}}{x+1.774 \times (x+1.182)^{-0.733}} \quad (80)$$

$$t_{dir} = e^{-k \times LAI_{shade_{Total}}} \quad (81)$$

$$Q_{dir_{ext}} = Q_{g_{ext}} - Q_{dif_{ext}} \quad (82)$$

$$\text{If } THshade_{corr_{row3}} < 0 \text{ then } Q_{dir_t} = 0 \quad (83)$$
$$\text{If } THshade_{corr_{row3}} \geq 0 \text{ then } Q_{dir_t} = Q_{dir_{ext}} \times t_{dir}$$

$$Q_t = Q_{dir_t} + Q_{dif_t} \quad (84)$$

$$Q_{t_{day}} = \frac{\sum Q_t \times 900}{10^6} \quad (85)$$

5.2.2. Model testing

5.2.2.1. Experimental data

For the model testing, an experiment was carried out in São Carlos, state of São Paulo, Brazil (lat 22°01’ S, long 47°53’ W, alt 860 m), from December 2014 to June 2016. The climate of this location is Cwa (Köppen) with a cool and dry season, from April to September (average air temperature of 19.9ºC and total rainfall of 250 mm), and another warm and wet, from October to March (average air temperature of 23.0ºC and total rainfall of 1100mm) (Alvares et al., 2013). The trial was composed by an open pasture of *Urochloa* (syn. *Brachiaria*) *brizantha* (Hochst ex A. Rich.) Stapf cv. BRS Piatã, which was the full sun system, and by an adjacent pasture, of the same cultivar, with rows of *Eucalyptus urograndis* (*Eucalyptus grandis x Eucalyptus urophylla*) of the GG100 clonal, which was the silvopastoral system. The experimental area totaled 12 ha, being 6 ha in each system. The trees were planted in April 2011 and arranged in simple rows, in a near East-West orientation, with 15 m between rows and 2 m between plants in the rows, totaling 333 trees ha^{-1}.

The full sun pasture was considered a treatment (FS) and in the silvopastoral system other four treatments were established. The silvopastoral treatments were settle considering the distance from the North row, which was responsible for causing shading in the assessed area in the most of the year, due to solar declination. These treatments were: 0.00 m (SP1); 3.75 m (SP2); 7.50 m (SP3) and 11.25 m (SP4) from the North row (Figure 32).

Five linear quantum sensors (Apogee, Logan, UT, USA) were installed at 0.6 m above the ground, being one in the open pasture and four in the silvopastoral system, to measure photosynthetically active radiation (PAR) in all the specified positions (Figure 32). These sensors were connected to a datalogger (CR3000, Campbell Scientific, Logan, UT, USA), configured to take measurements every 5 seconds and to record averages every 15 minutes and hour, and total values every day.

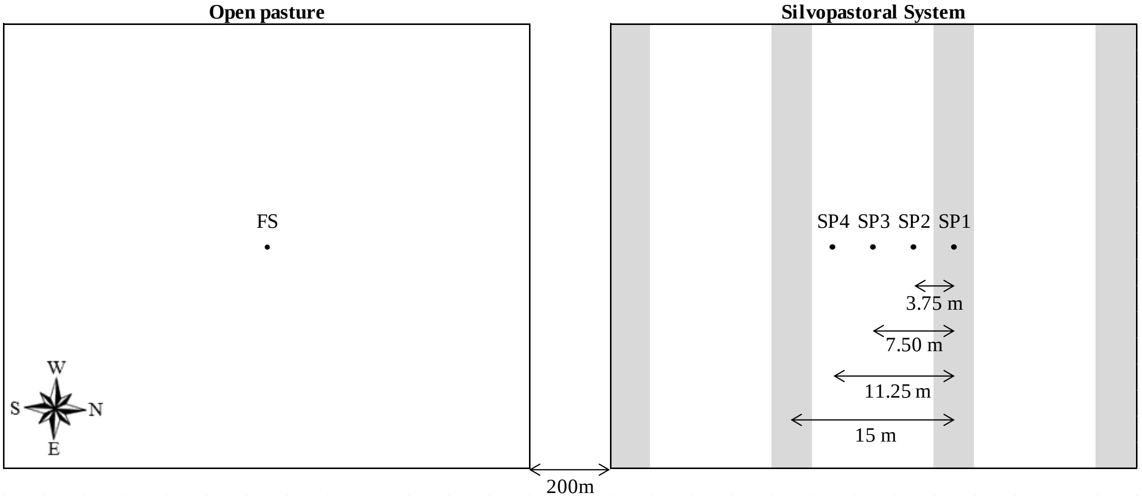

Figure 32. Schematic representation of the experimental area indicating where the photosynthetically active radiation data were collected in the open pasture (left) and in the silvopastoral system (right). FS: full sun, SP1: 0.00 m, SP2: 3.75 m, SP3: 7.50 m, SP4: 11.25 m from North row. Grey strips illustrate the tree rows.

During the experimental period, trees assessments were performed six times (12/26/2014, 02/03/2015, 05/26/2015, 10/01/2015, 01/27/2016, and 06/02/2016), consisting in measurements of tree height and canopy beginning height, with a clinometer; and canopy width and canopy width to North (considering the distance from the stem to the extremity of the wider branch at the North direction), with a metric tape.

In February 2015, the average leaf angle of 20 trees was measured with a LAI-2000 canopy analyzer (Li-Cor, Lincoln, Nebraska, USA), maintaining the fish-eye glass oriented to take measurements only from the canopy, excluding the stem. For this, a cap with 45º openness was used, requiring eight measurements to integrate the whole canopy circumference.

In July 2016, 10 trees were cut in order to measure their total leaf area. All the leaves of each tree were separated and weighed to determine the green biomass. Subsequently, a subsample of 0.2 kg was taken to determine its leaf area with a leaf area meter, model LI-3100C (Li-Cor, Lincoln, Nebraska, USA) and driven in an oven at 65ºC, until constant weight. The specific leaf area (SLA) was determined by dividing the leaf area of the subsample by its dry mass. The total leaf area was calculated multiplying the SLA by the total leaf biomass.

5.2.2.2. Testing process

The first step of the testing process was the shading sub-model calculations, considering Tm = -45º, RS = 15 m, RO = -7.28, GS = 1.35º, SO = 90º and Sd = 0º. The values of TH, Cbh, CW and CWN (Table 23) were taken from the trees assessments and their variations were performed by a linear interpolation between the values of the previous and the next assessment.

Table 23. Average tree height (TH), canopy beginning height (Cbh), canopy width (CW) and canopy width to North (CWN) of Eucalyptus trees cultivated in a silvopastoral systems.

Date	TH	Cbh	CW	CWN
			m	
12/26/2014	24.05	5.93	7.16	3.68
02/03/2015	23.01	5.27	7.54	4.06
05/26/2015	23.15	5.50	6.53	3.38
10/01/2015	25.40	6.58	8.09	4.13
01/27/2016	26.73	6.72	8.96	4.38
06/02/2016	29.40	9.26	8.07	4.61

For the LAI distribution calculations, the total leaf area of the trees, measured during the experiment, was multiplied by the population of trees (0.0333 trees m^{-2}), resulting in the LAI for the total area (1.97). This value was divided by the fraction of the total area covered by tree canopy (0.6) in order to obtain the average LAI considering the canopy projection area

(3.28), required as input by the model. This value was assumed to be the same in all the experimental period, considering that the leaf area variation was not significant.

As leaf area was not measured separated for each canopy layer specified in the model, the fraction of leaf area in each vertical or horizontal layer (f) was adjusted to achieve the best simulations of PAR transmission (Table 24).

Table 24. Fraction of leaf area in each vertical and horizontal layer calibrated for the PAR transmission simulations.

Vertical		Horizontal	
Layer	Fraction	Layer	Fraction
Low	0.150	Internal North	0.370
Intermediate	0.430	Middle North	0.240
High	0.380	External North	0.060
Top	0.040	Internal South	0.275
		Middle South	0.050
		External South	0.005

Finally, the radiation transmission calculations were performed using the x coefficient calculated through the equation 75 (0.70), for an ellipsoidal leaf angle distribution (Campbell and Norman 1998), considering the average leaf angle (ALA) measured during the experiment (66.5º). The measured data of external daily total incoming PAR (MJ m^{-2} day^{-1}) also were employed in these calculations. The diffuse PAR transmission was calculated through the model of Gou et al. (2017), using as input data a k = 0.67, calculated for a zenith angle of 45º, considering the Campbell and Norman (1998) approach (Eq. 80), and LA_V of the row 1, canopy width, row spacing and tree height.

$$x = -1.7433025 + \left(\frac{162.22848}{ALA}\right) \tag{86}$$

5.2.3. Statistical evaluation of the model

Several statistical indexes were used to evaluate the model capacity for estimating PAR transmission. These statistics were:

a) Linear regression between the observed (O) and the predicted (P) values of each variable, and the coefficient of determination (R^2) about this regression.

b) Agreement index (d) of Willmott (1981), which calculates the model accuracy:

$$d = 1 - \frac{\sum_{i=1}^{n}(O_i - P_i)^2}{\sum_{i=1}^{n}(|P_i - \bar{O}| + |O_i - \bar{O}|)^2} \tag{87}$$

c) Nash-Sutcliffe efficiency (NSE), which describes the model accuracy and, as suggested by Moriasi et al. (2007), means satisfactory model performance when its values are higher than 0.5, and good performance when greater than 0.65:

$$NSE = 1 - \frac{\sum_{i=1}^{n}(P_i - O_i)^2}{\sum_{i=1}^{n}(O_i - \bar{O})^2} \tag{88}$$

d) Mean error (ME).

$$ME = \left(\frac{1}{n}\right)\sum_{i=1}^{n}(P_i - O_i) \tag{89}$$

e) Mean absolute error (MAE).

$$MAE = \left(\frac{1}{n}\right)\sum_{i=1}^{n}|P_i - O_i| \tag{90}$$

f) Root mean square error (RMSE).

$$RMSE = \sqrt{\left[\left(\frac{1}{n}\right)\sum_{1=i}^{n}(O_i - P_i)^2\right]} \tag{91}$$

5.3. Results

Good agreement between observed and estimated data was achieved for PAR transmission in all the assessed positions (Figure 33 and Table 25). The simulations at the position 0.00 m achieved good precision (R^2 = 0.61), regular accuracy (d = 0.87 and NSE = 0.48) and low errors (ME = 0.31 MJ m^{-2} day^{-1}, MAE = 0.70 MJ m^{-2} day^{-1} and RMSE = 0.90 MJ m^{-2} day^{-1}) (Table 25). PAR transmission at 3.75 m from the North row also was satisfactorily simulated, achieving good agreement (R^2 = 0.83, d = 0.95, NSE = 0.77, ME = 0.40 MJ m^{-2} day^{-1}, MAE = 0.92 MJ m^{-2} day^{-1} and RMSE = 1.15 MJ m^{-2} day^{-1}) (Table 25). The simulations at the position 7.50 m presented good agreement (R^2 = 0.92, d = 0.97, NSE = 0.88, ME = 0.52 MJ m^{-2} day^{-1}, MAE = 0.76 MJ m^{-2} day^{-1} and RMSE = 0.93 MJ m^{-2} day^{-1}), such as at the 11.25 m from the North row (R^2 = 0.88, d = 0.96, NSE = 0.87, ME = 0.25 MJ m^{-2} day^{-1}, MAE = 0.68 MJ m^{-2} day^{-1} and RMSE = 0.84 MJ m^{-2} day^{-1}) (Table 25).

Time series of observed and estimated data are shown for the positions 0.00 m (Figure 34a), 3.75 m (Figure 34b), 7.50 m (Figure 34c) and 11.25 m (Figure 34d) from the North row. The model was able to capture several trends across all conditions. Some simulation problems were identified mainly during the transition between periods under intense shading and periods with high transmissivity, mainly for the positions 3.75 and 7.50 m from the North row. In the position 0.00 m, a PAR transmission underestimation occurred between September and October 2015 (Figure 34).

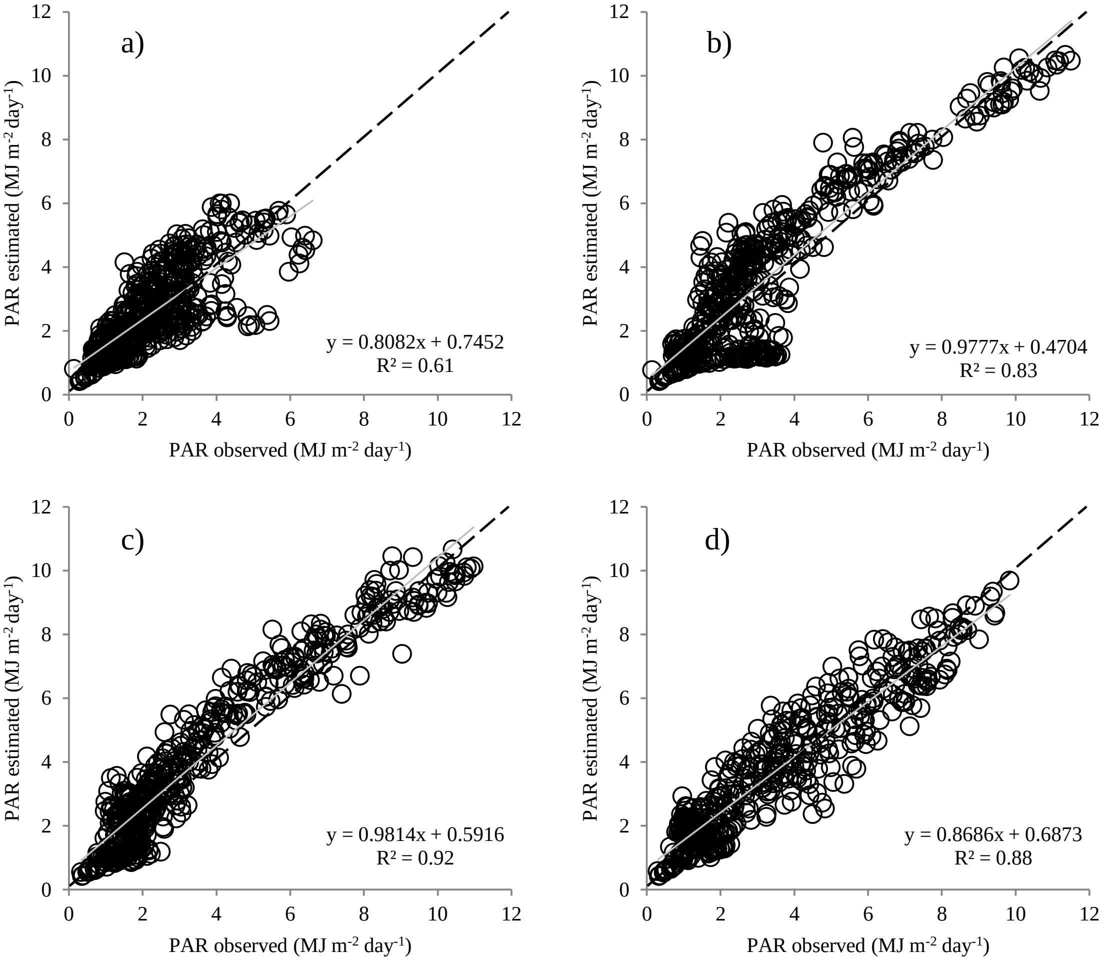

Figure 33. Relationship between estimated and observed daily PAR transmissions at 0.0 m (a), 3.75 m (b), 7.50 m (c) and 11.25 m (d) from the North row in a silvopastoral system.

Table 25. Statistical indexes for the simulations of photosynthetically active radiation transmission at 0.0 m, 3.75 m, 7.50 m and 11.25 m from the North row in a silvopastoral system. R^2 = coefficient of determination, d = agreement index, NSE = Nash-Sutcliffe efficiency, ME = mean error (MJ m^{-2} day^{-1}), MAE = mean absolute error (MJ m^{-2} day^{-1}), RMSE = root mean square error (MJ m^{-2} day^{-1}).

Position	Statistical index					
	R^2	d	NSE	ME	MAE	RMSE
0.00	0.61	0.87	0.48	0.31	0.70	0.90
3.75	0.83	0.95	0.77	0.40	0.92	1.15
7.50	0.92	0.97	0.88	0.52	0.76	0.93
11.25	0.88	0.96	0.87	0.25	0.68	0.84

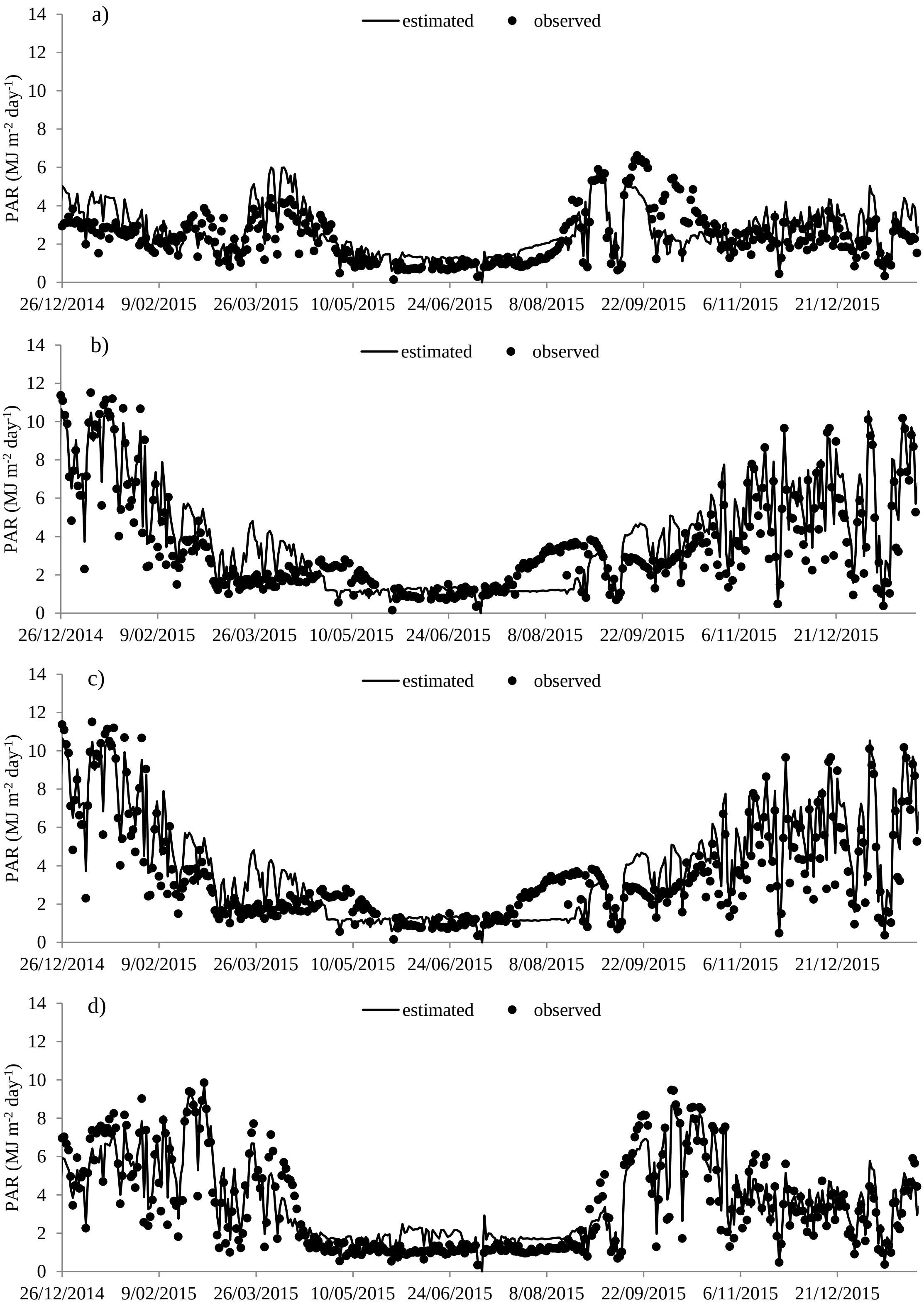

Figure 34. Time series of estimated and observed daily photosynthetically active radiation transmissions at 0.0 m (a), 3.75 m (b), 7.50 m (c) and 11.25 m (d) from the North row in a silvopastoral system.

5.4. Discussion

The model developed in this study showed to be able to simulate solar radiation transmission in agroforestry systems with eucalyptus arranged in rows and without significant spaces between the canopies in the rows. The results confirmed the efficiency of the model for estimating PAR transmission in several distances from the tree rows, different zenith angles, in all the seasons of the year, and under high or low shading. This capacity must allow future adaptations for several tree species in agroforestry systems and the use of such model to help in simulations of crop and pastures growth in understory of these systems. Therefore the model can be improved in many aspects to simulate with better accuracy the interactions between solar radiation and tree canopy, mainly estimating the distance crossed by the light beam within the canopy, and refining the leaf area distribution in the different canopy parts; and must be tested in several locations, for different latitudes and agroforestry arrangements.

The PAR transmission simulations showed a good agreement between observed and estimated data, achieving statistical results similar to several good studies available in the literature (Abraha and Savage 2010; Annandale et al. 2004; Charbonnier et al. 2013; Oyarzun et al. 2007), confirming the model efficacy. The results reached in the present study (R^2 between 0.61 and 0.92, d from 0.87 to 0.97, NSE between 0.48 and 0.88, ME from 0.25 to 0.52 MJ m^{-2} day^{-1}, MAE from 0.68 to 0.92 MJ m^{-2} day^{-1} and RMSE between 0.84 and 1.15 MJ m^{-2} day^{-1}) where similar to those obtained by Annandale et al. (2004) (R^2 between 0.62 and 0.99, d from 0.22 to 0.98 and RMSE between 0.60 and 5.90 MJ m^{-2} day^{-1}), Charbonnier et al. (2013) ($R^2 = 0.88$ and RRMSE = 30%), Oyarzun et al. (2007) (d from 0.65 to 0.92), and Abraha and Savage (2010) ($R^2 = 0.91$ and d = 0.96) for solar radiation transmission or interception.

The simulations at the position 0.00 m were less efficient due to the great variability of the distribution of lateral branches, which projected shade on this position in great part of the year. In systems with pruning of this non-uniform part of the canopy or low layer, this problem may be reduced. Another factor that influenced the model performance was the allocation of the quantum sensors, which were maintained at the same position all the time and without replications, promoting a great susceptibility of the measurements to differences in individual tree dimensions. Probably, this factor influenced the efficiency of the estimates during the transition between periods under intense shading and periods with high transmissivity, due to individual variations of tree height and canopy width. Experimental designs with replications of stationary sensors or the utilization of portable sensors that allow drawing grids of measurement throughout the system may help to solve these uncertainties.

The diffuse/direct radiation ratio may be different depending on the location and conditions (Dervishi and Mahdavi 2012). The partitioning between incoming direct and diffuse radiation (Eq. 77 and 78) was estimated empirically in the present study with an equation developed specifically for the experimental site, being necessary to test this equation for other locations and adapt it if necessary.

5.5. Conclusions

The model developed in this study was efficient for estimating PAR transmission in several distances from the tree rows, different zenith angles, in all the seasons of the year, and under high or low shading. This capacity must allow future adaptations for several tree species in agroforestry systems and the use of such model to help in simulations of crop and pastures growth in understory of these systems.

The model can be improved in many aspects to simulate with better accuracy the interactions between solar radiation and tree canopy, mainly estimating the distance crossed by the light beam within the canopy, and refining the leaf area distribution in the different canopy parts. Tests should be performed in several locations, for different latitudes and agroforestry arrangements.

The simulations were affected negatively by factors such as the great variability of the distribution of lateral branches and the allocation of the quantum sensors, which were maintained at the same position all the time and without replications, increasing the susceptibility of the measurements to differences in individual tree dimensions.

REFERENCES

Abraha, M.G., Savage, M.J., 2010. Validation of a three-dimensional solar radiation interception model for tree crops. Agric. Ecosyst. Environ. 139, 636-652. https://doi.org/10.1016/j.agee.2010.10.010

Alvares, C.A., Stape, J.L., Sentelhas, P.C., Goncalves, J.L.M., Sparovek, G., 2013. Köppen’s climate classification map for Brazil. Meteorol. Z. 22, 711-728. https://doi.org/10.1127/0941-2948/2013/0507

Annandale, J.G., Jovanovic, N.Z., Campbell, G.S., Du Sautoy, N., Lobit, P., 2004. Two-dimensional solar radiation interception model for hedgerow fruit trees. Agric. For. Meteorol. 121, 207-225. https://doi.org/10.1016/j.agrformet.2003.08.004

Campbell, G.S., Norman, J.M., 1998. An Introduction to Environmental Biophysics. Springer, Amsterdam.

Charbonnier, F., le Maire, G., Dreyer, E., Casanoves, F., Christina, M., Dauzat, J., Eitel, J.U., Vaast, P., Vierling, L.A., Roupsard, O., 2013. Competition for light in heterogeneous canopies: Application of MAESTRA to a coffee (*Coffea arabica* L.) agroforestry system. Agric. For. Meteorol. 181, 152–169. https://doi.org/10.1016/j.agrformet.2013.07.010

Chen, S.G., Ceulemans, R., Impens, I., 1994. A fractal based Populus canopy structure model for the calculation of light interception. For. Ecol. Manag. 69, 97-110. https://doi.org/10.1016/0378-1127(94)90222-4

Dervishi, S., Mahdavi, A., 2012. Computing diffuse fraction of global horizontal solar radiation: A model comparison. Sol. Energy 86, 1796-1802. https://doi.org/10.1016/j.solener.2012.03.008

Duursma, R.A., Mäkelä, A., 2007. Summary models for light interception and light-use efficiency of non-homogeneous canopies. Tree Physiol. 27, 859-870.

Duursma, R.A., Medlyn, B.E., 2012. MAESPA: a model to study interactions between water limitation, environmental drivers and vegetation function at tree and stand levels, with an example application to [CO2] × drought interactions. Geosc. Model. Dev. 5, 919-940. https://doi.org/10.5194/gmd-5-919-2012

Forrester, D.I., 2014. A stand-level light interception model for horizontally and vertically heterogeneous canopies. Ecol. Model. 276, 14-22.

Grace, J.C., Jarvis, P.G., Norman, J.M., 1987. Modelling the interception of solar radiant energy in intensively managed stands. N. Z. J. For. Sci. 17, 193-209.

Gou, F., Van Ittersum, M.K., Van der Werf, W., 2017. Simulating potential growth in a relay-strip intercropping system: Model description, calibration and testing. Field Crop. Res. 200, 122–142. https://doi.org/10.1016/j.fcr.2016.09.015

Monsi, M., Saeki, T., 1953. On the Factor Light in Plant Communities and its Importance for Matter Production. Jpn. J. Bot. 14, 22–52.

Moriasi, D.N., Arnold, J.G., Van Liew, M.W., Bingner, R.L., Harmel, R.D., Veith, T.L., 2007. Model evaluation guidelines for systematic quantification of accuracy in watershed simulations. Trans. Am. Soc. Agric. Biol. Eng. 50, 885-900.

Norman, J.M., Welles, J.M., 1983. Radiative transfer in an array of canopies. Agron. J. 75, 481–488. https://doi.org/10.2134/agronj1983.00021962007500030016x

Oyarzun, R.A., Stockle, C.O., Whiting, M.D., 2007. A simple approach to modelling radiation interception by fruit-tree orchards. Agric. For. Meteorol. 142, 12–24. https://doi.org/10.1016/j.agrformet.2006.10.004

Sinoquet, H., Bonhomme, R., 1992. Modeling radiative transfer in mixed and row intercropping systems. Agric. For. Meteorol. 62, 219-240. https://doi.org/10.1016/0168-1923(92)90016-W

Talbot, G., Dupraz, C., 2012. Simple models for light competition within agroforestry discontinuous tree stands: are leaf clumpiness and light interception by woody parts relevant factors? Agrofor. Syst. 84, 101-116. https://doi.org/10.1007/s10457-011-9418-z

Wang, Y.P., Jarvis, P.G., 1990. Description and validation of an array model: MAESTRO. Agric. For. Meteorol. 51, 257-280. https://doi.org/10.1016/0168-1923(90)90112-J

Willmott, C.J., 1981. On the validation of models. Phys. Geogr. 2, 184–194.

Zhao, W., Qualls, R.J., Berliner, P.R., 2003. Modeling of the short wave radiation distribution in an agroforestry system. Agric. For. Meteorol. 118, 185-206. https://doi.org/10.1016/S0168-1923(03)00108-4

6. APSIM-TROPICAL PASTURE AND CROPGRO-PERENNIAL FORAGE PERFORMANCES FOR SIMULATING PIATÃ PALISADEGRASS GROWTH IN A SILVOPASTORAL SYSTEM

ABSTRACT

Silvopastoral systems are important to intensify pasture production and mitigate climate change effects. However, very few studies were performed to adapt crop models to simulate these systems. The aim of this study was to test the APSIM-Tropical Pasture and the CROPGRO-Perennial Forage models for estimating Piatã palisadegrass growth in a silvopastoral system with eucalyptus. For this, a field experiment was carried out from December 2014 to January 2016, in a silvopastoral system with the trees arranged in simple rows, in East-West orientation, with 15 m between rows and 2 m between plants in the rows. This experiment was conducted under grazing management and rainfed conditions, during 11 growth cycles, with the pasture variables being assessed at four distances from the North row (SP1: 0.00 m, SP2: 3.75 m, SP3: 7.50 m and SP4: 11.25 m). APSIM testing was performed by three methods: considering only the soil water competition, by using the current silvopastoral simulation capability, and considering only the solar radiation competition, by using the measured data of solar radiation or by using data of radiation transmission estimated by a specific model. CROPGRO testing was performed based on the competition for solar radiation, using the measured data of this variable. The APSIM-Tropical Pasture was efficient to simulate pasture growth when competition by solar radiation was considered (R^2 from 0.69 to 0.88, d from 0.90 to 0.96, and NSE between 0.51 and 0.85), but inefficient when considering only competition by soil water (R^2 between 0.58 and 0.85, d between 0.58 and 0.82, and NSE from -4.07 to -0.14). The CROPGRO-Perennial Forage achieved good performance on pasture growth simulation at the positions SP1, SP2 and SP3 (R^2 from 0.75 to 0.90, d from 0.93 to 0.96, NSE between 0.74 and 0.85), but low agreement between observed and estimated growth at SP4 ($R^2 = 0.38$, d = 0.74 and NSE = -0.34). Despite the good results, improvements should be performed in both models for simulating all factors that affect forage growth in silvopastoral systems.

Keywords: Agroforestry; DSSAT; Grazing; Tree-crop interactions; Solar radiation; Soil water

6.1. Introduction

Modeling of crop growth and development in agroforestry systems is much more complex than for single crops. This complexity comes from the heterogeneity caused by the interactions between crops and trees, changing mass and energy fluxes between them and promoting a huge interdependence of these two systems. Therefore, a crop model for simulating these two systems will require, besides the simulation of the dynamic processes of each of them, to describe the changes caused by their interactions (Huth et al. 2002).

Many models employed for simulating agroforestry systems are based on this abstraction of the interaction between crop and tree. The WaNulCAS (Water, Nutrient and

Light Capture in Agroforestry systems) model (Van Noordwijk and Lusiana 1999), for example, uses a series of soil zones to calculate subsuperficial competition between trees and crops in several distances from the tree component. This model was used by Pinto et al. (2005) for estimating sugarcane productivity in an agroforestry system with eucalyptus. In a similar way, the SBELTS model (Qi et al. 2001) simulates crop yield according to several points under windbreaks, in order to calculate the effect of wind speed reduction on crop performance. In both cases, there are only studies about the system performance, but not of all the components that affect yield.

Matthews and Lawson (1997) combined the tree model HYBRID (Friend et al. 1997) with the cassava model GUMCAS (Matthews and Hunt 1994) aiming to evaluate several agroforestry management options. The HYBRID model also was incorporated into the HyPAR model, using the tropical crop model PARCH (Fry and Lungu 1996) to simulate crops growth.

Zuidema et al. (2005) used the SUCROS-Cocoa model for estimating cacao yield, taking into account solar radiation interception and photosynthesis, maintenance respiration, biomass accumulation and competition between plants, such as shading by trees. Balandier et al. (2003) evaluated the capacity of the ALWAYS model (Auclair 1996) to describe the interactions in silvopastoral systems, considering trees, pasture and animals. Brisson et al. (2004) adapted the STICS-CA model for integrated systems. Johnson et al. (2009) combined the ALMANAC (Kiniry et al. 1992) and SWAT models for estimating the yield of trees and understory crops.

Oijen et al. (2010) developed a simple model for estimating coffee yield in agroforestry systems, in Central America, taking into account vegetative and reproductive growth fisiology under several environmental conditions. The Yield-SAFE model (Van Der Werf et al. 2007) was also applied for agroforestry systems. This model was used by Kessman et al. (2007) for simulating crops growth and productivity in these systems, whereas Palma et al. (2007) and Graves et al. (2010) employed it for simulating crops and trees growth.

Gregory (1996), in a review about approaches for modeling water and nutrients uptake in agroforestry systems, mentioned that the basic principles that define the ability of roots to uptake water and nutrients from the soil were, respectively, first outlined by Bray (1954) and by Gardner (1960). These authors observed that the ability to uptake water and nutrients from the soil was not only dependent of the amount of each of them but also of their mobility in relation to the architecture of the root system. This means that the zone of competition between roots for water and mobile nutrients such as nitrate is much larger than that for immobile nutrients such as phosphate.

According to Celette et al. (2010), there are several models to estimate the partitioning of soil resources in intercropped systems (Lafolie et al. 1999; Ozier-Lafontaine et al. 1998; Van Noordwijk and Lusiana 1999). Most of them are fairly complex as they were designed to test hypotheses about the mechanisms of intercropped systems interactions (Malezieux et al. 2008). However, such kind of model should be kept simple, with few parameters and inputs, incorporating the main features relevant to the problem to be solved.

The Agricultural Production Systems Simulator (APSIM) (Holzworth et al. 2014; Keating et al. 2003) was applied sometimes for agroforestry systems (Huth et al. 2002; Smethurst et al. 2017), but never for silvopastoral systems. Huth et al. (2002) simulated the yield of eucalypt and chickpea associated, using a multipoint capability, modeling each point separately and aiming a distribution that promotes a good representation of the entire system. Smethurst et al. (2017) estimated maize yield in an agroforestry system with gliricidia. On the other hand, the CROPGRO model (Boote et al. 1998), available on the Decision Support System for Agrotechnology Transfer (DSSAT) platform, is not used frequently for agroforestry systems, since its platform does not have tree models. However, it was employed by Qi et al. (2001) to simulate soybean yield under windbreak systems, and by Zamora et al. (2009), for simulating cotton yield under several shading levels, in an agroforestry system with pecan nut. More specifically, the CROPGRO-Perennial Forage model was employed by Pedreira et al. (2011) and Pequeno et al. (2014) for Urochloa brizantha under full sun, but never in silvopastoral systems.

Considering that silvopastoral systems are of great importance to recover degraded pastures (Nair et al. 2009) and are tools for adapting agricultural systems and mitigating climate change effects (Steinfeld et al. 2006), the hypothesis of this study is that both APSIM-Tropical Pasture and CROPGRO-Perennial Forage can be adapted to simulate pasture growth in a silvopastoral system. Therefore, the aim of this study was to test the APSIM-Tropical Pasture and the CROPGRO-Perennial Forage models for estimating Piatã palisadegrass growth in a silvopastoral system with eucalyptus, considering different interaction conditions.

6.2. Material and methods

6.2.1. Experimental data

The data used to test the models were collected in a field experiment carried out in São Carlos, SP, Brazil (21°57'42" S, 47°50'28" W, 860 m), in a pasture of *Urochloa* (sin. *Brachiaria*) *brizantha* cv. BRS Piatã associated with rows of eucalypt (*Eucalyptus grandis x Eucalyptus urophylla)* (GG100 clonal), planted in April of 2011 and arranged in simple rows, in East-West orientation, with 15 m between rows and 2 m between plants in the rows. This experiment was conducted under grazing management and rainfed conditions during 11 growth cycles, from December 2014 to January 2016, totaling 44 pasture productivity data, with the pasture variables being assessed at four distances from the eucalypt North row (SP1: 0.00 m, SP2: 3.75 m, SP3: 7.50 m and SP4: 11.25 m) (Figure 35). The pasture was grazed by beef cattle of Canchim breed in rotational grazing. The resting period was 30 days and the period of occupation was six days. Fertiliser was applied as 50 kg N ha^{-1} in the 1st, 2nd, 3rd and 4th cycles, immediately after grazing. The meteorological conditions of each growth cycle, for the positions above described, are presented in Table 26.

During each cycle, five pasture assessments were performed at approximately 0, 9, 16, 23 and 30 days after grazing. These assessments were obtained by cutting the forage at 10 cm above the ground, being taken two subsamples per plot for quantifying the biomass accumulation (above 20 cm), using a 0.25 m^2 (0.5 x 0.5 m) quadrat. The forage collected was immediately weighed, and subsequently, both subsamples of each plot were mixed, from which two ~0.2 kg green mass samples were taken: one sample designed to perform morphological separation (leaf, stem and dead material) and another to determine the dry matter (DM). The percentage of dry matter from the morphological fractions was calculated by weighing both subsamples before and after drying them in an oven at 65ºC until they reached a constant weight. Having the weight of the green mass harvested in 0.25 m^2, the productivity of DM was estimated from the fractions in this area, and then extrapolated to 1 ha (kg ha^{-1}).

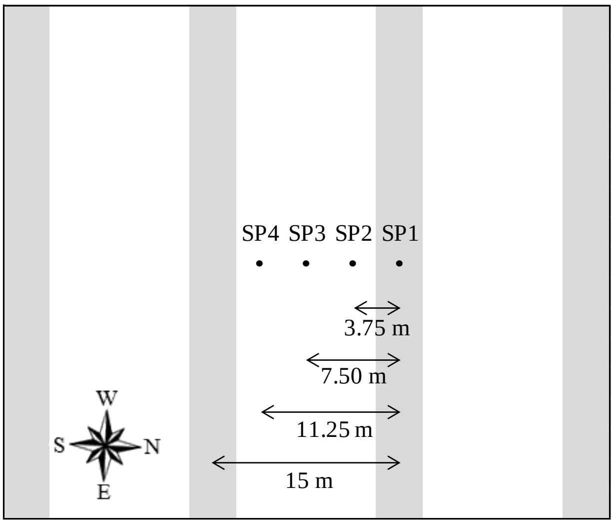

Figure 35. Schematic representation of the experimental area indicating where the pasture data were collected in the silvopastoral system. SP1: 0.00 m, SP2: 3.75 m, SP3: 7.50 m, SP4: 11.25 m from North row. Grey strips illustrate the eucalypt rows.

Table 26. Average air temperature (Tavg), average photosynthetically active radiation (PAR), and total rainfall (RF), during each cycle of the experiment at the positions SP1: 0.00 m, SP2: 3.75 m, SP3: 7.50 m, SP4: 11.25 m from eucalypt North row in the silvopastoral system.

	Weather	Cycle										
	variable	1	2	3	4	5	6	7	8	9	10	11
SP1	Tavg (ºC)	24.9	22.4	21.1	20.2	18.6	17.8	20.4	22.6	23.6	22.4	22.1
	PAR (MJ m^{-2} d^{-1})	7.9	6.6	6.9	7.5	3.1	3.3	6.5	10.8	7.7	6.0	5.2
	RF (mm $cycle^{-1}$)	167.6	218.4	272.1	49.5	26.4	41.1	5.8	166.9	168.9	239.5	616.2
SP2	Tavg (ºC)	24.9	22.4	21.1	20.2	18.6	17.8	20.4	22.6	23.6	22.4	22.1
	PAR (MJ m^{-2} d^{-1})	7.9	4.1	1.5	2.0	0.9	1.0	2.8	2.1	3.2	4.7	3.9
	RF (mm $cycle^{-1}$)	167.6	218.4	272.1	49.5	26.4	41.1	5.8	166.9	168.9	239.5	616.2
SP3	Tavg (ºC)	25.1	22.6	21.1	20.1	19.2	17.8	20.4	22.5	23.7	22.6	22.4
	PAR (MJ m^{-2} d^{-1})	7.7	5.9	2.2	1.3	1.5	1.5	1.9	2.3	5.4	4.5	3.7
	RF (mm $cycle^{-1}$)	160.3	212.8	260.4	58.2	35.3	51.6	4.8	161.8	167.4	210.3	541.8
SP4	Tavg (ºC)	25.1	22.6	21.1	20.1	19.2	17.8	20.4	22.5	23.7	22.6	22.4
	PAR (MJ m^{-2} d^{-1})	5.4	5.2	3.4	1.3	0.9	1.0	1.1	4.3	5.0	3.1	2.3
	RF (mm $cycle^{-1}$)	160.3	212.8	260.4	58.2	35.3	51.6	4.8	161.8	167.4	210.3	541.8

Once the morphological separation was performed, the fractions representing the leaves were used to determine the leaf area with a leaf area meter, model LI-3100C (Li-Cor, Lincoln, Nebraska, USA). With leaf area and the area from where forage was harvested (0.25 m^2), the leaf area index (LAI) was determined. The specific leaf area (SLA) was determined by dividing the leaf area of the samples by its dry weight.

To determine the forage biomass and biometric characteristics below 10 cm, four assessments were done, one in each season of the year, cutting the pasture until the ground level and submitting the samples to the same procedure above described. Crown mass was considered as the measured stem mass below 10 cm.

In July 2016, 10 trees were cut in order to measure their total leaf area. All the leaves of each tree were separated and weighed to determine the green biomass. Subsequently, a subsample of 0.2 kg was taken to determine its leaf area with a leaf area meter, model LI-3100C, and driven in an oven at 65ºC, until constant weight. The SLA was determined by dividing the leaf area of the subsample by its dry mass. The total leaf area of an individual tree was calculated multiplying the SLA by the total leaf biomass. This total leaf area was multiplied by the population of trees (0.0333 trees m^{-2}), resulting in the LAI for the total area (1.97). This value was divided by the fraction of the total area covered by tree canopy (0.6) in order to obtain the average LAI considering the canopy projection area (3.28), required as input by the model.

6.2.2. APSIM model testing

For the APSIM-Tropical Pasture test for pasture under grazing and in a silvopastoral system, it was necessary to add a function to change SLA by solar radiation incidence, assuming that SLA is changed when the daily total incoming radiation is lower than 15 MJ m^{-2} day^{-1} for several consecutive days, increasing linearly while incoming radiation decreases, achieving a maximum SLA increase of 40% at 0 MJ m^{-2} day^{-1}.

Specifically, in pastures under grazing, there are forage mass losses after a grazing event, which occur due to physical damages caused by the animals during grazing. Therefore, it was necessary to use the cutting management capability of the APSIM-Tropical Pasture to set the after grazing biomass losses. The losses were considered to occur at the first day after grazing and their values were assumed to be different for each position of the silvopastoral system, as specified in Table 27.

For the simulations, sowing was performed considering a population of 225 plants m^{-2}, with a sowing depth of 10 cm and space between rows of 20 cm. Initial nitrate content was 86.5 kg ha^{-1}, initial ammonium content was 59.6 kg ha^{-1}, initial organic carbon was 13.8 kg m^{-2} in which 7.7 kg m^{-2} were inert, and soil pH ranged from 5.5 in the surface layer to 6.3 in the deeper layer. The initial surface organic matter was considered as 1000 kg ha^{-1}.

As the APSIM modelling framework still has not a complete model to simulate silvopastoral systems, this testing process was performed by adopting three methods: a) considering only the soil water competition, by using the current silvopastoral simulation capability; b) considering only the solar radiation competition, by using the measured data of photosynthetically active radiation; and c) considering only the solar radiation competition, but using data of total solar radiation estimated by the model described in Chapter 5.

Table 27. Forage mass losses after grazing assumed for each cycle of the experiment in four positions (SP1: 0.00 m, SP2: 3.75 m, SP3: 7.50 m and SP4: 11.25 m from the North row) of a silvopastoral system, during the testing of APSIM-Tropical pasture to estimate forage growth in such system.

Cycle	Grazing end date	Forage mass losses after grazing (kg ha^{-1})			
		SP1	SP2	SP3	SP4
1	12/26/2014	160	1000	1000	1000
2	1/30/2015	150	300	500	900
3	3/6/2015	50	0	0	400
4	4/14/2015	50	0	0	0
5	5/19/2015	50	0	0	0
6	6/23/2015	0	0	0	0
7	7/29/2015	0	200	0	0
8	9/3/2015	0	0	0	0
9	10/9/2015	130	0	300	300
10	11/13/2015	0	330	300	0
11	12/21/2015	0	400	300	300

6.2.2.1. Simulations with soil water competition

The current silvopastoral simulation capability, built for APSIM Next Generation (Holzworth et al. 2014; Holzworth et al. 2015) is composed by: the pasture module; the soil water competition capability, composed by the APSIM SoilWat module (Probert et al. 1998), with a multi-root-zones approach; the Slurp module, which represents the tree component and allows setting a total tree root mass and length, and a leaf area index to calculate transpiration; and a simple approach for simulating radiation transmission by tree canopies.

The soil water competition capability allows to divide an agroforestry simulation into zones of influence, being the first zone composed by the tree and the crop together, and the others only by the crop, but allowing to add some tree root mass to compete by water and sending this water to be used by the trees.

The current APSIM’s tool for simulating radiation transmission by tree canopies in these systems calculates the radiation transmission through the Beer-Lambert law but considers that all the shading is projected on the first zone (below the trees), which causes wrong radiation distribution and transpiration estimates. Besides that, the pasture growth in the first zone is being calculated using the solar radiation intercepted by the pasture plus the intercepted by the trees, resulting in growth overestimations. The tree LAI used for the radiation transmission calculations was the measured in July 2016, assuming that it was the same during all the experimental period.

In order to test the model performance for estimating competition by soil water, the data of soil moisture for the considered positions, measured in the experiment described in Chapter 3, were used.

6.2.2.2. Simulations with measured solar radiation transmission

The simulations that considered only solar radiation competition were performed using the APSIM-Tropical Pasture model and changing the weather files by adding the solar radiation transmission measured in each position of the silvopastoral system. As only the PAR transmission was measured, as described in Chapter 2, data of daily total incoming solar radiation, measured under standard conditions, were used to calculate the total solar radiation transmission, by multiplying the incoming solar radiation at full sun by the transmissivity for each assessed position.

6.2.2.3. Simulations with estimated solar radiation transmission

In this case, the simulations were performed similarly to that described above, but using total solar radiation transmission data estimated by the model presented in Chapter 5. For this, the input data of incoming solar radiation under full sun were the same collected at full sun and in the standard conditions (Allen et al. 1998).

6.2.3. CROPGRO model testing

As the CROPGRO-Perennial Forage model was never before adapted for Piatã palisadegrass, the first step was to calibrate it for simulating this cultivar under full sun. For this, the parameterization of Pequeno et al. (2014) for Marandu palisadegrass (*Urochloa brizantha* cv. Marandu) was used as a reference. Taking into account that the two cultivars belong to the same species, the species and ecotype coefficients were kept the same, and only the cultivar coefficients were adjusted.

For the calibration process, the data collected in the Experiment 1, described in Chapter 4, were used. The first adjustment was to add the value of SLA under standard growth conditions (SLAVR), 200 cm^2 g^{-1}, correspondent to the average of the SLA values obtained from the irrigated plots of the Experiment 1 and only from periods when the growth and partitioning were not affected by initial plant development or flowering (the end of the cycle 3, the whole cycles 4 and 8, and the beginning of the cycles 5 and 6). The second adjustment was performed by calibrating the Maximum leaf photosynthesis rate (at 30ºC, 350 ppm CO_2, and high solar radiation incidence) (LFMAX), in mg CO_2 m^{-2} s^{-1}, aiming to achieve the best pasture growth simulations, compared to the values from the same periods used for the SLAVR adjustment. The calibrated value of LFMAX was 2.2 mg CO_2 m^{-2} s^{-1}. The rest of the cultivar coefficients were kept as determined by Pequeno et al. (2014).

The second step was to test the efficiency of the calibrated model for estimating Piatã palisadegrass growth under full sun and grazing, using the pasture data collected in the Experiment 2, described in Chapter 4.

Finally, the model was tested for estimating pasture growth at the four positions of the silvopastoral system above described. As CROPGRO has not the capability to simulate competition for soil water, the simulations were based on the competition for solar radiation. CROPGRO also has not models for simulating trees or radiation transmission by their canopies in agroforestry systems, so the simulations were performed using the CROPGRO-Perennial Forage model and changing the weather files by adding the solar radiation transmission measured in each position of the silvopastoral system. As only the PAR transmission was measured, as described in Chapter 2, data of daily total incoming solar radiation, measured under standard conditions, were used to calculate the total solar radiation transmission, by multiplying the incoming solar radiation at full sun by the transmissivity for each assessed position.

6.2.4. Models performance assessment

Several statistical indexes were used to assess the performance of the models for estimating pasture growth in relation to the environmental conditions and managements above described. These statistics were:

a) Linear regression between observed (O) and estimated (E) values of each variable, and the respective coefficient of determination (R^2);

b) Willmott (1981) agreement index (d), which quantifies model´s accuracy:

$$d = 1 - \frac{\sum_{i=1}^{n}(O_i - E_i)^2}{\sum_{i=1}^{n}(|E_i - \bar{O}| + |O_i - \bar{O}|)^2} \tag{92}$$

c) Nash-Sutcliffe efficiency (NSE), which describes model´s accuracy:

$$NSE = 1 - \frac{\sum_{i=1}^{n}(E_i - O_i)^2}{\sum_{i=1}^{n}(O_i - \bar{O})^2} \tag{93}$$

d) Mean error (ME)

$$ME = \left(\frac{1}{n}\right)\sum_{i=1}^{n}(E_i - O_i) \tag{94}$$

e) Mean absolute error (MAE)

$$MAE = \left(\frac{1}{n}\right)\sum_{i=1}^{n}|E_i - O_i| \tag{95}$$

f) Root mean square error (RMSE)

$$RMSE = \sqrt{\left[\left(\frac{1}{n}\right)\sum_{1=i}^{n}(O_i - E_i)^2\right]} \tag{96}$$

6.3. Results

6.3.1. APSIM-Tropical Pasture

6.3.1.1. Simulations with soil water competition

The agreement between observed and estimated data of pasture variables was unsatisfactory when the current APSIM silvopastoral capability was used. Forage live mass simulations presented regular precision (R^2 between 0.58 and 0.85), low accuracy (d between 0.58 and 0.82, and NSE from -4.07 to -0.14) and regular errors (Table 28 and Figure 36). Dry matter partitioning between the aboveground organs also was not satisfactorily simulated, with low precision and accuracy between observed and estimated data (R^2 between 0.20 and 0.87, d between 0.34 and 0.90, and NSE from -11.53 to 0.67) (Table 28). LAI simulations were efficient for the positions SP2, SP3 and SP4 (R^2 between 0.78 and 0.86, d from 0.94 to 0.95, and NSE between 0.77 and 0.84), however for the position SP1 the model performed unsatisfactorily (R^2 = 0.59, d = 0.80, and NSE = -0.19) (Table 28). The SLA simulations presented low precision and accuracy (R^2 between 0.02 and 0.18, d between 0.37 and 0.45, and NSE from -5.41 to -1.74) (Table 28).

Good performance was achieved for the simulations of soil water for the positions SP2, SP3 and SP4, but for the position SP1 the agreement between observed and estimated values was poor, due to the model deficiencies for simulating solar radiation transmission, affecting the transpiration. The simulations at the position SP1 achieved low precision (R^2 = 0.48), low accuracy (d = 0.62 and NSE = -1.27) and high errors (ME = 30.3 mm, MAE = 30.7 mm and RMSE = 34.6 mm) (Table 29). Soil water at SP2 was satisfactorily simulated, achieving good agreement (R^2 = 0.79, d = 0.94, NSE = 0.77, ME = 1.5 mm, MAE = 9.0 mm and RMSE = 11.8 mm) (Table 29). The simulations at the position SP3 presented good precision and accuracy and small errors (R^2 = 0.69, d = 0.91, NSE = 0.59, ME = 0.9 mm, MAE = 11.1 mm and RMSE = 14.3 mm), such as at the SP4 (R^2 = 0.76, d = 0.93, NSE = 0.72, ME = 1.1 mm, MAE = 9.5 mm and RMSE = 12.5 mm) (Table 29).

Time series of observed and estimated soil water content are presented for the positions SP1, SP2, SP3 and SP4 in Figure 37. The model was able to simulate satisfactorily the soil water variations for several conditions. For the position SP1, the simulations presented higher errors, since the model estimated shading excessively for this position, what promoted underestimations of pasture transpiration and, consequently, overestimations of soil water. For the other positions, some problems were identified during periods when natural shading occurred in some conditions (between April and May for SP2, April and August for SP3 and from April to June for SP4). As the model assumes that shading did not occur at these positions, it promotes overestimation of pasture transpiration and underestimation of soil water content (Figure 37). Other problems occurred during intense rainfall events in June, July and September 2015, when the model overestimated soil water recharges.

6.3.1.2. Simulations with measured solar radiation transmission

The simulations that considered only competition by solar radiation, using the measured data of PAR transmission at each position of the silvopastoral system, achieved good agreement between observed and estimated data of pasture variables. Forage live mass simulations reached good precision (R^2 from 0.69 to 0.86), good accuracy (d from 0.90 to 0.96, and NSE between 0.51 and 0.85) and regular errors (Table 30 and Figure 38). Dry matter partitioning between the aboveground organs also was well simulated, with regular precision and accuracy between observed and estimated data (R^2 from 0.41 to 0.88, d ranging from 0.78 to 0.95, and NSE between 0.09 to 0.82) (Table 30), except for the crown mass simulations that presented performance ranging from low to regular (R^2 between 0.09 and 0.88, d between 0.45 and 0.86, and NSE from -2.91 to 0.68). LAI simulations were regular to good (R^2 from 0.65 to 0.82, d ranging between 0.81 and 0.89, and NSE from 0.38 to 0.67) (Table 30). The SLA simulations presented low precision and accuracy (R^2 from 0.01 to 0.07, d from 0.30 to 0.33, and NSE ranging from -2.00 to -0.65) (Table 30).

Table 28. Statistical indexes for the simulations of forage live mass (FLM), leaf mass (Leaf), stem mass (Stem) and crown mass (Crown) (kg ha^{-1}); and of leaf area index (LAI) and specific leaf area (SLA) (m^2 g^{-1}), at 0.0 m (SP1), 3.75 m (SP2), 7.50 m (SP3) and 11.25 m (SP4) from the eucalypt North row in a silvopastoral system, using the current APSIM silvopastoral simulation capability and the APSIM-Tropical Pasture model. R^2 = coefficient of determination, d = agreement index, NSE = Nash-Sutcliffe efficiency, ME = mean error (kg ha^{-1}), MAE = mean absolute error (kg ha^{-1}), RMSE = root mean square error (kg ha^{-1}).

Variable	SP1					
	R^2	d	NSE	ME	MAE	RMSE
FLM	0.58	0.58	-4.07	946.84	954.5	1349.0
Leaf	0.67	0.63	-3.58	561.4	578.3	806.0
Stem	0.20	0.34	-11.53	348.5	360.2	551.7
Crown	0.85	0.90	0.67	50.1	58.0	71.5
LAI	0.59	0.80	-0.19	0.5	0.7	1.2
SLA	0.02	0.42	-1.74	-5.0	5.5	6.3
	SP2					
	R^2	d	NSE	ME	MAE	RMSE
FLM	0.85	0.81	-0.31	801.20	813.9	1036.6
Leaf	0.87	0.90	0.44	294.6	340.1	428.3
Stem	0.54	0.66	-1.82	382.0	406.8	538.6
Crown	0.65	0.77	-0.17	138.4	162.9	180.0
LAI	0.86	0.95	0.84	-0.2	0.5	0.6
SLA	0.18	0.45	-1.91	-6.6	6.6	7.7
	SP3					
	R^2	d	NSE	ME	MAE	RMSE
FLM	0.80	0.82	-0.14	773.42	793.3	997.0
Leaf	0.78	0.88	0.35	284.4	333.7	440.8
Stem	0.58	0.76	-0.46	296.5	355.8	467.3
Crown	0.72	0.61	-1.93	203.6	203.6	225.5
LAI	0.78	0.94	0.77	-0.1	0.5	0.6
SLA	0.18	0.40	-4.70	-6.6	6.6	7.1
	SP4					
	R^2	d	NSE	ME	MAE	RMSE
FLM	0.76	0.80	-0.43	735.32	810.5	1083.9
Leaf	0.84	0.85	-0.04	354.7	411.9	556.9
Stem	0.42	0.65	-1.56	302.5	368.2	490.4
Crown	0.76	0.86	0.48	90.7	100.2	124.5
LAI	0.84	0.95	0.82	-0.2	0.5	0.6
SLA	0.02	0.37	-5.41	-7.7	7.7	8.5

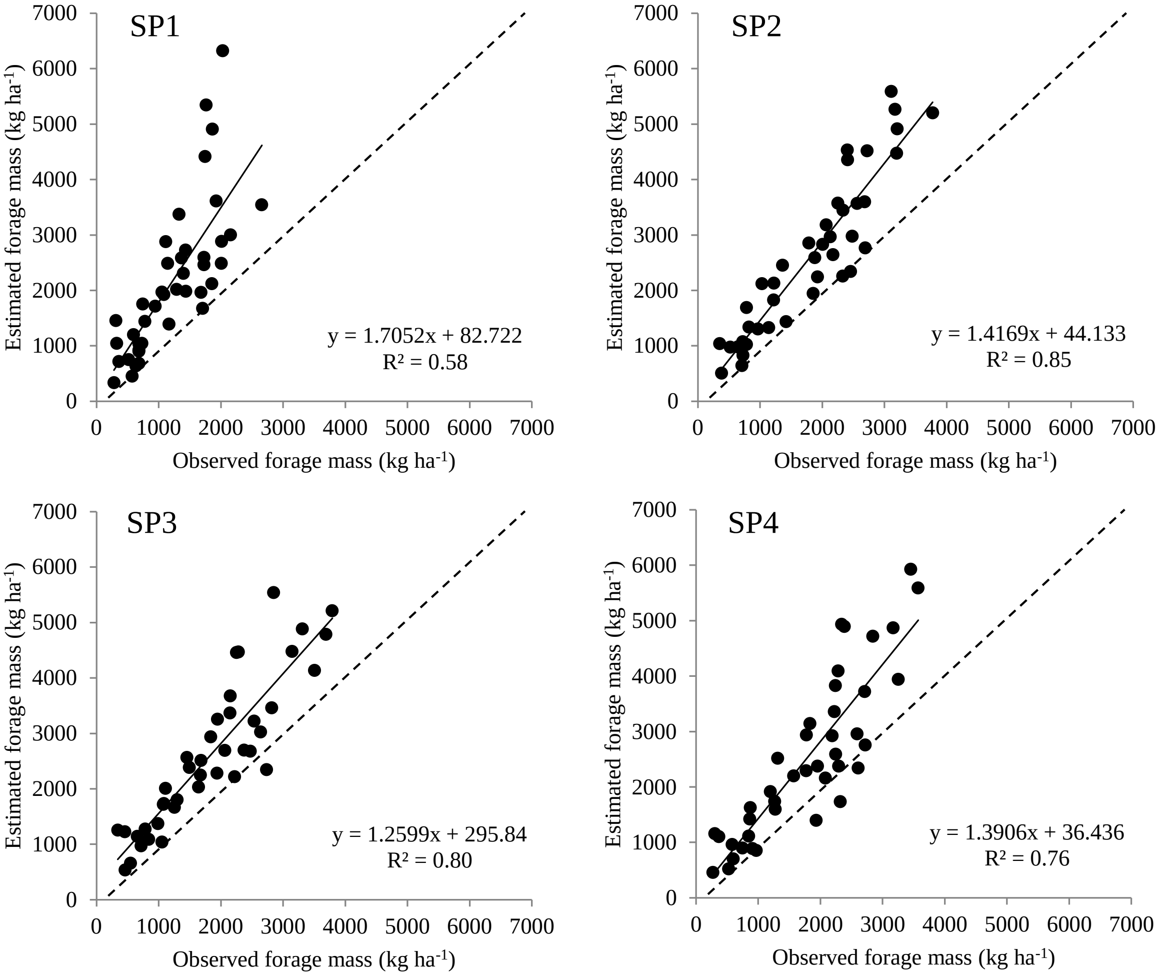

Figure 36. Relationships between observed and estimated forage live mass, using the current APSIM silvopastoral simulation capability and the APSIM-Tropical Pasture model, for the positions 0.0 m (SP1), 3.75 m (SP2), 7.50 m (SP3) and 11.25 m (SP4) from the eucalypt North row in a silvopastoral system.

Table 29. Statistical indexes for the simulations of soil water until 1-m depth at 0.0 m (SP1), 3.75 m (SP2), 7.50 m (SP3) and 11.25 m (SP4) from the eucalypt North row in a silvopastoral system, using the current APSIM silvopastoral simulation capability associated to the APSIM-Tropical Pasture model. R^2 = coefficient of determination, d = agreement index, NSE = Nash-Sutcliffe efficiency, ME = mean error (mm), MAE = mean absolute error (mm), RMSE = root mean square error (mm).

Position	Statistical index					
	R^2	d	NSE	ME	MAE	RMSE
SP1	0.48	0.62	-1.27	30.3	30.7	34.6
SP2	0.79	0.94	0.77	1.5	9.0	11.8
SP3	0.69	0.91	0.59	0.9	11.1	14.3
SP4	0.76	0.93	0.72	1.1	9.5	12.5

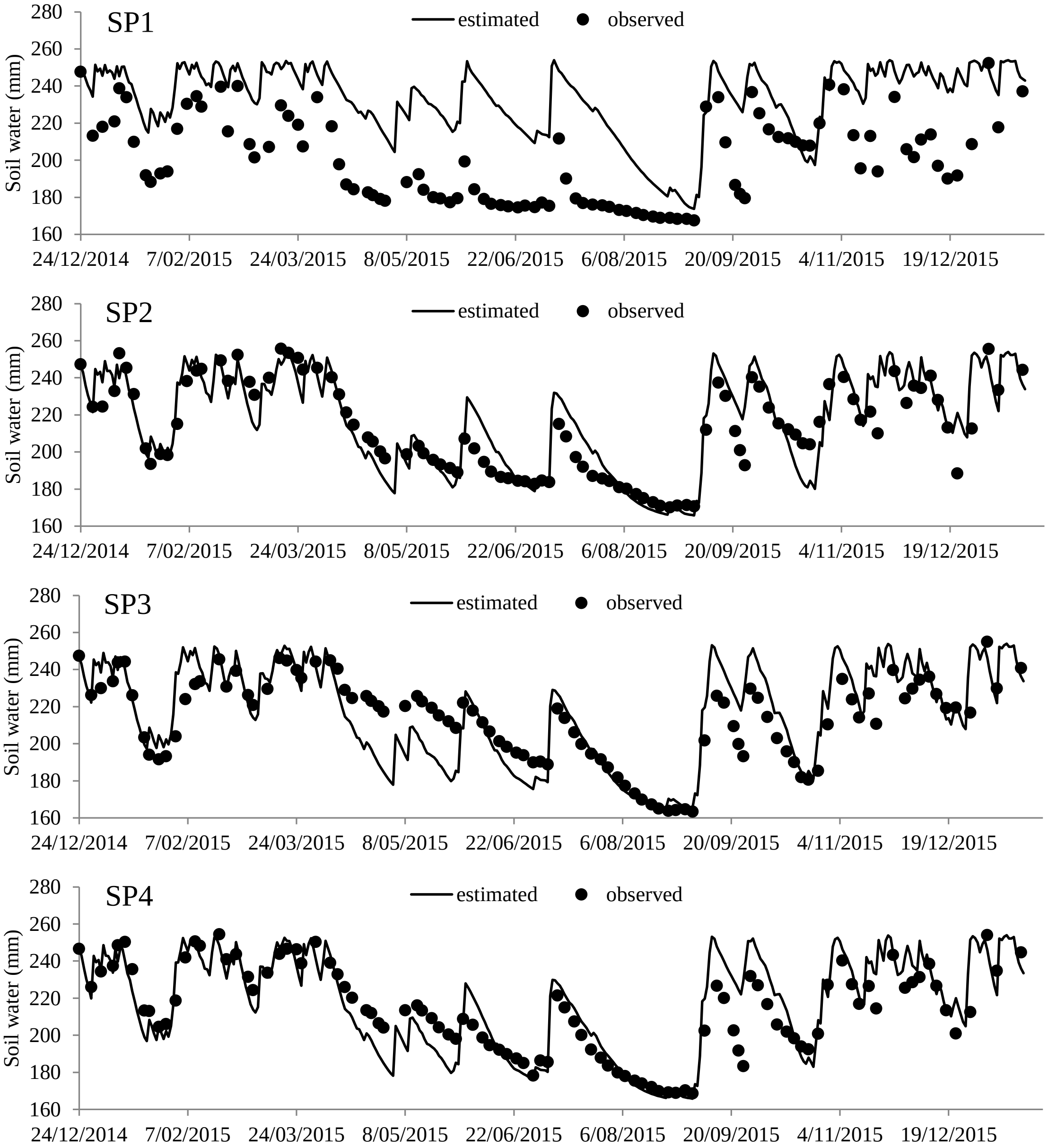

Figure 37. Time series of observed and estimated soil water content until 1-m depth, using the current APSIM silvopastoral simulation capability associated with the APSIM-Tropical Pasture model, for the positions 0.0 m (SP1), 3.75 m (SP2), 7.50 m (SP3) and 11.25 m (SP4) from the eucalypt north row in a silvopastoral system.

Time series of observed and estimated data of forage mass for these simulations with estimated solar radiation transmission are presented in Figure 39. The model was able to capture several trends related to the effect of environmental conditions on pasture growth. The simulations achieved good results, even considering only competition by solar radiation, since it was the most determinant factor once water deficit was not very intense during the experimental period, except in the cycle 7 (Figure 39). During the 7th cycle the model overestimated pasture growth since the water uptake by the tree roots was important to determine pasture growth (Figure 39). The assumed values of forage mass losses after grazing allowed good growth simulations, despite the uncertainties of these values.

Table 30. Statistical indexes for the simulations of forage live mass (FLM), leaf mass (Leaf), stem mass (Stem) and crown mass (Crown) (kg ha^{-1}), leaf area index (LAI) and specific leaf area (SLA) (m^2 g^{-1}) at 0.0 m (SP1), 3.75 m (SP2), 7.50 m (SP3) and 11.25 m (SP4) from the eucalypt north row in a silvopastoral system, considering only competition by solar radiation, using the measured data of PAR transmission at each position and the APSIM-Tropical Pasture model. R^2 = coefficient of determination, d = agreement index, NSE = Nash-Sutcliffe efficiency, ME = mean error (kg ha^{-1}), MAE = mean absolute error (kg ha^{-1}), RMSE = root mean square error (kg ha^{-1}).

Variable	SP1					
	R^2	d	NSE	ME	MAE	RMSE
FLM	0.86	0.96	0.85	-17.8	179.5	229.6
Leaf	0.88	0.95	0.82	-92.1	126.3	160.7
Stem	0.49	0.80	0.09	67.1	110.1	149.0
Crown	0.86	0.86	0.68	12.3	55.1	70.5
LAI	0.82	0.89	0.67	-0.4	0.4	0.6
SLA	0.07	0.30	-0.65	-2.4	3.7	4.9
	SP2					
	R^2	d	NSE	ME	MAE	RMSE
FLM	0.75	0.91	0.58	-200.9	481.8	586.5
Leaf	0.71	0.88	0.45	-228.9	324.0	421.4
Stem	0.47	0.82	0.18	-59.0	245.8	289.7
Crown	0.09	0.45	-0.33	90.6	161.7	191.8
LAI	0.71	0.81	0.38	-0.8	0.9	1.2
SLA	0.02	0.31	-0.80	-2.7	4.4	6.1
	SP3					
	R^2	d	NSE	ME	MAE	RMSE
FLM	0.69	0.90	0.51	-37.1	531.0	651.8
Leaf	0.63	0.87	0.36	-133.2	324.2	435.5
Stem	0.44	0.78	0.18	-138.7	307.2	350.6
Crown	0.61	0.48	-2.91	245.4	245.4	260.4
LAI	0.65	0.84	0.41	-0.6	0.7	1.0
SLA	0.01	0.30	-1.96	-3.0	4.3	5.2
	SP4					
	R^2	d	NSE	ME	MAE	RMSE
FLM	0.77	0.93	0.71	-63.6	396.6	484.6
Leaf	0.81	0.92	0.67	-179.2	263.6	314.4
Stem	0.41	0.80	0.19	-57.9	228.3	275.8
Crown	0.88	0.69	-0.32	187.9	187.9	199.2
LAI	0.80	0.83	0.46	-0.8	0.9	1.1
SLA	0.03	0.33	-2.00	-3.8	4.7	5.8

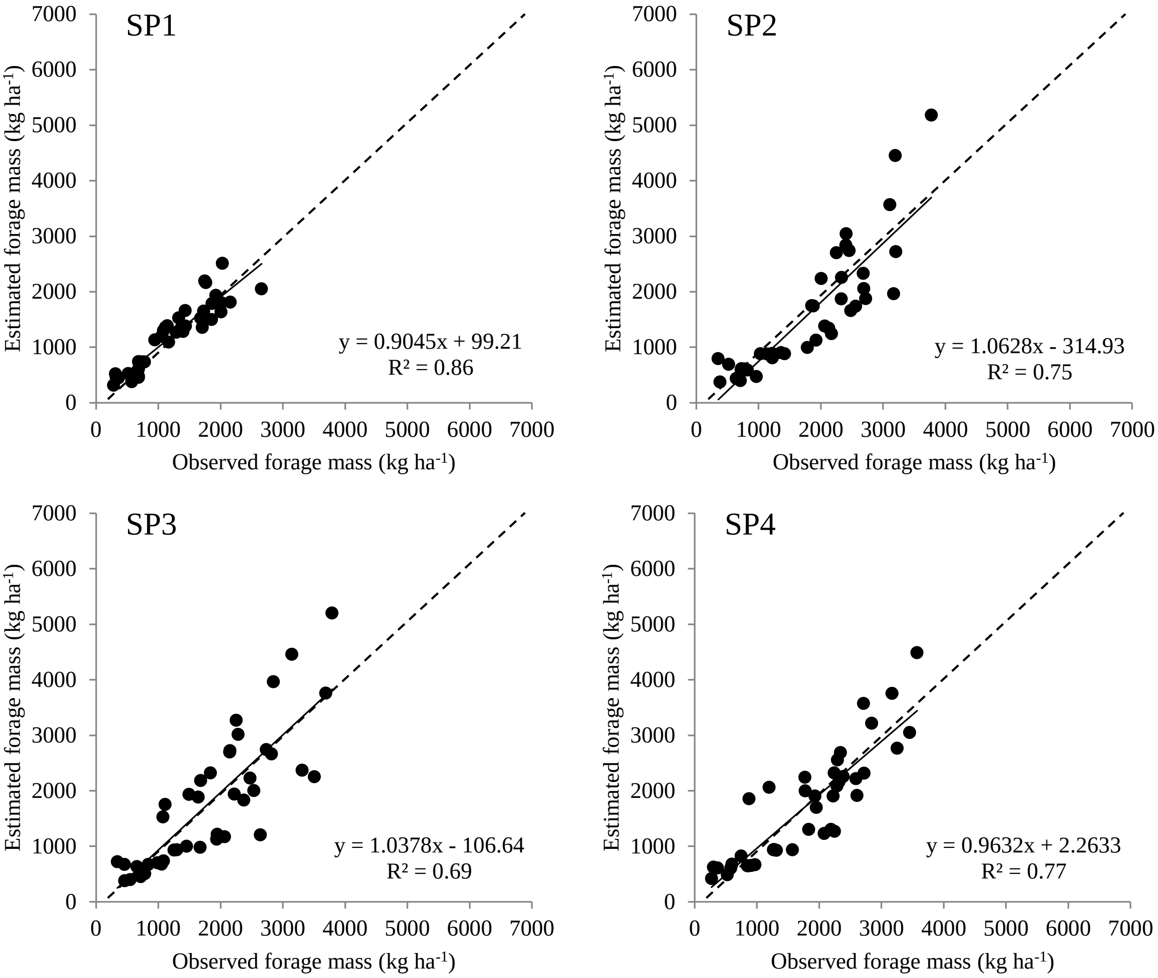

Figure 38. Relationships between observed and estimated forage live mass, considering only competition by solar radiation and using the measured data of PAR transmission at each position and the APSIM-Tropical Pasture model, for the positions 0.0 m (SP1), 3.75 m (SP2), 7.50 m (SP3) and 11.25 m (SP4) from the eucalypt north row in a silvopastoral system.

6.3.1.3. Simulations with estimated solar radiation transmission

The simulations that considered only competition by solar radiation, using data of radiation transmission estimated by the model described in Chapter 5, also reached a good agreement between observed and estimated data of pasture variables (Table 31 and Figure 40). Forage live mass simulations presented good precision (R^2 between 0.76 and 0.88), good accuracy (d between 0.91 and 0.96, and NSE from 0.56 to 0.83) and regular errors (Table 31 and Figure 40). Dry matter partitioning between the aboveground organs also was well simulated, with good precision (R^2 between 0.50 and 0.90) and regular accuracy between observed and estimated data (d between 0.73 and 0.97, and NSE from 0.28 to 0.87) (Table 31), except for the stem mass simulations for SP1 and SP2 (d = 0.80, and NSE from -0.10 to -

0.09) and crown mass for SP3 (d = 0.55, and NSE = -2.48), which presented low accuracy. LAI simulations showed good performance (R^2 between 0.70 and 0.90, d from 0.87 to 0.93, and NSE between 0.63 and 0.79 (Table 31), whereas SLA simulations presented low precision and accuracy (R^2 between 0.01 and 0.07, d between 0.22 and 0.33, and NSE from -2.30 to -0.18) (Table 31).

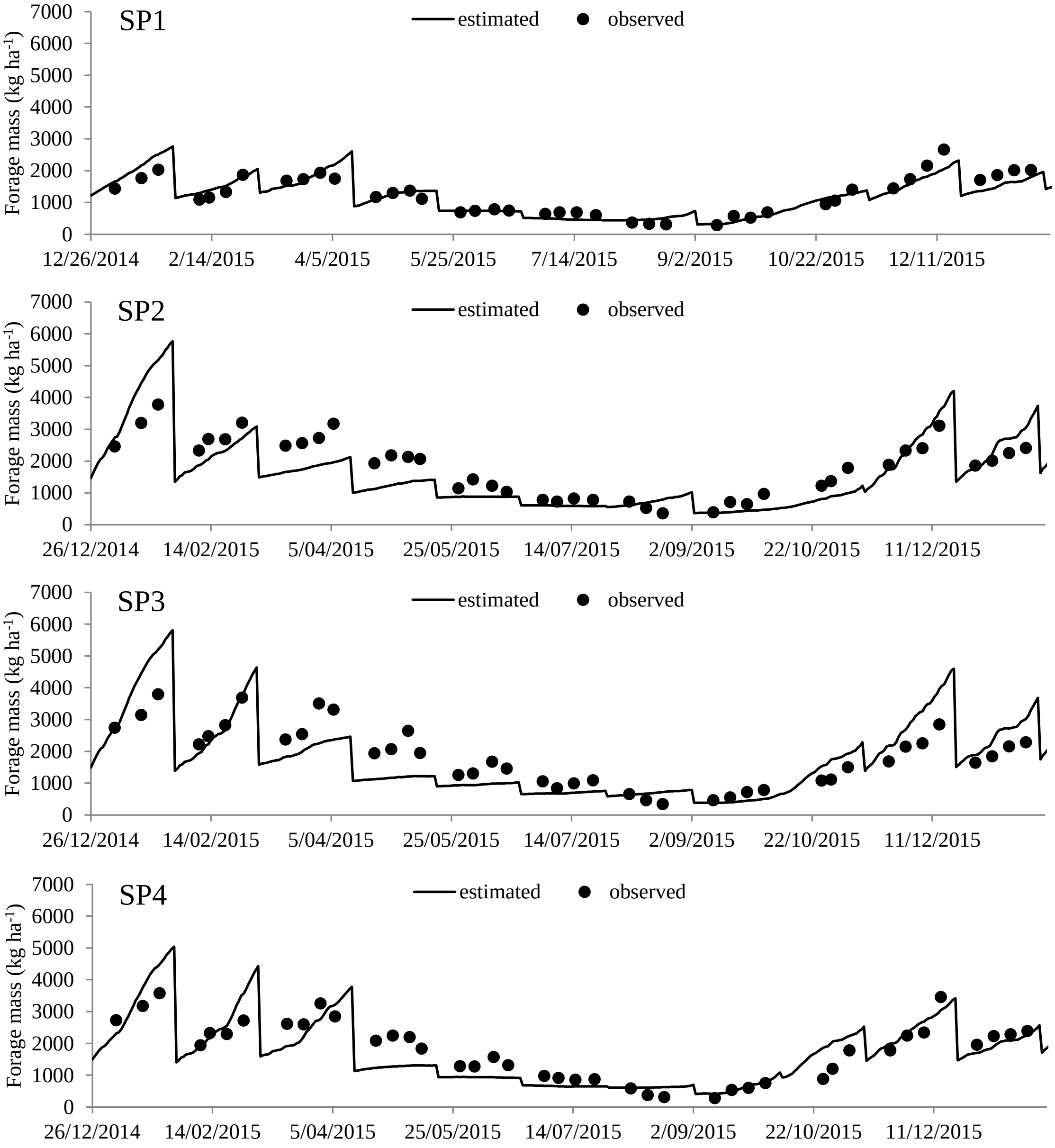

Figure 39. Time series of observed and estimated forage live mass, considering only competition by solar radiation and using the measured data of PAR transmission at each position and the APSIM-Tropical Pasture model, for the positions 0.0 m (SP1), 3.75 m (SP2), 7.50 m (SP3) and 11.25 m (SP4) from the eucalypt north row in a silvopastoral system.

Table 31. Statistical indexes for the simulations of forage live mass (FLM), leaf mass (Leaf), stem mass (Stem) and crown mass (Crown) (kg ha^{-1}); and of leaf area index (LAI) and specific leaf area (SLA) (m^2 g^{-1}) at 0.0 m (SP1), 3.75 m (SP2), 7.50 m (SP3) and 11.25 m (SP4) from the eucalypt north row in a silvopastoral system, considering only competition by solar radiation, using data of radiation transmission estimated by the model described in Chapter 5 and the APSIM-Tropical Pasture model. R^2 = coefficient of determination, d = agreement index, NSE = Nash-Sutcliffe efficiency, ME = mean error (kg ha^{-1}), MAE = mean absolute error (kg ha^{-1}), RMSE = root mean square error (kg ha^{-1}).

Variable	SP1					
	R^2	d	NSE	ME	MAE	RMSE
FLM	0.76	0.92	0.68	-84.1	255.3	336.7
Leaf	0.78	0.92	0.69	-91.5	160.2	210.7
Stem	0.55	0.80	-0.09	57.5	105.7	162.7
Crown	0.56	0.73	0.34	-44.9	85.7	101.1
LAI	0.71	0.88	0.63	-0.3	0.5	0.7
SLA	0.01	0.25	-0.18	-1.1	3.0	4.1
	SP2					
	R^2	d	NSE	ME	MAE	RMSE
FLM	0.88	0.94	0.69	201.6	372.9	503.3
Leaf	0.90	0.97	0.84	-60.4	177.4	227.6
Stem	0.56	0.80	-0.10	171.0	244.0	336.3
Crown	0.62	0.79	0.25	102.3	130.3	144.5
LAI	0.90	0.93	0.79	-0.4	0.5	0.7
SLA	0.07	0.22	-1.04	-1.8	5.0	6.5
	SP3					
	R^2	d	NSE	ME	MAE	RMSE
FLM	0.78	0.91	0.56	327.7	463.6	619.9
Leaf	0.70	0.91	0.64	-8.9	250.3	329.1
Stem	0.61	0.86	0.37	117.3	234.2	307.3
Crown	0.76	0.55	-2.48	233.6	233.6	245.8
LAI	0.70	0.87	0.63	-0.3	0.5	0.8
SLA	0.04	0.27	-2.30	-2.7	4.5	5.4
	SP4					
	R^2	d	NSE	ME	MAE	RMSE
FLM	0.85	0.96	0.83	59.8	293.8	373.1
Leaf	0.90	0.97	0.87	-81.3	154.7	196.7
Stem	0.50	0.83	0.43	23.1	174.5	230.6
Crown	0.87	0.80	0.28	129.8	129.8	146.7
LAI	0.89	0.92	0.75	-0.5	0.6	0.7
SLA	0.02	0.33	-1.32	-2.8	4.0	5.1

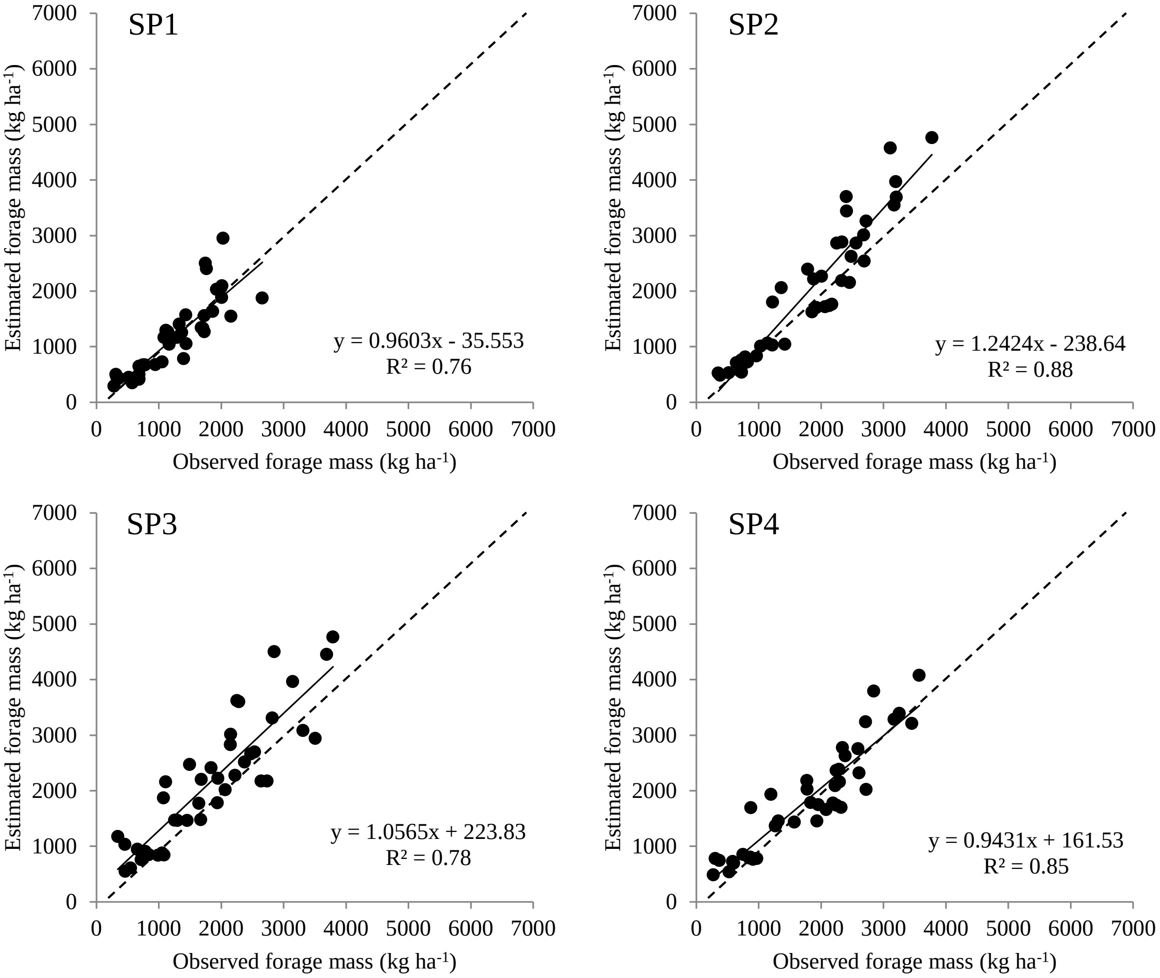

Figure 40. Relationships between observed and estimated forage live mass, considering only competition by solar radiation, using data of radiation transmission estimated by the model described in Chapter 5 and the APSIM-Tropical Pasture model, for the positions 0.0 m (SP1), 3.75 m (SP2), 7.50 m (SP3) and 11.25 m (SP4) from the eucalypt north row in a silvopastoral system.

6.3.2. CROPGRO-Perennial Forage

6.3.2.1. Model calibration for Piatã palisadegrass under cutting and full sun

The simulations for pasture under cutting management and full sun presented a good agreement between observed and estimated data, for both irrigated and rainfed pastures, for all growth variables, except SLA (Table 32). Forage live mass was simulated with good precision (R^2 = 0.86 and 0.93), good accuracy (d = 0.91 and 0.97, and NSE = 0.75 and 0.90) and low errors (Table 32 and Figure 41), but with some underestimations during the reproductive period. Dry matter partitioning between leaf and stem also was well simulated, with good precision and accuracy between observed and estimated data (R^2 between 0.73 and

0.90, d between 0.89 and 0.96, and NSE from 0.69 to 0.87). LAI simulations were efficient for both irrigated and rainfed systems (R^2 = 0.82 and 0.69, d = 0.94 and 0.87, and NSE = 0.81 and 0.44 (Table 32). The SLA simulations presented a regular precision and accuracy (R^2 = 0.10 and 0.02, d = 0.30 and 0.44, and NSE = -0.46 and -0.64) (Table 32), showing the limited performance of the model to simulate this variable. However, the errors in SLA did not influence substantially the forage mass simulations.

Table 32. Statistical indexes for the simulations of forage live mass (FLM), leaf mass (Leaf), and stem mass (Stem) (kg ha^{-1}); and of leaf area index (LAI) and specific leaf area (SLA) (m^2 g^{-1}), for the Experiment 1, used in the CROPGRO-Perennial Forage model calibration for Piatã palisadegrass under cutting management and full sun. R^2 = coefficient of determination, d = agreement index, NSE = Nash-Sutcliffe efficiency, ME = mean error (kg ha^{-1}), MAE = mean absolute error (kg ha^{-1}), RMSE = root mean square error (kg ha^{-1}).

Variable	Irrigated					
	R^2	d	NSE	ME	MAE	RMSE
FLM	0.86	0.91	0.75	-494.6	646.1	1025.8
Leaf	0.73	0.89	0.70	-112.3	342.8	505.0
Stem	0.76	0.90	0.69	-382.4	547.7	805.6
LAI	0.82	0.94	0.81	0.1	0.5	0.6
SLA	0.10	0.30	-0.46	1.3	2.6	3.3
	Rainfed					
	R^2	d	NSE	ME	MAE	RMSE
FLM	0.93	0.97	0.90	-136.5	446.7	587.7
Leaf	0.79	0.94	0.79	12.7	309.6	382.1
Stem	0.90	0.96	0.87	-149.2	280.8	412.2
LAI	0.69	0.87	0.44	0.5	0.7	1.0
SLA	0.02	0.44	-0.64	2.6	3.3	4.2

6.3.2.2. Model testing for Piatã palisadegrass under grazing and full sun

The comparison between observed and estimated forage live mass for pasture grown under rainfed conditions, full sun and grazing were good, even considering the great variability and difficulties to assess grazed pastures (Table 33 and Figure 42). The results prove such performance, as follows: R^2 = 0.65, d = 0.86, NSE = 0.60, ME = -289.3 kg ha^{-1}, MAE = 677.5 kg ha^{-1} and RMSE = 919.4 kg ha^{-1}. The leaf mass simulations were very good (R^2 = 0.79, d = 0.93, NSE = 0.75) but the stem mass presented low performance (R^2 = 0.45, d = 0.78, NSE = 0.29). The model was efficient to simulate LAI (R^2 = 0.77, d = 0.92, NSE = 0.68), but inefficient to simulate SLA (R^2 = 0.37, d = 0.52, NSE = 0.19).

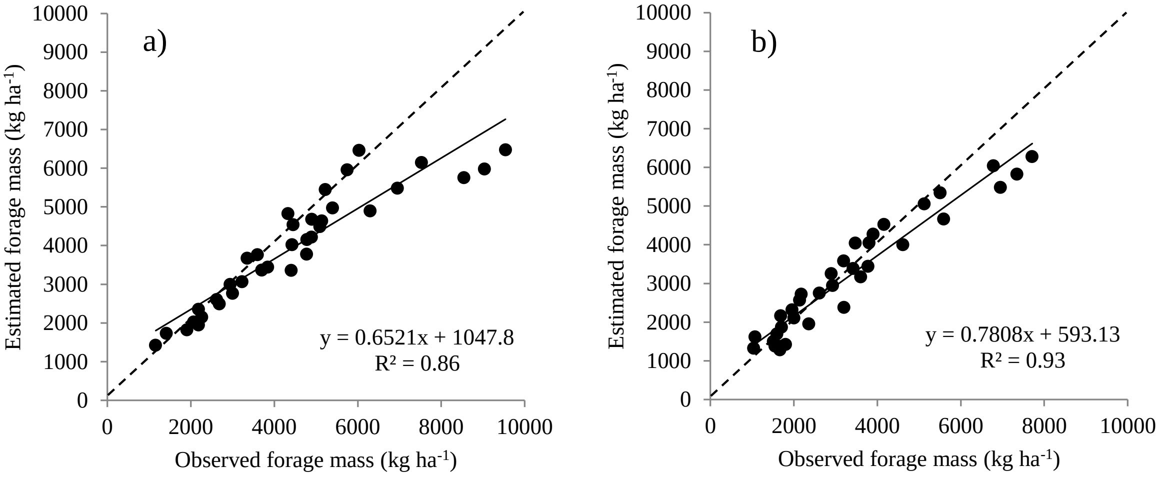

Figure 41. Relationships between observed and estimated forage live mass for the Experiment 1, used in the CROPGRO-Perennial Forage model calibration for Piatã palisadegrass under cutting management and full sun, irrigated (a) and rainfed (b).

Table 33. Statistical indexes for the simulations of forage live mass (FLM), leaf mass (Leaf), and stem mass (Stem) (kg ha^{-1}); and of leaf area index (LAI) and specific leaf area (SLA) (m^2 g^{-1}), for the Experiment 2, used in the CROPGRO-Perennial Forage model testing for Piatã palisadegrass under grazing management and full sun. R^2 = coefficient of determination, d = agreement index, NSE = Nash-Sutcliffe efficiency, ME = mean error (kg ha^{-1}), MAE = mean absolute error (kg ha^{-1}), RMSE = root mean square error (kg ha^{-1}).

Variable	Statistical index					
	R^2	d	NSE	ME	MAE	RMSE
FLM	0.65	0.86	0.60	-289.3	677.5	919.4
Leaf	0.79	0.93	0.75	96.1	225.5	281.1
Stem	0.45	0.78	0.29	-385.5	587.5	871.6
LAI	0.77	0.92	0.68	0.3	0.5	0.6
SLA	0.37	0.52	0.19	0.6	1.6	2.0

6.3.2.3. Model testing for Piatã palisadegrass in silvopastoral system

The simulations of pasture variables with the CROPGRO-Perennial Forage model, which considered only competition by solar radiation, using the measured data of PAR transmission at each position of the silvopastoral system, presented regular to good performance, except for the position SP4, and for SLA simulations at all positions. Taking into account the simulations for the positions SP1, SP2 and SP3, forage live mass simulations achieved good precision (R^2 from 0.75 to 0.90), good accuracy (d from 0.93 to 0.96, and NSE between 0.74 and 0.85) and regular errors (Table 34 and Figure 43). Dry matter partitioning between leaf and stem also was well simulated, with regular to good precision and accuracy (R^2 from 0.48 to 0.90, d ranging from 0.83 to 0.97, and NSE between 0.32 to 0.88) (Table

34). LAI simulations were good (R^2 from 0.57 to 0.90, d ranging between 0.86 and 0.97, and NSE from 0.55 to 0.90) (Table 34). On the other hand, the simulations related to the position SP4 presented low performance, with $R^2 = 0.38$, d = 0.74 and NSE = -0.34 for forage live mass; R^2 between 0.27 and 0.54, d between 0.69 and 0.82, NSE between -0.61 and 0.17 for partitioning between leaf and stem, and $R^2 = 0.15$, d = 0.63 and NSE = -0.51 for LAI (Table 34). The SLA simulations presented low precision and accuracy (R^2 from 0.01 to 0.18, d from 0.32 to 0.64, and NSE ranging from -0.68 to -0.09), as reported in Table 34.

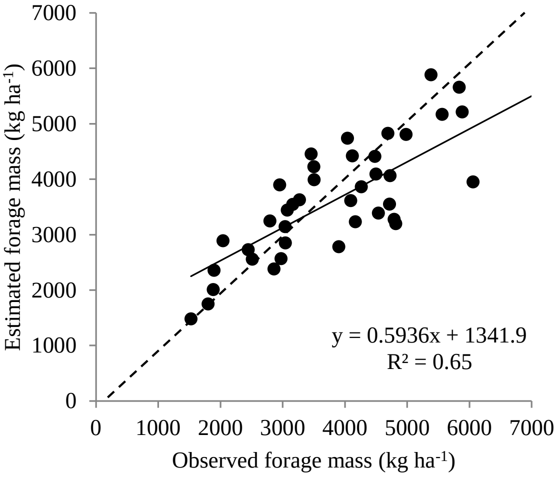

Figure 42. Relationships between observed and estimated forage live mass for the Experiment 2, used in the CROPGRO-Perennial Forage model testing for Piatã palisadegrass under grazing management and full sun.

Time series of estimated and observed data of forage live mass are presented for the simulations with the CROPGRO-Perennial Forage model for the four positions of the silvopastoral system in Figure 44. The results showed that the model was able to simulate the pasture growth in all experimental period, except in the 7th cycle for the positions SP1, SP2 and SP3; and for the 8th, 9th, 10th and 11th cycles for the position SP4. During the 7th cycle a very intense water deficit occurred, reducing forage productivity. Therefore, during this cycle only competition by solar radiation was not enough to explain pasture growth. For the simulations in the position SP4, factors such as low stubble mass, low N supply and high water deficit in the 7th cycle promoted the pasture death, reducing forage accumulation in the subsequent cycles (Figure 44).

Table 34. Statistical indexes for the simulations of forage live mass (FLM), leaf mass (Leaf) and stem mass (Stem) (kg ha^{-1}); and of leaf area index (LAI) and specific leaf area (SLA) (m^2 g^{-1}) at 0.0 m (SP1), 3.75 m (SP2), 7.50 m (SP3) and 11.25 m (SP4) from the eucalypt north row in a silvopastoral system, considering only competition by solar radiation, using the CROPGRO-Perennial Forage model. R^2 = coefficient of determination, d = agreement index, NSE = Nash-Sutcliffe efficiency, ME = mean error (kg ha^{-1}), MAE = mean absolute error (kg ha^{-1}), RMSE = root mean square error (kg ha^{-1}).

Variable	SP1					
	R^2	d	NSE	ME	MAE	RMSE
FLM	0.90	0.95	0.85	-123.1	182.2	233.2
Leaf	0.90	0.97	0.88	-51.7	103.9	132.0
Stem	0.70	0.87	0.61	-71.4	110.2	150.9
LAI	0.90	0.97	0.90	0.0	0.3	0.4
SLA	0.18	0.58	-0.09	1.9	3.3	4.0
	SP2					
	R^2	d	NSE	ME	MAE	RMSE
FLM	0.84	0.96	0.83	-61.7	305.1	377.0
Leaf	0.71	0.91	0.60	-5.7	264.9	360.6
Stem	0.86	0.95	0.83	-55.9	122.9	160.8
LAI	0.71	0.91	0.71	-0.1	0.5	0.8
SLA	0.01	0.32	-0.22	0.7	3.9	5.0
	SP3					
	R^2	d	NSE	ME	MAE	RMSE
FLM	0.75	0.93	0.74	-32.7	351.2	478.6
Leaf	0.48	0.83	0.32	17.9	333.5	451.2
Stem	0.88	0.96	0.86	-50.7	124.1	164.8
LAI	0.57	0.86	0.55	-0.1	0.6	0.9
SLA	0.01	0.36	-0.68	-0.1	3.3	3.9
	SP4					
	R^2	d	NSE	ME	MAE	RMSE
FLM	0.38	0.74	-0.34	-569.0	699.4	1048.8
Leaf	0.27	0.69	-0.61	-382.4	475.8	693.5
Stem	0.54	0.82	0.17	-186.8	251.8	372.4
LAI	0.15	0.63	-0.51	-1.0	1.1	1.8
SLA	0.15	0.64	-0.43	1.5	3.1	4.0

6.4. Discussion

The APSIM-Tropical Pasture and CROPGRO-Perennial Forage models showed to be able to simulate Piatã palisadegrass growth in silvopastoral systems under diverse environmental conditions, such as rainfed, low and high nitrogen supply, grazing managements, wet periods, and warm and cool seasons, mainly when the competition by solar radiation was the main limiting factor for pasture growth. Such performance will allow that many studies about pasture growth in silvopastoral systems could be conducted under the above described conditions. Therefore, the models can be improved in many ways to simulate with better accuracy silvopastoral systems and the interactions between trees, pasture, and animals, mainly if competition by soil moisture and forage mass damages caused by animals during grazing could be considered on pasture growth.

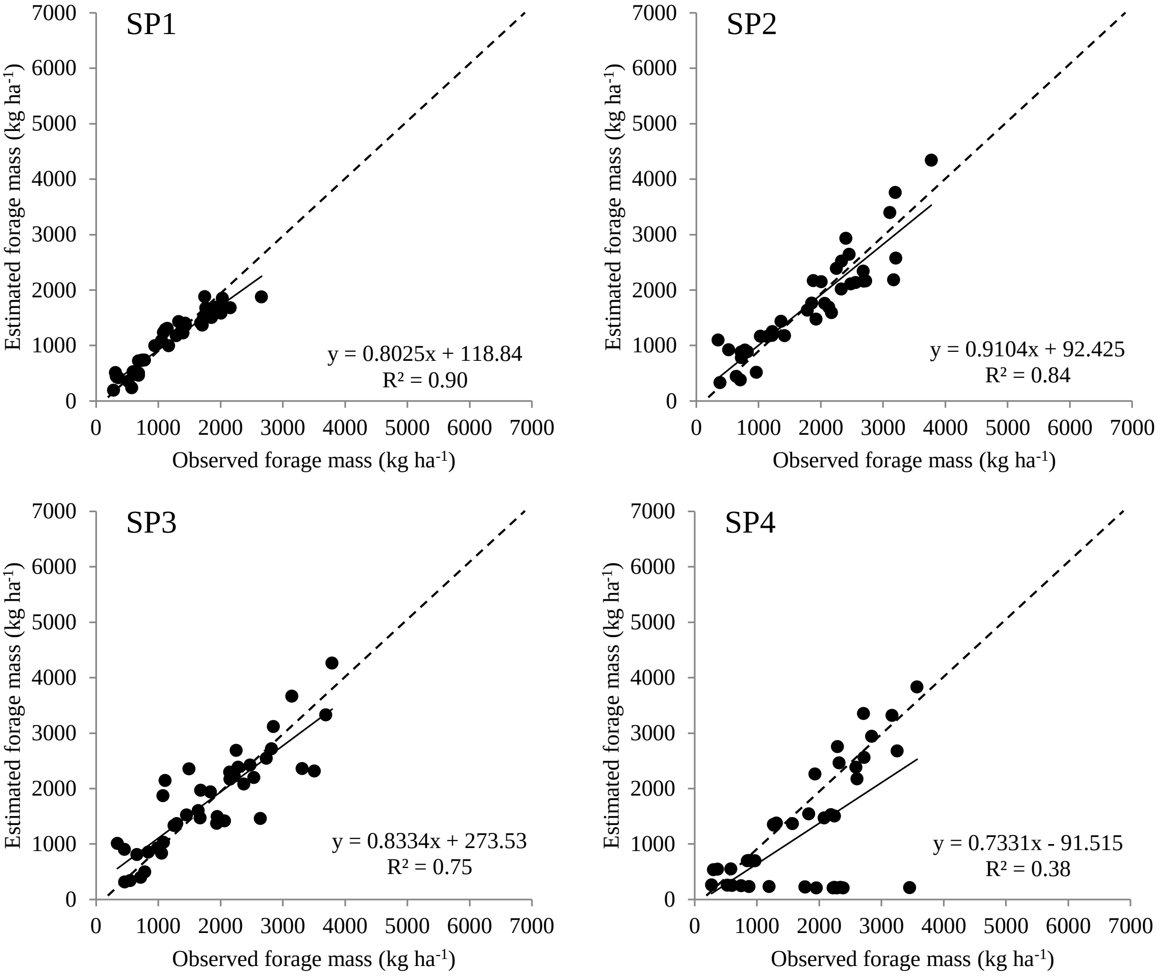

Figure 43. Relationships between observed and estimated forage live mass, considering only competition by solar radiation, using the CROPGRO-Perennial Forage model, for the positions 0.0 m (SP1), 3.75 m (SP2), 7.50 m (SP3) and 11.25 m (SP4) from the eucalypt north row in a silvopastoral system.

The simulations of forage mass with the APSIM-Tropical Pasture model showed a good performance when pasture growth was simulated considering only competition by solar radiation. These simulations were similar to those obtained by employing the APSIM modeling framework for simulating agroforestry systems by Smethurst et al. (2017) and Dilla et al. (2017). The results of the simulations with competition by solar radiation using the data of PAR measured (R^2 from 0.69 to 0.86, d from 0.90 to 0.96, and NSE between 0.51 and 0.85) and using the radiation transmission estimated by the model described in Chapter 5 (R^2 between 0.76 and 0.88, d between 0.91 and 0.96, and NSE from 0.56 to 0.83) were worse than those obtained by Smethurtst et al. (2017) (R^2 between 0.73 and 0.99, d between 0.90 and 1.00, and NSE from 0.67 to 0.98), simulating maize yields in an agroforestry system with gliricidia, and by Dilla et al. (2017) (R^2 between 0.94 and 0.95), for simulations of maize biomass under several artificial shading levels, but were still suitable taking into account the difficulties to simulate pasture growth in silvopastoral systems with grazing. On the other hand, the results for the simulations using the current APSIM silvopastoral capability were the worst obtained in this study (R^2 between 0.58 and 0.85, d between 0.58 and 0.82, and NSE from -4.07 to -0.14).

The APSIM silvopastoral simulation capability presented several problems, such as the inefficiency to simulate solar radiation transmission across the field transect between two rows of trees in the silvopastoral system, which resulted in difficulties to simulate pasture transpiration and, consequently, soil moisture. This problem may be corrected by adding a good solar radiation transmission model into the APSIM framework, for simulating with accuracy solar radiation incidence in any position of the system. The model described in Chapter 5 is a good alternative to solve this issue for silvopastoral systems with eucalyptus, such as shown by the results above discussed. Another deficiency of the silvopastoral capability was the simulation of pasture growth at the first zone, with trees and pasture together, in which it was calculated using the radiation intercepted by the pasture plus the intercepted by the trees, resulting in overestimation of forage accumulation. This problem should be fixed by changing the codes used for calculating radiation interception. Finally, the model must be improved to simulate automatically the tree root growth and its distribution in each zone of the silvopastoral system and soil layer. This improvement will be possible by coupling a eucalypt model in the APSIM silvopastoral simulation capability of the APSIM Next Generation platform, and by adding calculations that distribute the tree root growth estimated by the tree model horizontally and vertically in the soil, following a predetermined pattern related to the tree species.

Specifically for silvopastoral systems under grazing, the simulations should be improved by developing tools to simulate forage mass losses during and after grazing, caused by animals physical damages, since they are very important to estimate pasture growth in these conditions. SLA calculations also should be improved by changing and calibrating the relationships between shading and SLA increase, but more detailed experiments are required for that.

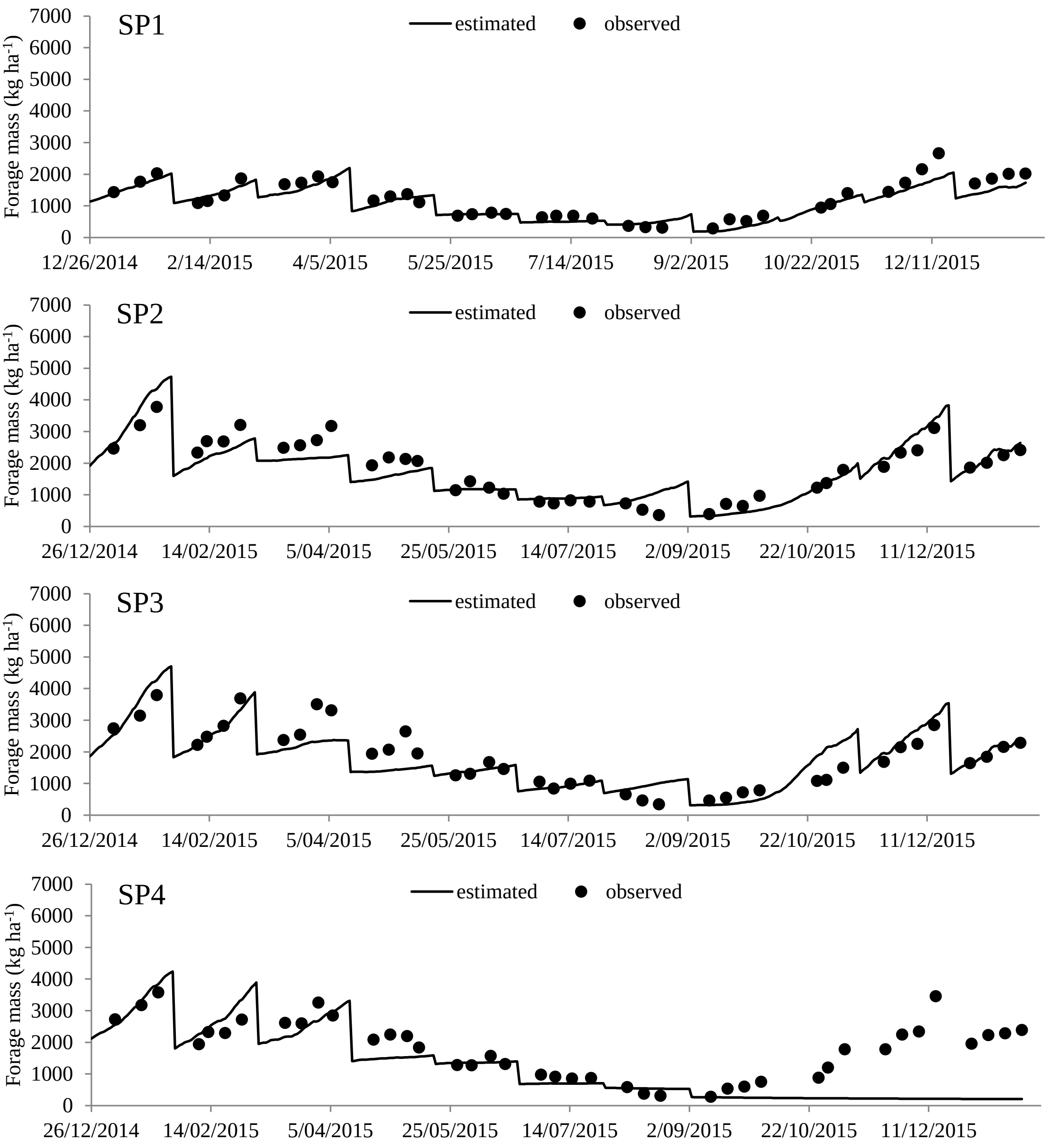

Figure 44. Time series of observed and estimated forage live mass, considering only competition by solar radiation, using the CROPGRO-Perennial Forage model, for the positions 0.0 m (SP1), 3.75 m (SP2), 7.50 m (SP3) and 11.25 m (SP4) from the eucalypt north row in a silvopastoral system.

The forage mass simulations for Piatã palisadegrass, under cutting management and full sun, with the CROPGRO-Perennial Forage model, showed a good performance, achieving results similar to the best parameterizations of such model for *Urochloa brizantha* available in the literature (Pedreira et al. 2011; Pequeno et al. 2014), confirming the model efficacy. The results for irrigated pasture under cutting management ($R^2 = 0.86$, d = 0.91, NSE = 0.75, ME = -494.6 kg ha^{-1}, MAE = 646.1 kg ha^{-1} and RMSE = 1025.8 kg ha^{-1}) where similar to those obtained by Pedreira et al. (2011) for Xaraés palisadegrass (d = 0.84 and RMSE = 538 kg ha^{-1}) and by Pequeno et al. (2014) for Marandu palisadegrass (d = 0.91 and 0.96 and

RMSE = 464 and 523 kg ha^{-1}). In the same way, the results for rainfed pasture under cutting management (R^2 = 0.93, d = 0.97, NSE = 0.90, ME = -136.5 kg ha^{-1}, MAE = 446.7 kg ha^{-1} and RMSE = 587.7 kg ha^{-1}) were similar to those obtained by Pequeno et al. (2014) for Marandu palisadegrass (d = 0.93 and 0.96 and RMSE = 526 and 501 kg ha^{-1}).

The results for the forage mass simulations with the CROPGRO-Perennial Forage model for rainfed pasture, under grazing management and full sun (R^2 = 0.65, d = 0.86, NSE = 0.60, ME = -289.3 kg ha^{-1}, MAE = 677.5 kg ha^{-1} and RMSE = 919.4 kg ha^{-1}) were also similar to those results obtained by Pequeno et al. (2014). Santos (2016), simulating Piatã palisadegrass growth under continuous stocking with the STICS model, obtained R^2 = 0.48 and RMSE = 1020 kg ha^{-1}.

The CROPGRO-Perennial Forage model forage mass simulations, for the silvopastoral system, presented good results at the positions SP1, SP2 and SP3 (R^2 from 0.75 to 0.90, d from 0.93 to 0.96, NSE between 0.74 and 0.85, and RMSE = 919.4 kg ha^{-1}), similar to those obtained by Pequeno et al. (2014) at full sun, and to those obtained by Zamora et al. (2009) (d between 0.94 and 0.98 and RMSE between 235 and 512 kg ha^{-1}) simulating cotton biomass with the CROPGRO-Cotton model, in an agroforestry system with pecan trees, considering only competition by solar radiation, such as in the present study. The forage mass estimations at SP4 were affected by the pasture death during the 7th cycle, probably promoted by the association between low N supply, low stubble mass, high shading and high water stress. However, more detailed studies should be carried out to evaluate the effects of these conditions on pasture growth and death.

The simulations of pasture growth with the CROPGRO-Perennial Forage model may be improved by adding calculations that take into account the differences of growth partitioning and senescence during flowering. Specifically for pastures under grazing, such model should be adapted to consider the forage mass losses during and after grazing, caused by animals physical damages, but for this, more detailed studies should be conducted to identify the specific factors that affect such losses.

Simulations of agroforestry systems in the DSSAT platform are very limited, since the models allow simulating only the competition by solar radiation, needing measurements of solar radiation at each position to be simulated, and do not have tree models. The good performance of CROPGRO-Perennial Forage model in the present study for the silvopastoral simulations are mainly due to the higher importance of solar radiation competition to determine pasture growth than competition by soil water. Therefore, when water deficit becomes more important to define pasture growth than solar radiation, the model will fail.

These problems could be solved in this platform by creating tree models and capabilities to simulate the interactions between trees and crops satisfactorily.

6.5. Conclusions

The APSIM-Tropical Pasture model was efficient to simulate pasture growth when only competition by solar radiation is considered, but when the simulations are performed with the current APSIM silvopastoral capability and considering competition by soil water, the model was inefficient.

The APSIM silvopastoral simulation capability presented several problems, such as: the inefficiency to simulate solar radiation transmission across a transect, affecting pasture transpiration and water balance; pasture growth simulations at the first zone is calculated using the radiation intercepted by the pasture plus the intercepted by the trees, resulting in overestimations of forage accumulation; and the model does not simulate the tree root growth automatically, neither its horizontal and vertical distribution. Therefore, this capability is a promissing tool for estimating soil water competition in integrated systems.

The CROPGRO-Perennial Forage model was efficient to simulate Piatã palisadegrass growth at full sun, under irrigated and rainfed conditions, and cutting and grazing management, except during flowering periods and when high forage mass losses after grazing occur.

The simulations of pasture growth in silvopastoral systems with the CROPGRO-Perennial Forage model were efficient when the competition by solar radiation is the only determining factor for pasture growth, however when soil water competition assumes a higher importance, the model is not efficient.

REFERENCES

Allen, R.G., Pereira, L.S., Raes, D., Smith, M., 1998. Crop evapotranspiration – guidelines for computing crop water requirements. FAO, Rome.

Auclair, D., 1996. Scientific and technical basis for silvopastoral systems in Europe, in: Etienne, M. (Ed.), Western European Silvopastoral Systems. INRA, Paris, pp. 195-206.

Balandier, P., Bergez, J.E., Etienne, M., 2003. Use of the management-oriented silvopastoral model ALWAYS: Calibration and evaluation. Agrofor. Syst. 57, 159-171. https://doi.org/10.1023/A:1024863408559

Boote, K.J., Jones, J.W., Hoogenboom, G., Pickering, N.B., 1998. The CROPGRO model for grain legumes, in: Tsuji, G.Y., Hoogenboom, G., Thornton, P.K. (Eds.), Understanding Options for Agricultural Production. Kluwer, Dordrecht, pp. 99-128.

Bray, R.H., 1954. A nutrient mobility concept of soil-plant relationships. Soil Sci. 78, 9-22.

Brisson, N., Bussiere, F., Ozier-Lafontaine, H., Tournebize, R., Sinoquet, H., 2004. Adaptation of the crop model STICS to intercropping: Theoretical basis and parameterization. Agron. 24, 409-421. https://doi.org/10.1051/agro:2004031

Celette, F., Ripoche, A., Gary, C., 2010. WaLIS—A simple model to simulate water partitioning in a crop association: The example of an intercropped vineyard. Agric. Water Manag. 97, 1749-1759. https://doi.org/10.1016/j.agwat.2010.06.008

Dilla, A., Smethurst, P.J., Barry, K., Parsons, D., Denboba, M., 2017. Potential of the APSIM model to simulate impacts of shading on maize productivity. Agrofor. Syst. (in press). https://doi.org/10.1007/s10457-017-0119-0

Friend, A.D., Stevens, A.K., Knox, R.G., Cannell, M.G.R., 1997. A process-based, terrestrial biosphere model of ecosystem dynamics (Hybrid v3.0). Ecol. Model. 95, 249-287. https://doi.org/10.1016/S0304-3800(96)00034-8

Fry, G.J., Lungu, C., 1996. Assessing the benefits of interventions to improve soil moisture conditions using the PARCH Crop Environment Model, in: Annual Scientific Conference, Proceedings of the Annual Scientific Conference. SADC-Land And Water Management Research Programme, Harare, pp.119-125.

Gardner, W.R., 1960. Dynamic aspects of water availability to plants. Soil Sci. 89, 63-73.

Graves, A.R., Burgess, P.J., Palma, J., Keesman, K.J., Van Der Werf, W., Dupraz, C., Van Keulen, H., Herzog, F., Mayus, M., 2010. Implementation and calibration of the parameter-sparse Yield-SAFE model to predict production and land equivalent ratio in mixed tree and crop systems under two contrasting production situations in Europe. Ecol. Model. 221, 1744-1756. https://doi.org/10.1016/j.ecolmodel.2010.03.008

Gregory, P.J., 1996. Approaches to modelling the uptake of water and nutrients in agroforestry systems. Agrofor. Syst. 34, 51-65. https://doi.org/10.1007/BF00129632

Holzworth, D.P., Huth, N.I., Devoil, P.G., Zurcher, E.J., Herrmann, N.I., Mclean, G., Chenu, K., Oosterom, E.J., Snow, V., Murphy, C., Moore, A.D., Brown, H., Whish, J.P.M., Verral, S., Fainges, J., Bell, L.W., Peake, A.S., Poulton, P.L., Hochman, Z., Thorburn, P.J., Gaydon, D.S., Dalgliesh, N.P., Rodriguez, D., Cox, H., Chapman, S., Doherty, A., Teixeira, E., Sharp, J., Cichota, R., Vogeler, I., Li, F.Y., Wang, E., Hammer, G.L., Robertson, M.J., Dimes, J.P., Whitbread, A.M., Hunt, J., Van Hees, H., Mcclelland, T., Carberry, PS., Hargreaves, J.N.G., Macleod, N., Mcdonald, C., Harsdorf, J., Wedgwood, S., Keating, B.A., 2014. APSIM - Evolution towards a new generation of agricultural systems simulation. Environ. Model. Softw. 62, 327-350.

Holzworth, D., Huth, N.I., Fainges, J., Herrmann, N.I., Zurcher, E., Brown, H., Snow, V., Verral, S., Cichota, R., Doherty, A., DeVoil, P., McLean, G., Brider, J., 2015. APSIM Next Generation: The final frontier?, in: 21st International Congress on Modelling and Simulation, Proceedings of the 21st International Congress on Modelling and Simulation, Gold Coast, pp. 347–353. http://www.mssanz.org.au/modsim2015 (accessed 19 August 2017).

Huth, N.I., Carberry, P.S., Poulton, P.L., Brennan, L.E., Keating, B.A., 2002. A framework for simulating agroforestry options for the low rainfall areas of Australia using APSIM. Eur. J. Agron. 18, 171-185. https://doi.org/10.1016/S1161-0301(02)00103-X

Johnson, M-V. V., Macdonald, J.D., Kiniry, J.R., Arnold, J., 2009. ALMANAC: a potential tool for simulating agroforestry yields and improving swat simulations of agroforestry watersheds. Int. Agric. Eng. J. 18, 51-58.

Keating, B.A., Carberry, P.S., Hammer, G.L., Probert, M.E., Robertson, M.J., Holzworth, D., Huth, N.I., Hargreaves, J.N.G., Meinke, H., Hochman, Z., Mclean, G., Verburg, K., Snow, V., Dimes, J.P., Silburn, M., Wang, E., Brown, S., Bristow, K.L., Asseng, S., Chapman, S., Mccown, R.L., Freebairn, D.M., Smith, C.J., 2003. An overview of APSIM, a model designed for farming systems simulation. Eur. J. Agron. 18, 267–288. https://doi.org/10.1016/S1161-0301(02)00108-9

Keesman, K.J., Van Der Werf, W., Van Keulen, H., 2007. Production ecology of agroforestry systems: A minimal mechanistic model and analytical derivation of the land equivalent ratio. Math. Biosci. 209, 608–623. https://doi.org/10.1016/j.mbs.2007.04.001

Kiniry, J.R., Williams, J.R., Gassman, P.W., Debaeke, J., 1992. A general process-oriented model for two competing plant species. Trans. Am. Soc. Agric. Eng. 35, 801-810. https://doi.org/10.13031/2013.28665

Lafolie, F., Bruckler, L., Ozier-Lafontaine, H., Tournebize, R., Mollier, A., 1999. Modeling soil-root water transport and competition for single and mixed crop. Plant Soil 210, 127-143. https://doi.org/10.1023/A:1004634102958

Malezieux, E., Crozat, Y., Dupraz, C., Laurans, M., Makowski, D., Ozier-Lafontaine, H. Rapidel, B., De Tourdonnet, S., Valantin-Morison, M., 2008. Mixing plant species in cropping systems: concepts, tools and models. A review. Agron. Sustain. Dev. 29, 43-62. https://doi.org/10.1051/agro:2007057

Matthews, R.B., Hunt, L.A., 1994. GUMCAS: a model describing the growth of cassava (Manihot esculenta L. Crantz). Field Crop. Res. 36, 69-84. https://doi.org/10.1016/0378-4290(94)90054-X

Matthews, R.B., Lawson, G.J., 1997. Structure and applications of the HyCas model, in: Agroforestry Forum, Proceedings Agroforestry Forum. University of Wales, Cardiff, pp. 14-17.

Nair, P.K.R., Kumar, B.M., Nair, V.D., 2009. Agroforestry as a strategy for carbon sequestration. J. Plant Nutr. Soil Sci. 172, 10-23. https://doi.org/10.1002/jpln.200800030

Oijen, M.V., Dauzat, J., Harmand, J-M., Lawson, G., Vaast, P., 2010. Coffee agroforestry systems in Central America: II. Development of a simple process-based model and preliminary results. Agrofor. Syst. 80, 361-378. https://doi.org/10.1007/s10457-010-9291-1

Ozier-Lafontaine, H., Lafolie, F., Bruckler, L., Tournebize, R., Mollier, A., 1998. Modelling competition for water in intercrops: theory and comparison with field experiments. Plant Soil 204, 183-201. https://doi.org/10.1023/A:1004399508452

Palma, J.H.N., Graves, H.R., Bunce, R.G.H., Burgess, P.J., Filippi, R., Keesman, K.J., Van Keulen, H., Liagre, F., Mayus, M., Moreno, G., Reisner, Y., Herzog, F., 2007. Modeling environmental benefits of silvoarable agroforestry in Europe. Agric. Ecosyst. Environ. 119, 320-334. https://doi.org/10.1016/j.agee.2006.07.021

Pedreira, B.C., Pedreira, C.G.S., Boote, K.J., Lara, M.A.S., Alderman, P.D., 2011. Adapting the CROPGRO perennial forage model to predict growth of Brachiaria brizantha. Field Crop. Res. 120, 370–379. https://doi.org/10.1016/j.fcr.2010.11.010

Pequeno, D.N.L., Pedreira, C.G.S., Boote, K.J., 2014. Simulating forage production of Marandu palisade grass (Brachiaria brizantha) with the CROPGRO-Perennial Forage model. Crop Pasture Sci. 65, 1335–1348. https://doi.org/10.1071/CP14058

Pinto, L.F.G., Bernardes, M.S., Stape, J.L., Pereira, A.R., 2005. Growth, yield and system performance simulation of a sugarcane–eucalyptus interface in a sub-tropical region of Brazil. Agric. Ecosyst. Environ. 105, 77-86. https://doi.org/10.1016/j.agee.2004.05.003

Probert, M.E., Dimes, J.P., Keating, B.A., Dalal, R.C., Strong, W.M., 1998. APSIM's water and nitrogen modules and simulation of the dynamics of water and nitrogen in fallow systems. Agric. Syst. 56, 1-18. https://doi.org/10.1016/S0308-521X(97)00028-0

Qi, X., Mize, C.W., Batchelor, W.D., Takle, E.S., Litvina, I.V., 2001. SBELTS: a model of soybean production under tree shelter. Agrofor. Syst. 52, 53-61. https://doi.org/10.1023/A:1010647118256

Santos, D.C., 2016. Características do capim-piatã e desempenho de bovinos em sistemas silvipastoris no cerrado brasileiro. PhD Thesis-Federal University of Goiás, Goiânia, 82 p.

Smethurst, P.J., Huth, N.I., Masikati, P., Sileshi, G.W., Akinnifesi, F.K., Wilson, J., Sinclair, F., 2017. Accurate crop yield predictions from modelling tree-crop interactions in gliricidia-maize agroforestry. Agric. Syst. 155, 70-77. https://doi.org/10.1016/j.agsy.2017.04.008

Steinfeld, H., Gerber, P., Wassenaar, T., Castel, V., Rosales, M., De Haan, C., 2006. Livestock’s Long Shadow: environmental issues and options. FAO, Rome.

Van Der Werf, W., Keesman, K., Burgess, P.J., Graves, A.R., Pilbeam, D., Incoll, L.D., Metselaar, K., Mayus, M., Stappers, R., Van Keulen, H., Palma, J., Dupraz, C., 2007. Yield-SAFE: a parameter-sparse process-based dynamic model for predicting resource capture, growth and production in agroforestry systems. Ecol. Eng. 29, 419-433. https://doi.org/10.1016/j.ecoleng.2006.09.017

Van Noordwijk, M., Lusiana, B., 1999. WaNuLCAS, a model of water, nutrient and light capture in agroforestry systems. Agrofor. Syst. 43, 217-242. https://doi.org/10.1023/A:1026417120254

Willmott, C.J., 1981. On the validation of models. Phys. Geogr. 2, 184–194.

Zamora, D.S., Jose, S., Jones, J.W., Cropper Junior, W.P., 2009. Modeling cotton production response to shading in a pecan alleycropping system using CROPGRO. Agrofor. Syst. 76, 423-435. https://doi.org/10.1007/s10457-008-9166-x

Zuidema, P.A., Leffelaar, P.A., Gerritsma, W., Mommer, L., Anten, N.P.R., 2005. A physiological production model for cocoa (Theobroma cacao): model presentation, validation and application. Agric. Syst. 84, 195-225. https://doi.org/10.1016/j.agsy.2004.06.015

7. GENERAL CONCLUSIONS

Based on the results obtained in this study and answering the aims proposed, it is possible to conclude that:

- A silvopastoral system with east-west oriented rows caused shadow movement throughout the year, which promoted more shading at the inter-row when solar declination is higher; and higher shading at the positions near the trees, when solar declination is close to the local latitude. Air temperature and relative humidity did not differ between the open area and silvopastoral system, what was caused by the high canopy porosity, which allowed enough air movement between these areas;

- Silvopastoral system promoted alterations on rainfall distribution and soil water availability due to the rainfall interception and water uptake by the trees. Available soil water until 1-m depth was affected by water uptake by the trees, decreasing it near them, and by shading and the windbreak effect, reducing evapotranspiration within the silvopastoral system;

- Soil water recharge was higher close to the trees, mainly when rainfall interception increased throughfall at this position or due to improvements on soil structure and porosity, which increase water infiltration and decrease runoff. Soil water withdraw is faster below the trees, which is caused by the higher roots density and, consequently, more water absorption at this position;

- The APSIM-Tropical Pasture model was able to simulate tropical pasture growth under various management and environmental conditions, such as drought and good water supply, low and high nitrogen fertilization, and cutting and grazing systems. Several requirements for future work have been identified during this study. The environmental factors that induce flowering are not completely clear for Piatã palisadegrass, so this presents a problem for applying a model for this species at a large scale. The pasture simulations under grazing must be improved to account for biomass losses during and after grazing due to the damage caused by animals. Finally, the model should be tested in other locations, climate conditions, soils, and grazing or cutting intensities, in order to improve its accuracy and achieve enough confidence to be applied for planning and decision-making in pastoral systems;

- The two-dimensional radiation transmission model developed in this study was efficient for estimating PAR transmission in several distances from the tree rows, different zenith angles, in all the seasons of the year, and under high or low shading. This capacity must allow future adaptations for several tree species in agroforestry systems and the use of such model to help in simulations of crop and pastures growth in understory of these systems. However, tests should be performed with such model in several locations, for different latitudes and agroforestry arrangements.

- The CROPGRO-Perennial Forage model was efficient to simulate Piatã palisadegrass growth at full sun, under irrigated and rainfed conditions, and cutting and grazing management, except during flowering periods and when high forage mass losses after grazing occurred;
- The APSIM-Tropical Pasture model was efficient to simulate pasture growth in the silvopastoral system when only competition by solar radiation is considered, but when the simulations are performed with the current APSIM silvopastoral capability and considering competition by soil water, the model was inefficient;
- The APSIM silvopastoral simulation capability presented several problems, such as: the inefficiency to simulate solar radiation transmission across a transect, affecting pasture transpiration and water balance; pasture growth simulations at the first zone was calculated using the radiation intercepted by the pasture plus the intercepted by the trees, resulting in overestimations of forage accumulation; and the model does not simulate the tree root growth automatically, neither its horizontal and vertical distribution. Therefore, this capability is a promising tool for estimating soil water competition in integrated systems;
- The simulations of pasture growth in silvopastoral systems with the CROPGRO-Perennial Forage model were efficient when the competition by solar radiation is the only determining factor for pasture growth, however, when soil water competition assumes a higher importance, the model is not efficient.